NOTE TO USERS

DISSERTATION

SURFACE MODIFICATION OF ULTRA HIGH MOLECULAR WEIGHT POLYETHYLENE WITH HYALURONAN FOR TOTAL JOINT REPLACEMENT APPLICATION

Submitted by

Min Zhang

Department of Mechanical Engineering

In partial fulfillment of the requirements

For the degree of Doctor of Philosophy

Colorado State University

Fort Collins, Colorado

Summer 2004

COLORADO STATE UNIVERSITY

July 5, 2004

WE HEREBY RECOMMEND THAT THE DISSERTATION PREPARED UNDER OUR SUPERVISION BY **MIN ZHANG** ENTITLED **SURFACE MODIFICATION OF ULTRA HIGH MOLECULAR WEIGHT POLYETHYLENE WITH HYALURONAN FOR TOTAL JOINT REPLACEMENT APPLICATION** BE ACCEPTED AS FULLFILING IN PART REQUIREMENTS FOR THE DEGREE OF DOCTOR OF PHILOSOPHY.

Committee on Graduate Work

Advisor

Department Head

ABSTRACT OF DISSERTATION

SURFACE MODIFICATION OF ULTRA HIGH MOLECULAR WEIGHT POLYETHYLENE WITH HYALURONAN FOR TOTAL JOINT REPLACEMENT APPLICATION

Wear debris generated from ultra high molecular weight polyethylene (UHMWPE) remains a cause of total joint replacement loosening and failure. Most efforts to improve UHMWPE wear resistance have focused on modification of the bulk material properties. Few studies have involved the enhancement of UHMWPE surface lubrication. Hyaluronan (HA), a natural lubricant molecule present in mammalian synovial fluid, was introduced into the UHMWPE surface to improve its hydrophilicity, lubricity and wear resistance for orthopedic applications.

Two novel hyaluronan derivatives were created so that micro-composites of hydrophilic HA and hydrophobic UHMWPE could be made by either a solvent infiltration or melt blending process. The silylated HA was hydrophobic and soluble in organic solvents, and thus was used in the solvent infiltration process. It was not possible to silylate HA directly. Its ion-paired complex with a long aliphatic chain quaternary ammonium salt (HA-CTA) was used as the starting material in the silylation reaction. The degree of silylation (DS) was controlled by changing the reaction parameters such as temperature and time. Silylated HA-CTA with a high DS was soluble in xylenes or

hexane, while that with a low DS was only soluble in acetone, THF or 1,2-dichloroethane. The HA regenerated from silylated HA-CTA via hydrolysis had the same structure as native HA.

Preforms with interconnected micro-pores were used as the UHMWPE starting material to form a micro-composite with HA, rather than starting with full dense, bulk UHMWPE. A xylene solution of silylated HA-CTA quickly diffused into the connected pores of the UHMWPE performs. Following this, the silylated HA-CTA infiltrating throughout the preform was chemically crosslinked in place and hydrolyzed, and then the preform was dipped in an aqueous solution of HA which was also crosslinked. The HA-treated preform was then molded to full density. Thus the microcomposite manufacturing process was simpler and faster compared to prior efforts to create an UHMWPE-poly-L-lysine interpenetrating network.

The presence of HA on the micro-composite surface was confirmed by X-ray photoelectron spectroscopy (XPS) and toluidine blue O dye assay. With appropriate process parameters, a uniform HA film layer was produced on the micro-composite surface, which quickly hydrated in water, forming a lubricious surface film that was fully wetted by water drops during contact angle measurements.

The HA surface on the micro-composite was more stable and resistant to enzymatic degradation than free HA in an aqueous solution. This was attributed to the HA crosslinking and the deep rooting of HA into the UHMWPE surface. The effect of HA on the mechanical properties of UHMWPE was significant, but within ASTM guidelines for implant-grade UHMWPE. Compared with the control, the micro-composite had a decreased strength and increased elongation to failure. As the thickness of the preform

surface layer increased, the composite strength decreased. There was evidence of inferior consolidation during the final molding cycle in all samples, including the non-HA treated control. Simple adjustments to the molding cycle should solve this problem and result in microcomposites with better tensile properties. The HA-UHMWPE micro-composites did have significantly lower wear and wear rates than conventional UHMWPE. The decreases were most significant when the sample treatment was appropriate. Material properties and surface chemistry are more important than surface roughness in determining the wear properties of materials. Lower molecular weight and incomplete consolidation made the wear and wear rates of the smoother porous UHMWPE control higher than that of the conventional polyethylene. Low HA content within the micro-composite, abundant HA on the surface, sufficient crosslinking and good film adhesion are necessary to achieve significant lubrication and improve wear resistance of UHMWPE.

A series of HA esters that could be used to create the microcomposites via melt blending was also developed by acylating silylated HA-CTA. HA esters with an acyl chain length greater than 10 carbon atoms melted before degrading. Thus, HA caprinate and higher esters are melt-processable. The HA regenerated from HA esters via saponification had the same structure as native HA. Future work will investigate the melt blending approach to manufacture microcomposites with hot-processed HA esters and UHMWPE powder.

Min Zhang
Department of Mechanical Engineering
Colorado State University
Fort Collins, CO 80523
Summer 2004

ACKNOWLEDGEMENTS

First I would like to thank my advisor and friend, Dr. Susan James, for her guidance and support over the past five years. Without her insight, encouragement and help, I could not have surmounted one by one the technical obstacles I encountered throughout my doctoral program.

Appreciation also extends to Dr. Don Radford of Mechanical Engineering for allowing me to use his DSC and TG instruments and answering some of my material science questions.

I would also like to thank the other members of my committee: Dr. Paul Wilbur, Dr. Walajabad Sampath and Dr. David Grainger, for taking time out of their busy schedules to serve on my committee. Their insight and suggestions have been invaluable in helping me shape the research ideas. I would like to especially thank Dr. David Grainger for allowing me to sit in on his research meetings, from which I learned much about chemistry and biology.

Thanks also go to Dr. Guy Beauregard and Ms. Elisha Rentfrow for their training on poly-L-lysine modified UHMWPE system, and their assistance when I started the project.

Special thanks go to Mr. Richard King and Dr. Mark Hanes at DePuy Orthopaedics, Inc. Without their kind help, UHMWPE-hyaluronan micro-composites would just be a dream and not a reality.

Special thanks also go to Mr. Philippe Pare, Dr. Dele Popoola and Mr. Bill Overton at Zimmer, Inc. Their efforts to perform the wear test on our samples in such a tight time frame are greatly appreciated.

Many thanks also go to my grandmother, parents, brothers and sister. They have been there these years when I needed support and encouragement.

Finally, I am deeply grateful to my husband, Lizhong. He has been waiting patiently as I pursued my academic goals. Without his love, patience and support, I can not imagine how I would have completed this difficult work.

TABLE OF CONTENTS

Chapter 1

Introduction and Overview

1.1 Introduction

Because of the limited ability of articular cartilage to repair itself, joint degeneration and injury often necessitate joint arthroplasty. In 1999, approximately 600,000 total hip and knee replacements (TJRs) were performed in the United States [Romanelli, 2000]. By 2003, this number increased to over 700,000 [NIH Guide, 1999].

Since Sir John Charnley first used ultra high molecular weight polyethylene (UHMWPE) in his total hip prosthesis design in 1962 [Charnley, 1968], total joint replacements with a metal or ceramic-on-UHMWPE combination have been the most widely accepted configuration [Kurtz, 1999]. UHMWPE is a linear homopolymer produced by polymerization of ethylene gas. The mechanical properties of the material improve with molecular weight up to 1.75×10^6 g/mole and then remain fairly constant [Oonishi et al., 1999]. The weight-average molecular weight of commercially available UHMWPE is 4.0×10^6 g/mole approximately ten times that of high molecular weight-high density polyethylene (HMW-HDPE) [Stein, 1988]. Due to the extremely long molecular chains and their excessive entanglements, UHMWPE exhibits excellent sliding wear resistance and impact toughness, and due to its semi-crystalline conformation, the

surface and subsurface structure is highly ordered, offering resistance to deformation [Kelly, 2000].

Although clinical successes have been achieved with UHMWPE as the weight-bearing surface in TJRs, wear debris generated from UHMWPE components remains a major cause of implant loosening and failure, limiting the longevity of current TJR [Kawate et al., 1999]. It has been demonstrated that several hundreds of particles are generated from the UHMWPE-bearing surface in the acetabular cups of total hip replacements (THRs) with each step (> 51 billion/year), and a large proportion of these particles are smaller than one micron [McKellop et al., 1995]. Cells from the immune system of the host identify the polyethylene particles as foreign and initiate a complex inflammatory response. This response may lead to osteolysis, bone resorption, loosening and/or fracture of the bone. Osteolysis around a total knee joint is less frequent than in a total hip replacement. This might be due to the relatively larger particle size of polyethylene debris generated from delamination and fatigue wear of the UHMWPE tibial plateaus under the point contact stress and sliding motion [Walker, 1993].

Many research efforts to reduce friction and wear of UHMWPE are currently underway, seeking either to improve the properties of the bulk UHMWPE material or modify its surface. Crosslinked UHMWPE did markedly improve wear resistance, but at the sacrifice of its toughness and mechanical properties [Muratoglu et al., 1999]. The surface treatment of UHMWPE with plasma and ion implantation also improved its hydrophilicity and tribological properties [Widmer and Spencer 2001; Dong, 2000], but the surface modification is relatively short-lived. Beauregard modified UHMWPE by introducing a synthetic polypeptide (poly-l-lysine) into the surface to form a semi-

interpenetrating polymer network between polypeptide and UHMWPE. However, the decrease in the coefficient of friction was not very significant, and no wear data were available [Beauregard, 1999]. A more promising method to reduce friction and wear of UHMWPE with hyaluronan was explored in this study.

The following is a comprehensive review of both UHMWPE modification and hyaluronan. Attempts to apply a soft layer on the surface of UHMWPE to enhance lubrication of TJRs are also summarized.

1.2 Literature Review

1.2.1 Improving the Properties of UHMWPE Bulk Material

Three approaches have been used to improve the properties of UHMWPE bulk material: modification of the manufacturing process, UHMWPE composites, and crosslinking UHMWPE.

1.2.1.1 Modification of UHMWPE Processing

It is well known that processing can substantially influence the morphology of semi-crystalline polymers, so by modifying the manufacturing process, the performance and wear of UHMWPE can be changed. As stated by Eyerer et al. [1990], crystallinity of UHMWPE used for TJRs should not be greater than 70%. However, when below this level, increase in crystallinity can improve resistance to crack initiation, crack propagation, and oxidation, and hence, wear.

Hylamer^{TM} is an "enhanced" UHMWPE produced using hot isostatic press (HIP) [Li and Howard 1991; Sun et al., 1994; Li et al., 1990]. The modified UHMWPE shows

higher crystallinity and density than the surgical implant grade. It also has a very high ratio of modulus to yield strength. This is undesirable as such a high ratio could lead to increased contact and subsurface shear stresses in bearing surfaces fabricated from the materials, and consequently, increased wear.

The Hylamer™ family has two members: Hylamer™ material for accetabular components and Hylamer™ -M for knee components. The clinical results of Hylamer™ are mixed, ranging from significantly greater incidence of excessive wear *in vivo*, to comparable incidence, to improved wear resistance when compared with conventional UHMWPE [Kurtz, 1999]. It was found that Hylamer™ was more susceptible to oxidative degradation and had greater contact stresses than conventional UHMWPE [King et al., 1996].

1.2.1.2 UHMWPE Composites

In the 1970s, a carbon-reinforced UHMWPE, known as Poly II™ was created for orthopedic bearing materials, under the assumption that increasing the modulus and ultimate tensile strength of the bearing, as well as decreasing its creep, would increase its longevity. The inclusion of short chopped carbon fibers did improve the mechanical properties of UHMWPE. So Poly II™ was expected to be more resistant to the pitting and delamination often seen in knee arthroplasties. Unfortunately, the promise shown by Poly II™ in the laboratory was not borne out in the clinical setting, and within a short time after implantation many patients presented with osteolysis and complete mechanical failure of their tibial bearing inserts [Busanelli et al., 1996; Wright et al., 1988]. Investigation indicated that the poor crack propagation resistance of Poly II™ was the

reason, resulting from the poor bonding between carbon fibers and UHMWPE matrix [Connelly et al., 1984].

To improve the physical compatibility and produce better interfacial bonding between fiber and matrix, UHMWPE fiber-reinforced UHMWPE composites were studied [Deng, 1997]. It was found that the tensile properties, creep resistance and impact strength of the self-reinforced UHMWPE composites are superior to plain UHMWPE, while the wear properties are similar to plain UHMWPE.

1.2.1.3 Crosslinked UHMWPE

Interest in crosslinked UHMWPE has increased during the past several years, due to confirmation that crosslinking dramatically reduces the wear rate of UHMWPE [Shen et al, 1996; Wang et al., 1998]. UHMWPE can be crosslinked through chemical reactions or ionizing radiation.

Peroxides and silanes have been used to crosslink UHMWPE. The dialkyl peroxides often used include dicumyl peroxide[De Boer et al, 1984] and 2,5-dimethyl-2,5-bis(tertbutylperoxy)-3-hexyne (Peroxide 130) [Narkis et al., 1987]. At the elevated temperatures associated with compression molding or hot isostatic pressing of UHMWPE, the peroxide decomposes by a free radical reaction and leads to the formation of the crosslinks between adjacent polymer chains [Gul, 1997]. Peroxide-crosslinked UHMWPE can also improve wear resistance, but its apparent oxidative instability still is a problem [Gul, 1997].

The use of silane crosslinked polyethylene in total hip arthroplasty was first proposed by Atkinson et al. [1980]. They used vinyl trimethoxysilane to crosslink high-density

polyethylene (HDPE), and found the crosslinked HDPE had better creep resistance and wear resistance at high sliding velocities under unidirectional motion compared to uncrosslinked UHMWPE (RCH 1000). Wroblewski's clinical studies (8 years and 3 months, 19 patients) [1996] showed that the average linear wear rate of the silane crosslinked HDPE was 0.022mm/yr, similar to the result of UHMWPE crosslinked by other methods.

Gamma and electron beam radiation have been used for UHMWPE crosslinking. Radiation crosslinking can increase wear resistance by increasing surface smoothness and hardness [Lee et al., 1991], preventing molecular alignment and the associated cross-shear weakening [Ramamurti, 1995], and even decreasing wear particle generation [Bragdon et al., 1999]. However, the radiation can cause oxidation that has been known to accelerate fatigue wear through main-chain scission [Trieu et al., 1997]. Some efforts have been made to optimize radiation techniques that minimize oxidation. One example is the electron-beam irradiation and subsequent melt-annealing technique, which results in crosslinked UHMWPE that exhibits excellent oxidation resistance, due to the eradication of free radicals during the melt-annealing process [Gsell et al., 2001].

Crosslinking UHMWPE and HDPE markedly improve the wear resistance of these materials. However the structural changes that result from crosslinking compromise its toughness, fatigue crack growth resistance and mechanical properties (yield and ultimate tensile strength) [Muratoglu et al, 1999; Eberhardt et al., 2001]. With increased levels of crosslinking, the tensile elongation and impact strength decrease dramatically [Greer, 2001]. This might raise questions regarding its use in weight bearing components such as total knee replacements, which are subject to pitting and delamination failures.

The above attempts to lower friction and wear focus only on the prosthetic materials themselves, ignoring the important influence of the UHMWPE surface and its interaction with the synovial fluid. Some surface treatments can also be used to modify the UHMWPE surface microstructure without affecting the bulk characteristics. These are summarized next.

1.2.2 Modifying the Surface Structure of UHMWPE

1.2.2.1 Plasma Treatment

Klapperich et al. [1999] used Ar/C_3F_6 plasma to lightly crosslink the subsurface of UHMWPE and graft or deposit CF_X groups on the surface. The crosslinked surface was expected to inhibit alignment of the crystalline regions along the sliding direction and enhance the wear resistance, while the low-surface energy CFx groups were expected to reduce the surface adhesion (friction). The surface treatment was intended for total knee replacements (TKRs) in order to avoid fully crosslinking the bulk UHMWPE, which lowers the resistance to crack propagation making the TKRs subject to fatigue and delamination failures. The results indicated that the coefficient of friction was only marginally affected by the plasma treatment, but a significantly improved wear resistance was observed with the appropriately tailored treatments.

1.2.2.2 Ion Implantation Treatment

It has been demonstrated that nitrogen or carbon ion implantation can improve the wear resistance of UHMWPE by crosslinking the surface polymer chains [Chen et al., 2000; Shi et al., 2003], however, it is difficult to uniformly treat such three-dimensional

objects as hip joint sockets without using sophisticated manipulating devices. Dong et al. [2000] developed plasma immersion ion implantation (PI^3) technology to overcome this problem. The specimens were immersed in a low-pressure radio frequency plasma discharge and treated with a pulsed voltage source. It was found that PI^3 treatment could improve the UHMWPE' s surface hardness, elastic modulus, and hydrophilicity, and the average wear rate could be reduced from 3.45×10^{-8} mm^3 N^{-1} m^{-1} for untreated materials to 1.41×10^{-8} mm^3 N^{-1} m^{-1} for high dose PI^3 treated samples.

In the above bulk material or surface structure modification, the effect of UHMWPE surface chemistry was not considered. UHMWPE is extremely hydrophobic, while the natural joint surface, articular cartilage, is very hydrophilic and negatively charged. It is the interaction of articular cartilage and synovial fluid that plays a key role in the very low friction and wear of synovial joints [Dowson, 1967]. The composition of synovia present after postoperative healing following implantation was reported very similar to that present in a healthy joint [Black, 1998]. Therefore, some efforts have been made to modify the surface chemistry of UHMWPE, which are summarized in the following.

1.2.3 Modifying the Surface Chemistry of UHMWPE

1.2.3.1 Plasma Surface Treatment

Widmer and Spencer [2001] treated UHMWPE with oxygen-plasma. The treated surface was hydrophilic, and had a faster and modified protein adsorption. A denser boundary layer of human serum albumin (HSA) protein was found on the UHMWPE surface, which appeared to enhance boundary lubrication, leading to a 50% reduction of dynamic friction, as well as to a reduction of stiction. This surface modification is

relatively short-lived, but lasts long enough to verify the concept that adsorption of protein from synovial fluid can be influenced by changing surface chemistry, and can potentially improve boundary lubrication.

1.2.3.2 IPN Surface Modification

Beauregard [1999 & 2001] modified UHMWPE by introducing poly-L-lysine (PLL) (a polypeptide) into the surface to form a semi-interpenetrating polymer networks (IPN) between UHMWPE and PLL. PLL was first silylated with N,O-bis(trimethylsilyl) acetamide (BSA) (Figure 1.1) to improve its hydrophobicity. The silylated PLL could diffuse into the UHMWPE surface through swelling in xylene solution for a long time (250-500 hours), and then be crosslinked there. After hydrolysis, the silylated –NHx (x = 1 or 2) groups were returned to their initial state, which were expected to attract proteoglycans in synovial joint fluid for lowering the friction and wear of UHMWPE. The results showed that appropriately synthesized IPN did lower the friction, but no wear data are available.

1.2.4 Cushion Form Bearings

Current total joint replacements operate in the mixed or boundary lubrication regimes, relying on the inherent low friction and wear properties of ultra high molecular weight polyethylene (UHMWPE) [Unsworth, 1978 & 1995]. Lubrication using the body's own lubricant has not, to date, been a feature of artificial joint design. The continuous rubbing between the two articular surfaces results in wear of the softer material (i.e., UHMWPE). To take advantage of elastohydrodynamic lubrication (EHL) and to enhance fluid film lubrication, a thin compliant layer with low elastic modulus was attached to the

acetabular surface [Auger et al., 1993; Sawae et al., 1996], which could act like a cushion form bearing, maintaining an effective lubricant film through elastic surface deformation.

Two classes of materials have been investigated for this application. One class is the biocompatible elastomers, including various polyurethanes [Blamey et al., 1991; Auger et al., 1993; Caravia et al., 1993] and silicone rubbers [Sawae et al., 1996]. Artificial cartilage made of these materials exhibits a significantly lower coefficient of friction than UHMWPE, and shows fluid film lubrication under certain conditions. The polyurethane cushions exhibit a coefficient of friction as low as 0.005 under the best conditions [Unsworth, 1995]. These elastic cushions work well during steady-state sliding due to the resultant full fluid-film lubrication conditions, but the friction increases to an unacceptable level during periods of heavy loading with little movement or at the start-up of motion due to the resultant boundary lubrication conditions [Caravia et al., 1993].

Hydrogel cushions, the second class of materials investigated, were hypothesized to solve the above problem by introducing weeping lubrication as a supplemental lubrication mechanism under severe operation conditions. Hydrogels are a class of soft, porous, permeable, crosslinked hydrophilic polymer networks with a structure more like articular cartilage than the above elastomers. They readily absorb water and maintain high water contents, typically 40-60% [Goldsmith et al., 1998; Corkhill et al., 1990]. When the articulating surfaces come into contact, the water trapped in the hydrogel is squeezed out under pressure helping to maintain the separation of surfaces. This supplemental weeping effect may contribute to the advantage of hydrogels over elastomers [Sawae et al., 1996].

The hydrogels most often used, such as polyvinyl alcohols (PVA) and poly hydroxyethyl methacrylate (poly HEMA), are made from vinyl monomers. The structures of typical vinyl monomers are illustrated in Figure 1.2 [Corkhill et al., 1990]. The conventional homogeneous hydrogels are not suitable for artificial cartilage materials because of their very weak mechanical properties. The strategy to enhance the mechanical properties of synthetic hydrogels includes the development of copolymers and the use of semi-interpenetrating polymer networks (SIPNs). Copolymerization between hydrophilic vinyl monomers and hydrophobic vinyl monomers largely increases the strength and modulus of hydrogels, but meanwhile reduces the elongation to break and water content. The mechanical properties can thus be tailored by controlling composition and molecular structure. Cellulose acetate (CA) and cellulose acetate butyrate (CAB) have very high strengths and moduli, and have been used to reinforce hydrogels by forming SIPNs with crosslinked vinyl monomers. The typical properties for these materials [Corkhill et al., 1990; Caravia et al., 1993; Sawae et al., 1996] are listed in Table 1.1. Modified hydrogel bearings have mechanical properties comparable to natural articular cartilage and exhibit much lower coefficients of both start-up and steady friction than the elastomer cushions, but this may not necessarily give good wear and durability [Caravia et al., 1993].

The use of soft cushions has not exhibited clinical or commercial success to date [Sariri et al., 2000]. The main difficulties include the degradation or fatigue of cushion materials and de-bonding of the soft layer from its much stiffer substrate [Unsworth, 1995; Blamey et al., 1991].

1.2.5 Improvement in Femoral Head Materials

The above review addressed the effect of the bulk properties and surface features of UHMWPE on the wear of UHMWPE in total joint replacements. However, as pointed out by Dowson [1995], the surface topography of the femoral heads and the geometrical conformity of the mating components also play a key role in the wear of UHMWPE. The geometrical conformity is a design and manufacturing issue, and is not the direct purview of materials science research, so it will not be discussed here. For a detailed review, please see Lewis's paper [1997].

UHMWPE is the standard material for the acetabular cups, while commercially available femoral heads are made from either metal alloys (Cr-Co) or ceramics (alumina or zirconia) [Affatato et al., 1999]. It has been demonstrated that very hard, smooth and inert femoral head counterfaces are beneficial in reducing abrasive wear of UHMWPE [Dowson, 1995]. Ceramics are apparently superior to metal alloys due to their good surface finishes, high hardness and resistance to oxidation and corrosion [Skinner, 1999]. Diamond coatings were supposed to improve hardness and polish of Cr-Co femoral heads, but have not achieved commercial success yet. Alumina femoral heads were marketed in the United States in the early 1980s, and Zirconia in the late 1980s [Skinner, 1999]. Clinical results indicated that the wear rate of UHMWPE against ceramic femoral heads was only about 50% of the corresponding wear rate against the metal heads [Dowson, 1995; Heisel et al., 2004]. In addition its smooth surface and high hardness, the ionic structure of ceramic materials should lead to reduced wear due to the hydrophilic, ionic surface, which results in lower contact angles. A low contact angle has been correlated with low coefficient of friction, and reduced wear [Skinner, 1999].

In spite of these attractive properties, *in vivo* fracture of ceramic femoral heads, due to subcritical crack growth, remains a big concern. A fracture rate of 0.22% was reported with 10-15 year follow-up of more than 5000 alumina femoral heads [Aza et al., 2002; Skinner, 1999]. Efforts have been made to improve the toughness and crack growth resistance, for example, by developing alumina-zirconia nano-composites [Aza et al., 2002; Affatato et al., 1999].

1.2.6 Hyaluronan, Its Derivatives and Their Biomedical Applications

1.2.6.1 Hyaluronan and Its Derivatives

Hyaluronan is a naturally occurring polysaccharide with a large unbranched structure consisting of repeating disaccharides of N-acetylglucosamine and glucuronic acid (Figure 1.3). It is present in all vertebrate tissues and body fluids with relatively high concentrations in the vitreous humor of eye, the umbilical cord, synovial joint fluid and rooster combs [Laurent, 1970].

Hyaluronan was first isolated from bovine vitreous humor in acid form by Karl Meyer and John Palmer of Columbia University in 1934. They named the new polysaccharide "hyaluronic acid" meaning uronic acid from hyaloid (vitreous). The term "hyaluronan" was introduced by Endre Balazs in 1986 to encompass the different forms the molecule can take – for example, the acid form, hyaluronic acid, and the salts, such as sodium hyaluronate, which form at physiological pH [Laurent, 1989]. Endre Balazs pioneered the medical use of hyaluronan. He derived the main concepts for many applications and prepared the first non-inflammatory fraction of sodium hyaluronate, called NIF-NaHA, which was free of impurities that could cause inflammatory reactions [Laurent, 2003].

Hyaluronan has a unique set of physical and biological properties compared with other polysaccharides:

Viscoelasticity Hyaluronan carries one carboxyl group (-COOH) per disaccharide unit, which is dissociated at physiological pH thereby conferring a polyanionic characteristic to the compound. The negatively charged flexible chains take on an expanded conformation and entangle with each other at very low concentrations, which may contribute to the unusual rheological properties and viscoelastic behavior of hyaluronan. Solutions made of hyaluronan are primarily viscous at low shear rates, but primarily elastic at high shear rates [Laurent, 1970].

Hydrophilicity It has been demonstrated that hyaluronan acts as a water-retaining polymer in many tissues [Balazs, 1970 & 1984A], including skins [Yates, 1971; Bettelheim, 1971]. The hydrodynamic volume of hyaluronan in solution is 1000 times larger than the space occupied by the unhydrated polysaccharide chain [Laurent, 1970]. The large molecular volume forces the overlap of individual hyaluronic acid molecular domains, resulting in extensive chain entanglement and interaction. As a result, the polymer network can hold large amounts of water (up to ~1000 times its weight) like a molecular sponge [Hoekstra, 1999]. This property is unique to hyaluronan. Other glycosaminoglycans (GAG), such as heparin, chondroitin sulfates and keratan sulfate, may form viscous solutions, but they never form viscoelastic polymer networks [Balazs, 1983].

Lubricity The extraordinary viscoelastic properties also make hyaluronan ideal as a lubricant. Hyaluronan in synovial fluid complexes with proteins and penetrates the surface of cartilage, forming a 1-2 μm-thick layer of HA protein complex, which serves

as the primary isolating and lubricating layer in joints. Under slow mechanical loading it behaves as a viscous oil-like lubricant. However at higher mechanical loading rates the HA layer changes to a highly deformable elastic system. It absorbs and converts the imposed stress to an elastic deformation, and then rebounds to the original condition when the stress is removed [Balazs et al., 1970]. It should be noticed that biological lubrication by hyaluronan is not confined to joints. It occurs at most tissue surfaces that slide along each other [Hoekstra, 1999; Ogston 1970].

Regulator of Cellular Activity Hyaluronan is not just an inert compound, acting as a vital structural component of connective tissues. It also plays an important role in diverse biological processes, such as cellular migration, mitosis, inflammation, cancer, angiogenesis and fertilization. Hyaluronan influences cell behavior by binding some specific proteins, termed hyaladherins. Many reports have been published in the last decade on the role of hyaluronan-receptors [Heinegard, Lesley, Day and Toole, 1998].

However, hyaluronan's high solubility, rapid degradation and short residence time in water still limit the biomedical application of naturally occurring hyaluronan, particularly in tissue engineering and viscoseparation applications. Many researchers have modified hyaluronan in order to obtain a more stable solid material. Two groups of widely used and commercialized hyaluronan derivatives, Hylan and Hyaff, are discussed below.

Hylan is the generic name for crosslinked hyaluronan in which crosslinking only occurs on hydroxyl groups, not affecting carboxyl and acetamide groups [Balazs et al., 1989A]. Balazs and his co-workers in Biomatrix have patented a large group of hylans via various cross-linking methods since the mid 1980s [Balazs et al., 1995]. By adjusting the crosslinking reactions (which will be reviewed in Section 1.2.6), hylans can be

customized to particular medical applications and provided in different forms (fluids, gels and solids). The derivatives have enhanced rheological properties and longer residence time in the tissue than hyaluronan, and proved to be just as biocompatible as the native hyaluronan.

Hyaff is a class of hyaluronan esters with the free carboxyl group of glucuronic acid esterified using different types of alcohols (see Figure 1.4a). They are the patented products of Fidia Advanced Biopolymers in Italy [Della Valle et al.,1989]. Through reducing the hydrophilic carboxyl groups and introducing hydrophobic alkylation components, the stability of the polymer in an aqueous environment is improved. The hydration extent and degradation rate depends on the type of substituent alcohol and degree of esterification. Hyaluronan and pharmacologically active alcohols are their biodegraded products [Rastrelli et al., 1990], which are biocompatible, so these materials are intrinsically safe to use. Little or no evidence of cytotoxicity has yet been found. Hyaff can also be manipulated to obtain different biological properties. Hyaff with least hydration, such as Hyaff 11 - total benzyl ester, promotes cell adhesion, while very hydrated Hyaff, such as Hyaff 11 p75 – 75% benzyl ester, is not cell-adhesive. Campoccia's paper describes the biocompatibility and biological effects of Hyaff [Campoccia et al., 1998].

During the past two decades, hyaluronan and its derivatives have become important therapeutic agents in medicine and biocompatible materials due to their unusual rheological properties and interactions with cell receptors. Their biomedical applications are summarized as follows.

1.2.6.2 Viscosupplementation

Viscosupplementation is a therapeutic treatment for arthritis in which hyaluronan or hylans are used to replace the pathologic synovial fluid and supplement the elasticity and viscosity of the endogeneous hyaluronan for restoring the normal joint functions [Biomatrix, 2000A; Weiss, 2000]. In arthritic (especially osteoarthritic) joint fluid, the concentration and molecular weight of hyaluronan is significantly reduced (normal joints: concentration – 3~4 mg/ml, MW – 4~5 million; arthritis: concentration – 1~2 mg/ml, MW –1~4 million) [Balazs, 1970 & 1982], causing a dramatic drop in the rheological properties of the synovial fluid. The synovial fluid with decreased molecular weight can not protect the articular cartilage from the impact loading stresses, nor the synovium cells from noxious substances [Adams, 1998].

Healon® is the first hyaluronan product used for viscosupplementation, developed by Biotrics, Inc. (Arlington, MA) in 1970s, but licensed to Pharmacia AB (Uppsala, Sweden) later. It is a 1% solution of NIF-NaHA (non-inflammatory fraction of Na-hyaluronan) with a weight-average molecular weight of 2-3 million. Its rheological properties were nearly as high as those of healthy human synovial fluid [Denlinger, 1998]. With this viscosupplementation, low elastoviscosity of the joint fluid was immediately elevated and maintained at that level for a few days. The pain decreased, the joint mobility increased [Balazs et al., 1985A]. However, it was not successful when brought into the field of human arthritis due to its quick degradation. Healon® was never marketed for viscosuppplementation of human arthritic joints [Biomatrix, 2002A].

Dr. Balazs and his co-worker were convinced that high viscoelasticity is necessary for the effective viscosupplementation, so they developed Hylan A and B. Hylan A is a

aldehyde crosslinked HA liquid with a weight –average molecular weight of 6-26 million, and Hylan B is a hydrated divinyl sulfone-crosslinked gel with an infinite molecular network [Balazs, 1985A, 1986 and 1987A; Biomatrix, 2002D]. An elastoviscous solution containing both hylans became the first hylan-derived product available for human and equine arthritis therapy: Synvisc® and Gelvisc®Vet.

In the late 1980s, two other NIF-NaHA viscosupplementation products were marketed: one in Japan (Arzt, Seikagaku and Kaken) and one in Italy (Hyalgan, Fidia) [Balazs, 1995]. Another viscosupplementation product marketed in Canada in 1998 was Orthovisc (Anika Therapeutics, Inc., Woburn, MA). Their properties are listed in Table 1.2.

1.2.6.3 Viscoseparation

Viscoseparation is the use of viscoelastic gels, membranes and fluids to separate tissues, prevent adhesions, and cover internal and external wounds to facilitate wound healing and decrease scar formation [Weiss, 1998]. Tissue adhesion, which often occurs after operations, leads to various surgical traumas and undesirable symptoms such as intestinal obstruction, chronic pelvic pain, infertility and so on [Miyoshi et al., 2002].

Adhesions are connective tissue fibrous bands that join together adjacent tissues or organs in abnormal configurations, which is initiated by protracted inflammatory activity [Larsen, 1998]. Barriers are often used to provide mechanical separation between traumatized tissues in order to prevent adhesions. The ideal anti-adhesion barrier product should be biocompatible, self-adherent and resorbable, with an adequate residence time and the ability to modulate fibrous formation without interfering with normal wound healing. Compared with the synthetic and other natural polymer adhesion-prevention

products, hyaluronan is the best choice due to its exceptional biocompatibility and the ability to regulate cell behaviors and promote wound healing [Savani et al., 2000].

In 1971, Healon® was first used to reduce adhesions around injured tendons in rabbits. It was reported that the NIF-NaHA was beneficial in preventing adhesion formation between the lacerated tendon and the tendon sheath [Rydell et al., 1971]. However, the unmodified hyaluronan did not provide adequate effectiveness owing to its relatively short residence time at the site of implantation [Diamond et al., 2000]. In the mid 1980s, it was found that hylans could provide a more consistent and prominent reduction in adhesion formation due to its longer residence time at the site of injury.

The first commercially available hyaluronan-based viscoseparation product is Seprafilm® produced by Genzyme Corp. (Cambridge, MA). In this product, hyaluronan and carboxymethylcellulose (CMC) were chemically modified first, and then combined together to form an insoluble HA-CMC complex, which can be formed into membranes suitable for placement on injured tissue surfaces [Burns et al., 2000]. Table 1.3 lists these HA-based anti-adhesion products. Some of them are already marketed, but some are still under development.

1.2.6.4 Viscosurgery

Viscosurgery is the surgical procedure in which an elastoviscous solution or viscoelastic gel is used as a surgical tool or implant to protect sensitive tissues from mechanical damage while creating and maintaining space for surgical manipulation by separating the tissues [Biomatrix, 2002C]. Viscosurgical tools are applied during the surgical procedure, while implants are left in the site after the surgery. This new surgical

procedure was developed during the 1970s with the introduction of NIF-NaHA in ophthalmic surgery [Balazs et al., 1972 & 1979], and became widely used in the early1980s with the worldwide commercialization of NIF-NaHA under the trademark Healon®.

The mechanical function of viscosurgical devices depends on their visco-elasticity and permeability to molecules of different sizes. Its special rheological properties and excellent biocompatibility make hyaluronan a logical choice for viscosurgery [Balazs et al, 1989B].

NIF-NaHA as a viscosurgical device is primarily used in cataract surgery. It minimizes the surgical trauma during the removal of the cataractous lens and the introduction of its replacement polymeric intraocular lens [Balazs et al, 1989B; Arshinoff, 2002]. It is also used to push back the detached retina during retinal surgery to help keep the retina in its normal position after surgery [Balazs, 1960]. The unmodified NIF-NaHA cannot provide sufficient viscoelasticity to retain the retina in its reattached position, so Hylans are used to keep longer efficacy in vitreoretinal surgery and other medical conditions.

The principles of viscosurgery are also extended to other surgical specializations, such as orthopedic surgery and otolaryngology. In orthopedic surgery, Hylans have been used to protect the articular cartilage from scuffs caused by instruments during arthroscopy. In otosurgery, HA-based viscosurgical devices have been used in middle ear surgery and the healing of tympanic membranes [Balazs, 1989B; Denlinger, 1998; Laurent, 1998].

Since Healon® was marketed, numerous other HA-based ophthalmic viscosurgical devices have appeared, which are listed in Table 1.4. They have a broad spectrum of rheological properties to meet different surgical requirements.

1.2.6.5 Viscoaugmentation

Viscoaugmentation is the replacement or augmentation of the intercellular matrix of the dermal and other soft tissues with viscoelastic gels [Denlinger, 1998; Biomatrix, 2002D]. Augmentation has been practiced with various materials for nearly 100 years [Matton et al., 1985]. The widely used materials include paraffin, silicone and collagen [Larsen et al., 1998]. Paraffin and silicone have been reported to produce foreign-body reactions, and to migrate from the site of injection. The problems associated with collagen are its short residence time, and possible hypersensitivity reaction [Knapp et al., 1977].

The extended residence time, enhanced viscoelasticity, high biocompatibility and natural hydrating properties of Hylan make it a good choice to augment soft tissues. Hylan B gel was first used in ophthalmic surgery to replace the partially liquefied vitreous [Denlinger, 1998]. It was later marketed for dermal augmentation in Europe under the trademark Hylaform® (Biomatrix, Ridgefield, NJ) [Biomatrix, 2002D]. Hylaform® can be injected through a needle as small, elastically deformable gel particles, into skin to correct dermal wrinkles and depress scars.

Tissue augmentation with hylans and other HA-based gels was also extended for use in urology, laryngology and plastic surgery. Hylan B can be injected into the urethral sphincter muscle for the treatment of urinary stress incontinence [Balazs et al., 1995]. It

can also be used for treating hoarseness (due to glottic insufficiency) by injection into vocal cords [Hallén et al., 2000].

Besides Hylaform®, several other HA-based gels that are also marketed in Europe, primarily for correction of facial wrinkles and scars, are listed in Table 1.5.

1.2.6.6 Drug Delivery

The use of hyaluronan and its derivatives as drug carriers is a relatively new area, but some specific properties make them ideally suitable for this purpose. (1) HA is biocompatible and non-immunogenic [Gustafson, 1998]. (2) It exists naturally in very high molecular weight, but is subject to degradation by enzymes widely distributed throughout the body [Pouyani, 1994]. (3) Various functional groups (carboxyl, hydroxyl and acetamido) give HA many ways for chemical modification and attachment of drugs [Band, 1998; Prestwich, 2003]. (4) The binding of HA with some cellular receptors also opens up a perspective of HA application in targeting delivery [Gustafson, 1998].

The native hyaluronan is eliminated very rapidly in body. To increase the residence time and functionalize it, a variety of hyaluronan derivatives have been developed through different chemical modifications, such as crosslinking [Balazs et al., 1984B & 1985B], esterifying the carboxyl group with alcohols [Della Valle et al., 1989], de-acetylating acetamido groups to get free amines [Dahl et al., 1988], and coupling the carboxyl group with dihydrazide to get free hydrazido group [Pouyani et al., 1994]. These modifications will be reviewed in Section 1.2.6.

Drugs can be chemically bound to or dispersed in hyaluronan or its derivatives for controlled release devices [Balazs et al., 1992]. If there are no interactions between drug

substance and the polymer, the carrier just acts as a drug "reservoir" or "cage" [Balazs et al., 1986 & 1995], which stores the drug and retards its diffusion, resulting in a slow release rate. Drugs can also be attached to HA or its derivatives through ionic or covalent bonding to produce pro-drugs. Della Valle et al. [1988] described in their patent how to prepare various salts of hyaluronic acid with pharmacologically active bases, such as gentamycin, amikacin and so on. Hydrazide-HA allows the attachment of carboxyl-containing drugs, such as ibuprofen modified with N-hydroxysuccinimide (NHS) [Pouyani et al, 1994].

By trapping or complexing drugs, HA and its derivatives significantly alter the pharmacokinetics and increase the residence time of the drugs. A wide range of pharmacologically active substances can interact with these polymers to achieve a controlled release. The combination of HA or crosslinked HA with antibiotics, such as tobramycin [Gustafson, 1998] and gentamycin [Larsen et al, 1991], gives significantly increased corneal residence time and better therapeutic results in topical ophthalmic medication. Carbodiimide activated HA can anchor on the surface of liposomes, forming hyaluronan-phospholipid adduct. Liposomes coated with hyaluronan function as site-adherent and sustained-release depots of epidermal growth factor for the topical therapy of wounds [Yerushalmi, 1994]. Yun et al. incorporated DNA and antigen into hydrazide-modified HA microspheres for sustained gene delivery and site-specific targeting [Yun et al., 2004].

Gustafson [1998] also discussed the possibility of targeting HA-drug complexes to cells carrying one or more HA-binding proteins. He thought if drug attachment does not interfere with the biological properties of the polymer, and the uptake of drugs by the

liver is reduced, targeting of the complex to accessible unoccupied HA binding sites can be used.

1.2.6.7 Tissue Engineering

Tissue engineering can provide cell- or molecular-based tissue therapies for developmental anomalies, defects from excised tissue (tumor excision), or for adult-onset deficiencies (diabetes). Functional tissue engineering means the controlled restoration of tissue morphology and function [Caplan, 2003].

Hyaluronan and its derivatives are promising scaffolds for tissue engineering due to their specific biological functions. Hyaluronan, extensively present in the extracellular matrix (ECM), has been shown to play a fundamental role during embryonic development [Toole et al., 1989]. HA-rich scaffolds provide an "embryo-like" environment for stem or adult cells to differentiate and divide [Campoccia et al., 1998]. High molecular weight HA enhances chondrogenic development, and inhibits angiogenesis and the entry of vessels into stem cell regions. In distinct contrast, low molecular weight HA (i.e., HA oligomers) is highly stimulatory to angiogenesis. The change of HA from high to low molecular weight triggers a series of biological events, which occur during embryonic tissue formation and tissue regeneration of very young animals [Solchaga et al, 2002; Caplan, 2003].

The capabilities for HA to exhibit different signals at different stages of the repair process are necessary for functional tissue engineering. The kinetics and sequence of the repair process can be precisely controlled through changing the degradation characteristics of HA and its derivatives.

Chondrocytes [Grigolo et al., 2001], mesenchymal stem cells (MSC) [Bernard et al., 2000 and Solchaga et al, 2000], keratinocytes [Hollander et al., 2000] and endothelial cells [Brun et al., 2000] have been successfully cultured in HA-based scaffolds for cartilage, bone, skin and vessel repair. The use of three-dimensional HA scaffolds favored the maintenance of the cells' original phenotype. The preliminary clinical results demonstrated that most patients with full-thickness knee cartilage defects were relieved from symptoms and had mobility improvements after treatment with Hyalograft® C (Fidia Advanced Biopolymers, Italy) [Pavesio et al., 2003]. Hyalograft® C is a tissue-engineered graft consisting of autologous chondrocytes grown on a three-dimensional HYAFF®11 scaffold in a non-woven configuration, while HYAFF®11 is a HA ester with carboxyl group esterified by benzyl alcohol. Autologous fibroblasts and keratinocytes also cultured on HYAFF®11 have been applied to treat diabetic foot ulcers with high percentage of healing and low incidence of complications [Caravaggi et al., 2000].

1.2.6.8 Wound Repair

Hyaluronan (HA) is distributed throughout the dermis extracellular matrix as two pools, a large pool of free (>75%) HA and a small pool of bound HA. The half-life of bound HA normally is 2-4 days, while the free pool turns over with a half-life of 8-16 hr [Balazs et al., 2000].

Wound healing is a complex process [Garg et al., 2000; Weigel et al., 1989], in which HA has been demonstrated to function as a dominant and multiforous regulator [Ioconoet al., 2000; Balazs et al., 2000; Savani et al., 2000]. HA mediates the cell response in

wound repair through binding some cell receptors, such as CD44 and RHAMM. These HA-cell receptors can control cell attachment, motility, and cell cycle.

Some other specific physical properties of HA are also beneficial to wound healing. High molecular weight HA ($>10^3$-10^6 kDa) can trap large amounts of water, contributing to tissue viscosity and edema that follow injury. The ability of HA to coil and self-associate may also contribute to tissue elasticity.

It is well accepted that scarless healing of fetal wounds is associated with a prolonged increased HA content. Initially after injury, both adult and fetal wounds increase their HA content. The elevated HA level is maintained throughout the fetal repair, but only present for several days in adult wounds [Navsaria, 2000]. Therefore, it is necessary to apply exogenous HA onto the adult wound beds to keep high HA levels and mimic scarless fetal wound healing.

Both HA and its derivatives have been used for wound therapy, including: (1) pure HA water solution [Abatangelo et al., 1983; Breuing et al., 1991], or sponges [King, et al., 1991] and artificial skin [Murashita et al., 1996] soaked with the solution; (2) crosslinked HA (Hylan) in fluid, solid, gel, slurry, absorbent powder forms, or in combination with other polymers [Balazs et al., 1995]; (3) HA esters as sheets, nonwoven fleeces, ropes or meshs [Zacchi et al., 1998].

Naturally occurring HA rapidly degrades, limiting its application in wound healing. Hylan and HA esters have long residence times, and their degradation rate can be tailored by changing crosslinking degree or esterification percentage. HYAFF is a series of HA esters developed by Fidia Advanced Biopolymers (Italy), which has been used to produce a wide range of wound dressings, such as Hyalofill series [Brun et al., 2000; Harding,

2000]. Hylalofill is a 75% esterified derivative of HA. It forms a gel on contact with a moist environment. The molecule degrades completely within 48-72 hr, creating an HA rich wound environment. Wounds pre-treated with Hyalofill before applying keratinocyte autograft show a well-organized neodermis structure very similar to that found in normal skin. [Navsaria, 2000]

1.2.6.9 Biocompatible and Lubricious Coatings

A biocompatible and lubricating surface is very important for the materials used in biomedical devices. For example, catheters and endoscopes must have a slippery surface for easy insertion and removal, and for protecting the mucous membrane from mechanical injury [Ikada et al., 1993]. Also the surface must be biocompatible to avoid any foreign-body reaction. However, many widely used polymeric biomaterials, such as polyurethane, acrylic resin, vinyl resin, polyolefin, nylon and rubber [Fan, 1990], do not satisfactorily meet the above requirements. As a natural lubricant present in all tissues of animals, hyaluronan can impart both biocompatibility and lubrication to the surface of these materials.

Balazs et al. [1985C] developed azirdine-crosslinked HA to coat onto or disperse in various prosthetic devices, such as artificial valves, intraocular lenses, vascular grafts, pacemakers and so on, for improving device biocompatibility. HA coatings can also be immobilized onto optical devices, such as contact lenses (often made from polycarbonate), aircraft enclosures (often made from polymethyl methacrylate) and windshields (made from glass), through grafting [Beavers et al., 1987 & 1992] or crosslinking [Halpern et al., 1989 & 1990] to avoid optical distortion and get acute vision

when wetted by water. DeFife et al. [1999] utilized photochemical immobilization technology to covalently couple HA onto the surface of silicon rubber indwelling catheter to prevent occlusion. The results showed that HA coating effectively inhibited cell attachment and fibrosis/fibrin deposition, which is part of the host response to an implanted device and a reason for catheter occlusion. There are many other papers about HA coatings in the literature.

1.2.7 Chemical Modifications of Hyaluronan

Hyaluronan has many unique advantages as a starting point for biomedical products, but its high water solubility and quick turnover in the body limit the application of native hyaluronan. Improving rheological properties and functionalization of HA for attaching various pharmacophores have driven the extensive efforts to derivatize hyaluronan. Two main strategies have been employed to chemically modify the physical properties and impart novel functionalities to hyaluronan: modification of pendant groups and cross-linking.

1.2.7.1 Modification of Pendant Groups

Four groups on hyaluronan are available for chemical modification: carboxyl, hydroxyl, acetamido group and the reducing end-group. Although the derivatives via accetamido group and the end-group have been synthesized, most efforts are directed at modification of carboxyl and hydroxyl groups.

(1) Modification of Carboxyl Groups

HA-aliphatic quaternary ammonium salt complexes: The dissociated anionic carboxylate group on hyaluronan can be electrostatically combined with aliphatic quaternary ammonium cations forming a salt for separation from other polysaccharides or as an intermediate for further modification.

Scott [1955 & 1960] found that long paraffin-chain quaternary ammonium compounds, including cetyltrimethylammonium bromide (CTAB) and cetylpyridinium chloride (CPC), could be used to precipitate polyanions of hyaluronan and various sulfated polysaccharides from aqueous solution as polysaccharide-ammonium salt complexes, soluble in salt solutions of varying concentrations. For example, HA-CP complex is soluble at sodium concentrations above 0.2 M, while complexes with sulfated polysaccharides (such as keratosulfate, chondroitin sulfate, heparin and so on) usually require higher salt concentrations for solubility. This fact can be used to separate hyaluronan from other charged polysaccharides [Balazs, 1970]. Also, these complexes were soluble in some highly polar organic solvents. For example, HA-CP could dissolve in formamide, methyl formamide and pyridine [Scott, 1960].

Della Valle et al. of Fidia Advanced Biopolymer prepared a tetrabutylammonium salt ($^{+}N(Bu)_4$) of HA as a starting material for esterification. Sodium hyaluronate solution was passed through a thermostatic column containing sulphonic resin in tetrabutylammonium form (Dowex 50×8) at 4°C. HA- $N(Bu)_4$ complex was obtained by freeze drying the eluate [Della Valle et al., 1989], which was soluble in dimethylsulfoxide (DMSO) and dimethylformamide (DMF).

Yui et al. [2002] heated a mixture of sodium hyaluronate and distearyldimethyl-ammonium chloride (DSDMAC) to get an HA-DSDMA complex precipitate, which could be used as the starting material for esterification of the hydroxyl group on HA.

Esterification: The first HA ester was synthesized by Jeanloz and Forchielli [Jeanloz et al., 1950; Jäger et al., 1979] to determine the hyaluronan structure. This methyl ester was obtained by treatment of free hyaluronic acid with diazomethane in ether solution, and it was shown that all the carboxyl groups had been esterified.

Della Valle et al. [1989] treated HA- $N(Bu)_4$ with alkyl halides in DMSO solution to produce carboxylic esters of hyaluronan, commercially known as HYAFF® (Figure 1.4a). A variety of alcohols (aliphatic, araliphatic, cycloaliphatic and so on) can be used for the esterification, but only the ethyl and benzyl esters, respectively termed HYAFF®7 and HYAFF®11, have been well characterized. Using precise stoichiometric amounts of alkyl halide, HA esters with controlled substitution degree were obtained, such as HYAFF® 11 p75 with only 75% of carboxyl groups esterified. HYAFF® underwent hydrolytic degradation of the ester bonds in an aqueous environment even without enzymes present [Campoccia et al., 1998]. These esters can be processed into membranes, fibers, sponges, microspheres and other devices for a variety of biomedical applications.

Carbodiimide-activated reactions: A wide range of hydrazides can be used as nucleophilic agents to couple the carboxyl groups activated by carbodiimide on HA (Figure 1.4b) [Pouyani et al., 1994; Prestwich et al., 1998; Vercruysse, 1997]. The use of dihydrazide, such as adipic dihydrazide (ADH), provided multiple pendant hydrazide groups for further derivatization with drugs, and for cross-linking agents.

(2) Modification of Hydroxyl Groups

Esterification: Jeanloz and Forchielli [1950] also prepared an HA derivative with esterified hydroxyl groups to study the structure of HA. They acetylated sodium hyaluronate with acetic anhydride in a mixture including formamide and anhydrous pyridine. The final product was a mixture of di- and triacetates, which did not dissolve in organic solvents.

In their US patent application, Yui et al. [2002] described how to treat an HA / quaternary ammonium salt (HA-DSDMA) complex with an acid halide carrying photoreactive groups, such as cinnamoyl chloride, in DMF solution in the presence of an acid binder, such as pyridine (Figure 1.5a). The product precipitated with methanol was dissolved in DMF, and was subjected to ultraviolet radiation to crosslink the HA. The modified HA is useful for pharmaceuticals, foodstuffs, cosmetics, etc.

Smeds and Grinstaff [2001] modified the $-CH_2OH$ groups of HA with methacrylate groups to create a photo-crosslinkable hydrogel. The methacrylated HA (HA-MA) was prepared by reacting HA solution with a 20-fold excess of methacrylic anhydride at pH 8.0. Upon exposure to an argon ion laser, the viscous HA-MA solution was crosslinked into a soft and flexible hydrogel, useful for wound sealing and tissue engineering.

Sulphation: Heparin is a natural polysaccharide with the ability to prevent blood coagulation, but heparin does not have a regularly repeating unit, meaning that heparins of different molecular weights may vary in structure [Barbucci et al., 1998]. Unlike heparin, HA consists of a regular sequence of disaccharide units, resulting in a better understanding of the structure-property relationships [Magnani et al., 1998]. A series of sulphated hyaluronic acid derivatives (HyalSx) have been developed to obtain a blood-

compatible (i.e., non-coagulating) material for medical device coatings. The reaction was carried out in DMF using the tributylammonium salt of HA obtained by ion exchange resin (Dowex). The sulphation occurs through a nucleophilic attack of the alcoholic oxygen on the sulfur atom of the SO_3-pyridine complex (Figure 1.5b) [Barbucci et al., 1996]. By controlling the HA/ SO_3-pyridine molar ratio, HA derivatives with different degrees of sulphation were obtained, HyalSx, where x = 1-4. Sulphated HA has been successfully immobilized onto a plasma–treated polyethylene surface using a diamine polyethyleneglycol (PEG) spacer molecule, in order to improve hemocompatibility [Favia et al., 1997 & 1998].

Cyanogen bromide activation: The hydroxyl groups of HA have been activated with cyanogen bromide (CNBr) to produce a highly reactive isourea intermediate (Figure 1.5c). The therapeutic agents containing amine were then attached to one of the hydroxyl groups via a urethane bond by reacting with the isourea [Glabe et al., 1983; Prestwich, 2003].

Oxidation: Oxidation of hydroxyl groups on HA can be accomplished via two different methods. One is periodate oxidation, in which reactive bisaldehyde was created from the vicinal secondary alcohol functions by oxidation with sodium periodate (Figure 1.5d). Peptide containing cell attachment sequences could be covalently coupled to periodate-activated HA by reduction using sodium cyanoborohydride ($NaCNBH_3$) [Glass et al., 1996]. This chemistry is a standard method for chemical activation of glycoproteins for affinity immobilization [Prestwich, 2003].

Another oxidation method was reported by Jiang and de Nooy et al. They regioselectively oxidized the primary alcoholic functions (C6) on HA under the

mediation of 2,2,6,6-tetramethylpiperidin-1-oxyl (TEMPO) and converted them into carboxyl groups (Figure 1.5e) to increase the charge density for more effectively attracting biologically active counter ions, such as Zn(II) [Jiang et al., 2000; de Nooy et al., 2000; Crescenzi et al., 2001].

(3) Modification of Acetamido Groups

Free amino groups could be obtained on HA after deacetylation of the acetamido groups by hydrazinolysis with hydrazine sulfate as a catalyst (Figure 1.6) [Dahl et al., 1988; Crescenzi, et al., 2002], but at the same time HA molecules were also severely degraded due to base-induced backbone cleavage.

(4) Reducing End Modification

Reductive amination of the reducing end of hyaluronan has been employed to prepare affinity chromatography media, radioactive probes and synthetic cell culture surfaces. Raja et al. synthesized an HA derivative with a free amino attachment at the molecular chain end. The synthesis included three steps: (i) reduction (i.e. ring opening) of the terminal reducing sugar with sodium borohydride ($NaBH_4$), (ii) controlled sodium periodate ($NaIO_4$) oxidation to generate an aldehyde group only at the reduced end, (iii) coupling this aldehyde to an α,ω–alkyldiamine (e.g. 1,6-hexanediamine) in the presence of sodium cyanoborohydride ($NaCNBH_3$) (Figure 1.7) [Raja et al., 1984]. The modified HA provides a branch point for the preparation of new materials.

1.2.7.2 Crosslinking

Several different methods have been used to crosslink hyaluronan. By controlling the extent of crosslinking, the type of covalent bond and the hyaluronan group involved, it is possible to create a wide range of physically diverse materials from highly viscoelastic solutions to insoluble gels or solids.

(1) Crosslinking through Hydroxyl Groups

Hylan is a series of hyaluronan derivatives with the hydroxyl groups crosslinked, while leaving the carboxyl and acetamido groups unreacted. Retention of carboxyl groups is very important because the polyanionic character of hyaluronan is critical to its physicochemical and biological properties [Balazs et al., 1995].

Hylan polymers currently used in medicine are Hylan A and Hylan B. Hylan A is a viscoelastic fluid, developed by Balazs et al. by cross-linking hyaluronan chains to specific protein molecules with formaldehyde during recovery of the polymer from animal tissues [Balazs et al., 1987A]. A protein bridge is created between hydroxyl groups of hyaluronan in the reaction [Band, 1998], but the polymer remains soluble in aqueous media due to the small amount of formaldehyde used. The precise nature of the chemical events is not fully understood yet.

Hylan B is synthesized by reacting hyaluronan with divinyl sulphone in aqueous alkaline solutions at room temperature [Balazs et al., 1986]. With this reagent bis-(ethyl) sulphone crosslinks are formed (Figure 1.8a), producing an infinite hyaluronan network that is no longer water soluble. The degree of cross-linking can be controlled to create a

wide range of materials that range from soft deformable gels to solid membranes and tubes, with prolonged or permanent residence times [Band, 1998; Balazs et al., 1995].

Polyfunctional epoxy compounds are also used to crosslink hyaluronan in alkali solution with a water-soluble organic solvent present, such as acetone and methanol, which may prevent the HA from decomposing [Sakurai et al., 1987]. Depending on the ratio of epoxy compound to HA, different crosslinked polymers can be obtained. The products with a small molar ratio (<10) are soluble, while those with a high ratio (> 10) are insoluble.

A similar crosslinked insoluble HA polymer was developed by Tomihata et al. [1997A] through the reaction of poly(ethylene glycol) diglycidyl ether (a diepoxy compound) with HA under acidic or neutral conditions (Figure 1.8b). The crosslinked HA film showed good degradation-resistance.

Phosphate-crosslinked HA is a type of ester obtained by esterifying HA with phosphoric acid derivatives, such as phosphoryl chloride ($POCl_3$), in an alkaline medium. This reaction occurs very quickly with gel formation within a few minutes, and the excess of crosslinking agent is easily hydrolyzed and removed [Malson, et al., 1998] (Figure 1.8c).

A high degree of HA crosslinking has been achieved by reacting glutaraldehyde (GA) with an HA film in an acetone-water mixture under hydrochloric acid [Tomihata et al., 1997B]. It was shown that intermolecular formation of hemiacetal bonds between GA and the hydroxyl groups of HA led to crosslinking (Figure 1.8d). The crosslinked product was stable in phosphate buffer solution.

Polyisocyanates were used to permanently crosslink HA in anhydrous organic solvents [Balazs et al., 1987B], such as acetone, or to immobilize HA coatings on polymeric surfaces [Beavers et al., 1987 & 1992; Halpern et al., 1989 & 1990]. Due to the stability of the urethane linkage (Figure 1.8e), the crosslinked products are durable and resistant to decomposition in aqueous solutions [Lowry et al., 1994].

(2) Crosslinking through Carboxyl Groups

In the above crosslinking reactions, HA plays the role of a polymeric poly-hydroxyl component. The other category of crosslinked HA derivatives can be obtained through reactions in which HA plays the role of a poly-carboxylic acid.

Ionic crosslinking reactions are possible through the reaction of HA carboxyl groups and polyvalent cations. $BaCl_2$, $CaCl_2$ and $FeCl_3$ were used by Halpern et al. [1989] to treat HA coatings, producing stable products. Intergel®, an anti-adhesion product of Lifecore, is a hydrogel of HA formed by chelation with ferric hydroxide [Larsen, 1998].

The polymeric network of HA can also be synthesized via three- or four-component condensation known, respectively, as the Passerini reaction and the Ugi reaction [Crescenzi et al., 1998 & 2003]. In the Passerini reaction, a given amount of water-soluble dialdehyde (e.g. glutaraldehyde) and a highly reactive isocyanide (e.g. cyclohexylisocyanide) were added to HA solution with pH 3.5-4.0, which is stirred at room temperature until a gel forms (Figure 1.8f). In Ugi four-component condensation, the mixture contains HA, formaldehyde, cyclohexylisocyanide and lysine ethyl ester (Figure 1.8g). The degree of crosslinking is controlled by the amount of dialdehyde in the

Passerini reaction and diamine in the Ugi reaction. Hydrogels obtained from both reactions are transparent and mechanically stable.

(3) Crosslinking through both Hydroxyl and Carboxyl Groups

ACP™ is an auto-crosslinked HA product developed by Fidia Advanced Biopolymer used for adhesion prevention or tissue engineering scaffolds [Solchaga et al., 2000]. ACP™ is generated by condensation between the hydroxyl and carboxyl groups of hyaluronan [Mensitieri et al., 1996].

A low-water content hyaluronan hydrogel film was made by crosslinking an HA film in an aqueous mixture containing an organic solvent (ethanol or acetone) and a water-soluble carbodiimide (WSC). WSC does not chemically bind to HA molecules, but it mediates the reaction. Ester bonds formed between hydroxyl and carboxyl groups on different HA molecules result in crosslinking (Figure 1.8h) [Tomihata et al., 1997C].

The above review of the chemical modifications of HA supports the concept that esterification of either carboxyl or hydroxyl groups of HA can improve the hydrophobicity of HA and its solubility in highly polar organic solvents, such as DMSO and DMF.

1.3 Dissertation Objectives and Overview

The literature review indicates that current joint replacements do not enjoy the low friction and wear of natural joints, due to the extreme hydrophobicity of UHMWPE and its surface chemistry that is very different from that of articular cartilage. UHMWPE materials with improved bulk properties or modified surface microstructures cannot take

advantage of the natural joint lubrication mechanisms either, as they maintain hydrophobic surface chemistry similar to conventional UHMWPE. Hydrophilicity obtained via plasma treatment is successful but short-lived. Although the application of soft cushion bearings has achieved desirable lubrication, the degradation and debonding problems block its commercial success. As shown in Section 1.2.5, HA is a natural lubricant, and has been used for hydrophilic and lubricious coatings of a variety of medical devices, but it has not been used in total joint replacements yet due to the difficulty of fixing it to the articular surface of UHMWPE components in a manner that would survive under severe shear stresses.

The **overall goal** of this work is to create a hydrophilic, lubricious, more wear-resistant UHMWPE bearing through the surface application of hyaluronan (HA). Under this research goal, two specific aims were developed. In **specific aim I**, two different methods were used to introduce HA into the surface of UHMWPE to improve its tribological properties. In the solvent infiltration method (main method), hyaluronan was silylated first, and then introduced into UHMWPE porous preforms through solution, producing a micro-composite. In the non-solvent melt blending method (alternative method), a series of hot-processable hyaluronan esters were developed, which can be blended with UHMWPE powder, and then hot molded into the designed shape. In **specific aim II**, surface characterization and property evaluation were performed on the new materials.

Chapter 2 covers silylation of hyaluronan (the main method of specific aim I). In the solvent infiltration method, a novel micro-composite surface between hyaluronan and UHMWPE was created. Native hyaluronan cannot be directly introduced into UHMWPE

due to its extreme hydrophilicity and insolubility in organic solvents, so HA first needs to be modified to increase its hydrophobicity and compatibility with UHMWPE. Beauregard [1999] demonstrated that xylenes were the best solvents of UHMWPE. A modified HA should be able to dissolve in xylenes so that HA can be easily introduced into UHMWPE using xylenes. The modification reactions reviewed in Section 1.2.6 cannot meet these requirements, so a new hyaluronan derivative soluble in xylenes was created through silylation reaction. The silylated HA should easily revert to its original state, restoring the lubricious and other excellent properties of native HA.

Chapter 3 covers the fabrication of the micro-composite between UHMWPE and hyaluronan using the solvent infiltration method (the main method of specific aim I). UHMWPE preforms with a porous surface layer were used. It is much easier for the silylated HA molecules in xylenes to diffuse into the connected micro-pores of UHMWPE surface layer than into the solid bulk material. After diffusing in the HA, the porous preform is molded to full density. Due to entangling and crosslinking within UHMWPE, the HA surface layer should be stable, and able to withstand the severe stress conditions acting on the artificial joint surface. Various characterization methods (specific aim II) were used to verify the presence of HA layer on the UHMWPE surface, and examine the hydrophilicity of the micro-composites fabricated with different processes.

Chapter 4 covers the property evaluation of the new material (specific aim II). How does the micro-composite layer affect the mechanical and tribological properties of UHMWPE? Is the created HA layer stable in the body environment? These questions will be answered in Chapter 4.

Chapter 5 covers esterification of HA (alternative method of specific aim I). In the non-solvent melt blending method, HA needs to be hot molded with UHMWPE powder. However, HA degrades before it melts, and none of the HA derivatives reviewed in Section 1.2.6 can be melt processed. Therefore, a novel melt-processable HA derivative needs to be synthesized through appropriate reactions. Esterification of silylated HA was employed to confer thermo-plasticity on HA. The research on the non-solvent, melt-blending system is relatively preliminary compared with the solvent infiltration system. Yet, it does lay a foundation for future work.

1.4 Tables

Table 1.1 The Properties of Typical Materials Used for Artificial Joint Cushion

Material	Tensile Strength (MPa)	Tensile Modulus (MPa)	Elongation to break (%)	Equilibrium Water Content (%)
Natural cartilage	10-30	10-100	80	75
Silicone rubber	-	6	-	*
Polyurethane	20	49	423	*
PVA	-	0.5	-	79
Poly HEMA	0.5	0.5	180	40
NVP/PhEMA copolymer	4.0	21.3	109	54.4
NVP-MMA-CAB SIPN	10	90	120	45

- not available; * not applicable.

Table 1.2 Rheological Properties of Viscosupplementation Products [Adams, 1998]

Trade Name (Manufacturer)	Composition	MW ($\times 10^6$)	Elasticity (%, at 3 Hz)	Complex Viscosity (Pa.s at 0.002Hz)	Concentration (mg/ml)
Hyalgan®(Fidia)	NIF-NaHA	0.5-0.65	26	<0.1	10
Artz®(Seikagaku)	NIF-NaHA	0.75	33	0.3	10
Orthovisc®(Anika)	NIF-NaHA	1.5	66	42	15
Synvisc®(Biomatrix)	Hylans	6	88	213	8

Table 1.3 Hyaluronan-Based Anti-Adhesion Products

[Larsen, 1998; Biomatrix, 2002B; Wiseman, 2002]

Product	Company	Description	Applications	Regulatory Status
Seprafilm®	Genzyme	Bioresorbable HA-CMC film	Abdominal, pelvic and cardiac surgery	Approved by FDA Marketed worldwide
HylaSine®	Biomatrix	Hylan B gel	Nasal-sinus surgery	Marketed in U.S.
Hylan B	Biomatrix	Crosslinked hylan Membrane	Abdominal and pelvic surgery	Pre-clinical studies, Pilot U.S. clinical trials
Intergel®	Lifecore Biomedical	Ferric HA	Peritoneal cavity surgery	Marketed in Europe
Incert®	Anika Therapeutics	Hylan	General surgery	Awaiting CE* mark approval
Repel®	Life Medical Sciences	Bioresorbable HA-based film	Gynecological and general surgery	Pre-clinical studies

CE*: European Community

Table 1.4 HA-Based Ophthalmic Viscosurgical Devices

[Biomatrix, 2002C; Arshinoff, 2002]

Product	Distributor and manufacturer	Composition	Molecular Weight ($\times 10^6$)	Zero Shear Viscosity (Pa.s)
Healon®	Pharmacia	1.0%NaHA	4.0	230
Healon®5		2.3% NaHA	4.0	7000
Healon®GV		1.4% NaHA	5.0	2000
Amvisc®	Bausch & Lomb and Anika	1.2% NaHA	1.0	60
Amvisc®Plus		1.6% NaHA	1.0	100
Viscoat®	Alcon and Genzyme	3.0% NaHA, 4.0%CDS	0.5, 0.025	50
Provisc®		1.0% NaHA	2.0	280
Microvisc®	I-MED Parma and Bohus Bio. Tech.	1.4% NaHA	6.1	1000
Microvisc®		1.4% NaHA	7.9	4800

NaHA: NIF-NaHA; CDS: Chondroitin sulfate.

Table 1.5 HA-Based Gels for Viscoaugmentation

[Hallén et al., 2000; Biomatrix, 2002D]

Product	Manufacturer	Composition	Applications	Regulatory Status
Hylaform®	Biomatrix	Hylan B	Dermal augmentation	Marketed in Europe
Restylane®& Perlane®	Q-Med AB	Hylan crosslinked by epoxy	Dermal augmentation	Marketed in Europe
Deflux®	Med AB	HA solution, dextran	Pediatric urology	Clinical trials
Hylan B	Biomatrix	Hylan B	Urology, laryngology	Pre-clinical Studies

* Q-Med AB: in Uppsala, Sweden.

1.5 Figures

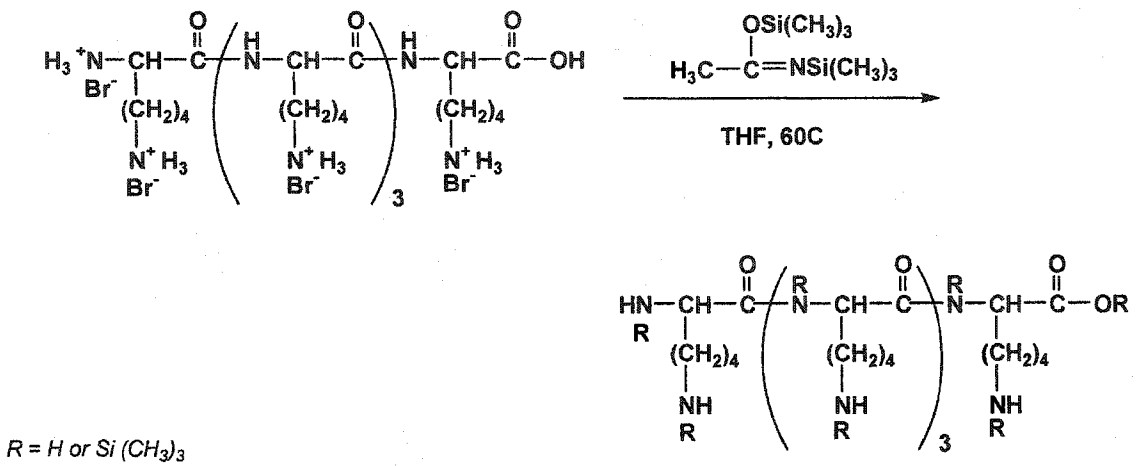

Figure 1.1 Silylation of poly-L-lysine

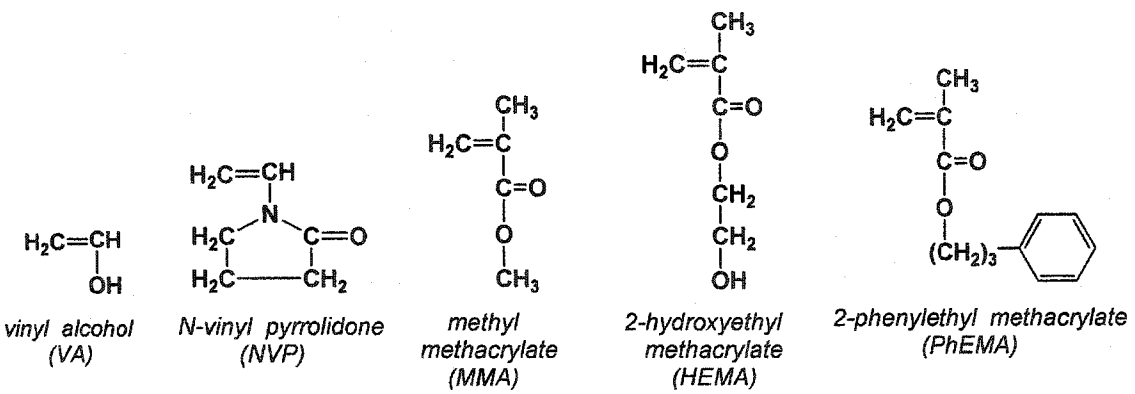

Figure 1.2 Structures of vinyl monomers used for hydrogel synthesis

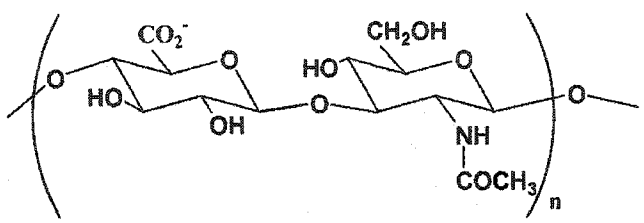

Figure 1.3 Structure of Hyaluronan

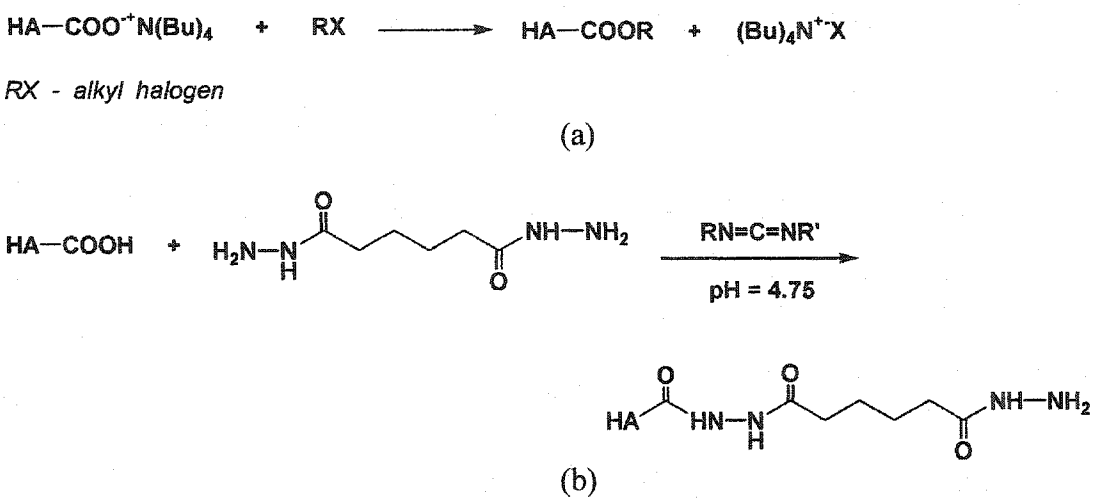

Figure 1.4 Chemical modifications of carboxyl groups of HA: (a) esterification with alkyl halogens, (b) bishydrazide modification.

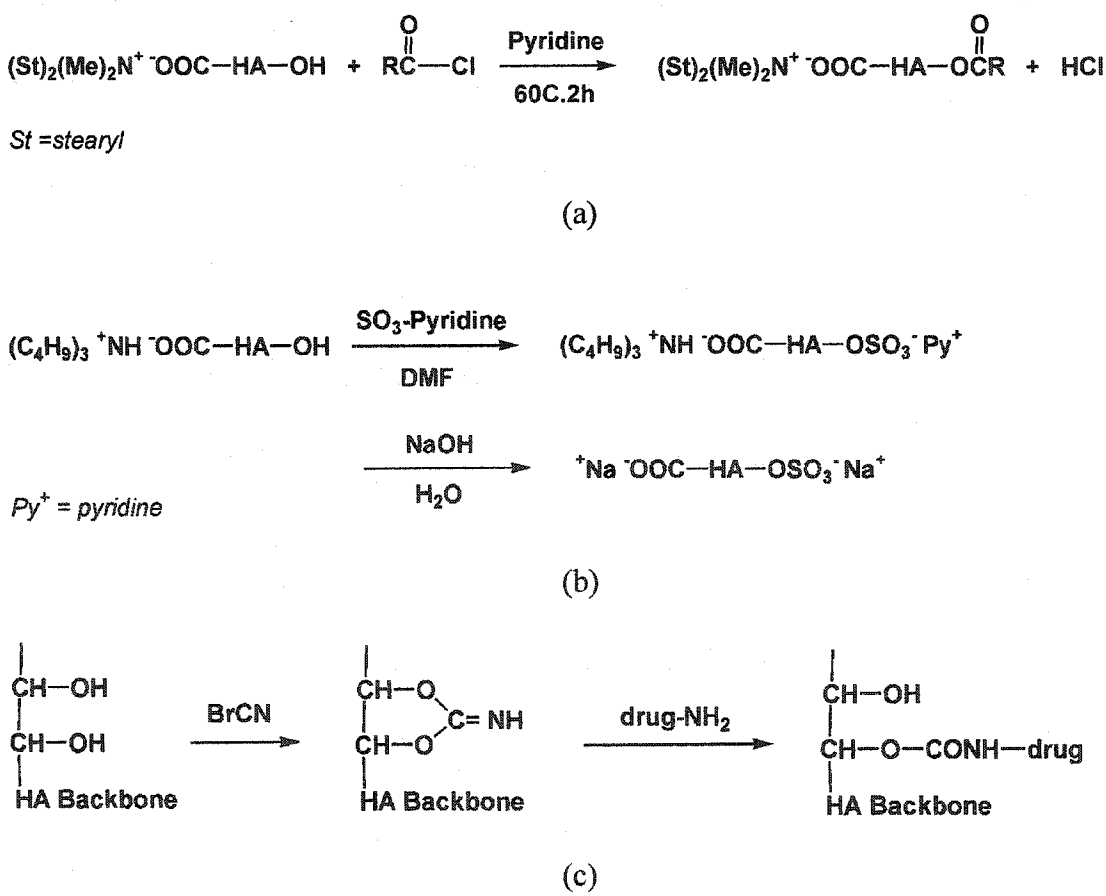

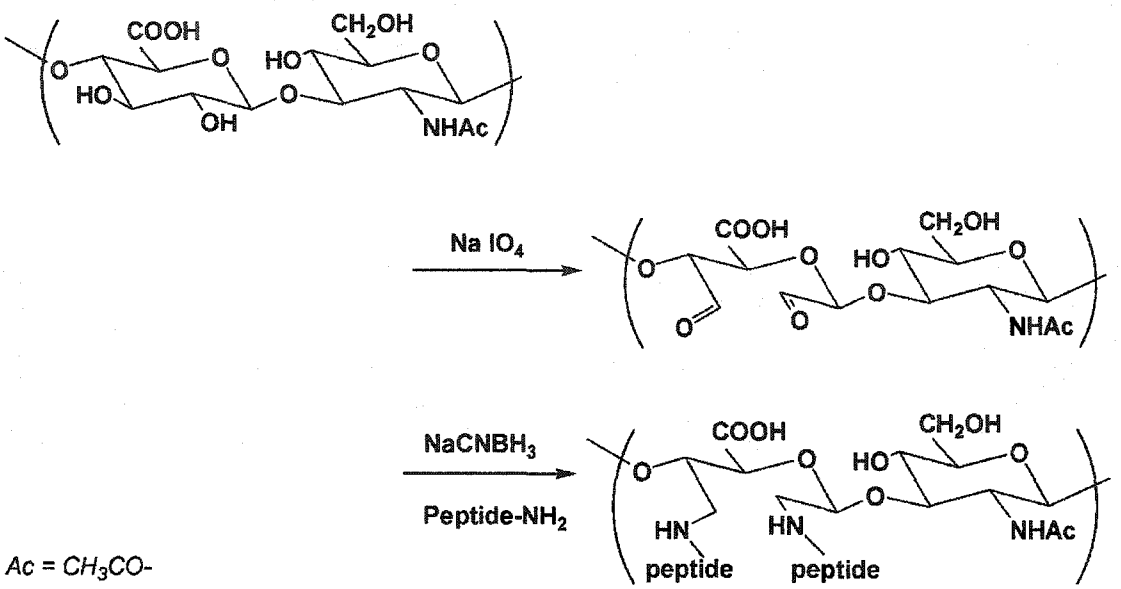

(d)

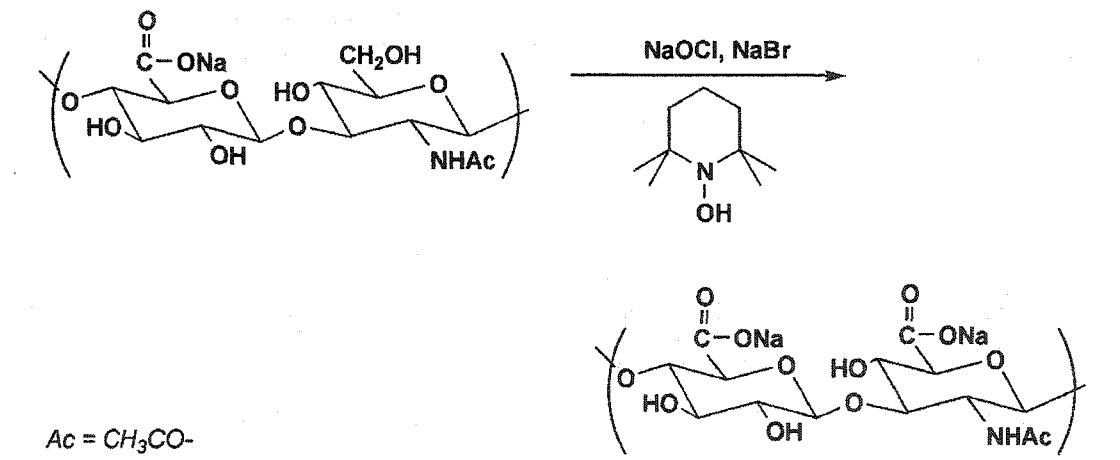

(e)

Figure 1.5 Chemical Modifications of hydroxyl groups of HA: (a) esterification, (b) sulphation, (c) cyanogen bromide activation, (d) periodate oxidation, (e) TEMPO-mediated oxidation.

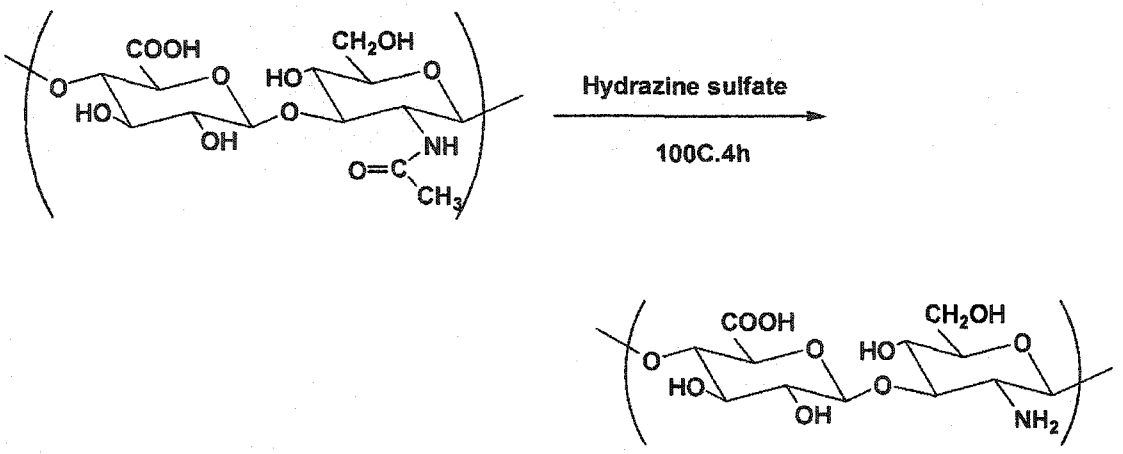

Figure 1.6 Deacetylation of acetamido groups of HA

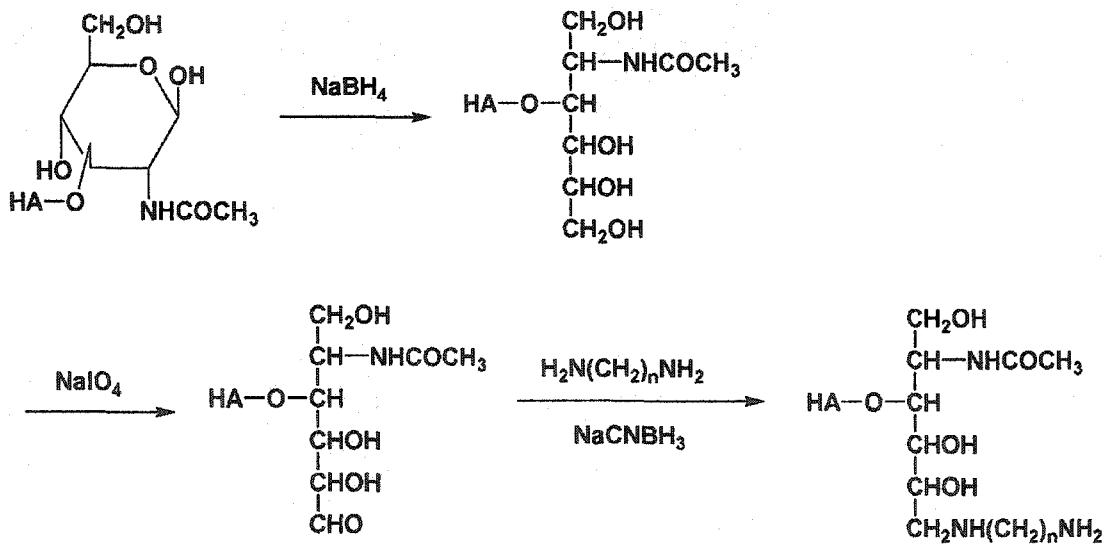

Figure 1.7 Reducing end modification of HA

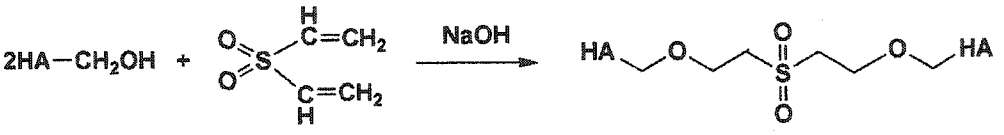

(a)

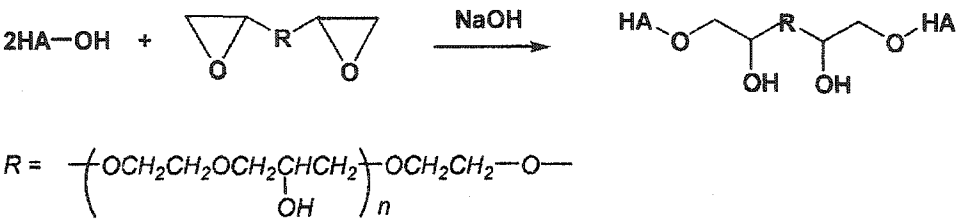

(b)

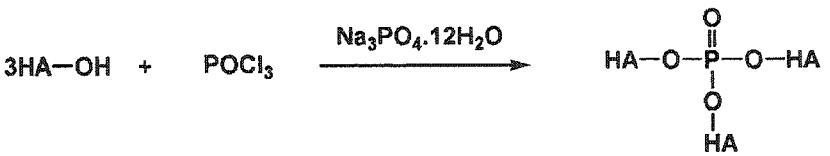

(c)

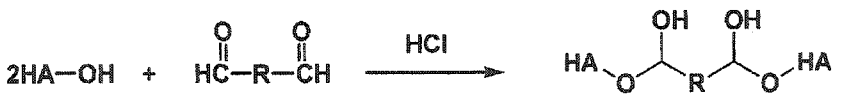

(d)

(e)

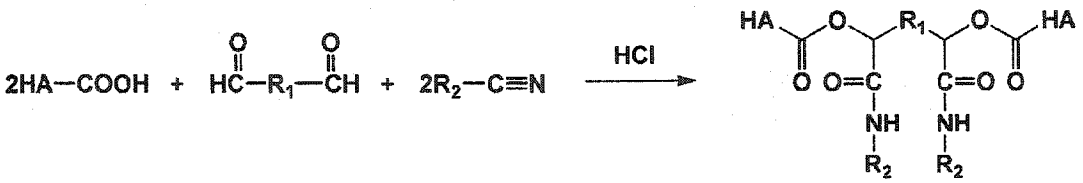

(f)

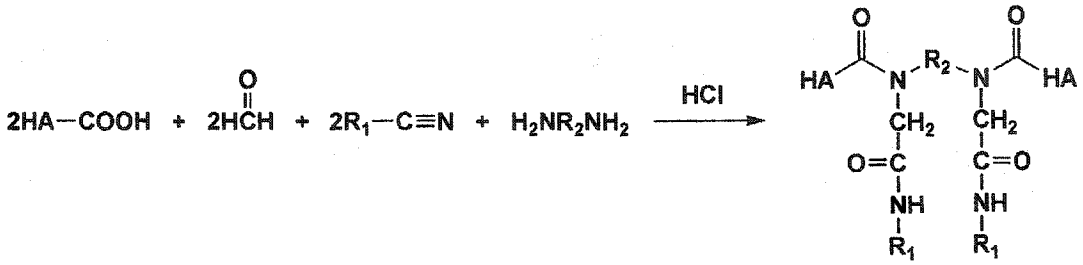

(g)

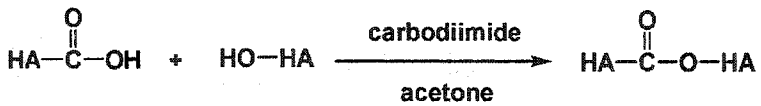

(h)

Figure 1.8 Crosslinking reactions of HA with crosslinking agents: (a) divinyl sulphone, (b) poly(ethylene glycol) diglycidyl ether, (c) phosphoryl chloride, (d) glutaraldehyde, (e) poly-isocyanate, (f) dialdehyde via Passerini reaction, (g) diamine via Ugi reaction, (h) carbodiimide.

1.6 References

Abatangelo G, Martelli M, and Vecchia P (1983). Healing of hyaluronic acid-enriched wounds: histological observations. *Journal of Surgical Research*, 35: 410-416.

Adams ME (1998). Viscosupplementation as articular therapy. In *the Chemistry, Biology and Medical Applications of Hyaluronan and Its Derivatives* (edited by Laurent TC). Portland Press Ltd: London, pp.243-253.

Affatato S, Testoni M, Cacciari GL and Toni A (1999). Mixed oxides prosthetic ceramic ball heads. Part 1: effect of ZrO_2 fraction on the wear of ceramic on polyethylene joints. *Biomaterials*, 20: 971-975.

Arshinoff SA (2002). The use of ophthalmic viscosurgery devices in cataract surgery. In *Hyaluronan 2000* (edited by Kennedy JF et al.). Woodhead Publishing Limited: Cambridge, England, 2: 120-128.

Atkinson JR, Dowling JM, and Cicek RZ (1980). Materials for internal prostheses: the present position and possible future developments. *Biomaterials*, 1: 89-96.

Auger DD, Dowson D, and Fisher J (1993). Friction of cylindrical cushion form bearings for artificial joints. In *Thin Films Tribology* (edited by Dowson D). Elsevier Science Publishers B.V.: Amsterdam, pp.683-692.

Aza AH De, Chevalier J, and Fantozz G et al. (2002). Crack growth resistance of alumina, zirconia and zirconia toughened alumina ceramics for joint prostheses. *Biomaterials*, 23:937-945.

Balazs EA (1960). Physiology of the vitreous body. In *Importance of the Vitreous Body in Retina Surgery with Special Emphasis on Reoperations* (edited by Schepens CL). Mosby: St. Louis, 27-48.

Balazs EA and Gibbs DA (1970). The rheological properties and biological function of hyaluronic acid. In *Chemistry and Molecular Biology of the Intercellular Matrix* (edited by Balazs EA). Academic Press: London & New York, 3: 1241-1253.

Balazs EA, Freeman MI, and Klöti R et al. (1972). Hyaluronic acid and replacement of vitreous and aqueous humor. In *Modern Problems in Ophthalmology* (edited by Streiff EB). S. Karger: Basel & New York, 10: 3-21.

Balazs EA (1979). Ultrapure hyaluronic acid and the use thereof. US Patent 4141973.

Balazs EA (1982). The physical properties of synovial fluid and the special role of hyaluronic acid. In *Disorders of the Knee* (edited by Helfet AJ, 2nd edition). JB Lippincott: Philadelphia, pp.61-74.

Balazs EA (1983). Viscosurgery in the eye. *Ocular Inflammation Therapy*, 1:91-92.

Balazs EA and Band P (1984A). Hyaluronic acid: its structure and use. *Cosmetics and Toiletries*, 99:65-72.

Balazs EA and Leshchiner A (1984B). Crosslinked gels of hyaluronic acid and products, US Patent 4582865.

Balazs EA and Denlinger JL (1985A). Sodium hyaluronate and joint function. *Journal of Equine Veterinary Science*, 5:217-228.

Balazs EA, Leshchiner A, and Band P (1985B). Chemically modified hyaluronan acid and preparation and method of recovery thereof from animal tissues. US Patent 4713448.

Balazs EA and Leshchiner A (1985C). Hyaluronate modified polymeric articles (prosthetic devices). US Patent 4500676.

Balazs EA and Leshchiner A (1986). Cross-linked gels of hyaluronic acid and products containing such gels. US Patent 4582865.

Balazs EA, Leshchiner A, and Band P (1987A). Chemically modified hyaluronic acid preparation and method of recovery thereof from animal tissues. US patent 4713448.

Balazs EA and Leshchiner A (1987B). Water insoluble preparations of hyaluronic acid and processes therefore. UK Patent GB 2151244B.

Balazs EA and Leshchiner A (1989A). Hyaluronan, its crosslinked derivative-hylan, and their medical applications. In *Cellulosics Utilization* (edited by Inagaki H). Elsevier Applied Science: London, pp.233-239.

Balazs EA and Denlinger JL (1989B). Clinical uses of hyaluronan. In *the Biology of Hyaluronan, Ciba Foundation Symposium* (edited by Evered D et al.). John Wiley & Sons: Chichester, 143: 265-273.

Balazs EA, Leshchiner A, and Larsen NE (1992). Drug delivery systems based on hyaluronans derivatives thereof and their salts and methods of producing same. US Patent, 5128326.

Balazs EA and Leshchiner EA (1995). Hyaluronan biomaterials: medical applications. In *Encyclopedic Handbook of Biomaterials and Bioengineering*(edited by Wise DL). Marcel Dekker Press: New York, pp.2719-2741.

Balazs EA and Larsen NE (2000). Hyaluronan: aiming for perfect skin regeneration. In *Scarless Wound Healing* (edited by Garg HG et al.). Marcel Dekker, Inc.: New York, 143-160.

Band PA (1998). Hyaluronan derivatives: chemistry and clinical applications. In *the Chemistry, Biology and Medical Applications of Hyaluronan and its Derivatives* (edited by Laurent TC). Portland Press Ltd: London, pp.33-42.

Barbucci R, Magnani A, Lamponi S, and Casolaro M (1996). Different sulphation degree and biological performance of hyaluronic acid as heparin-like molecule. *Macromolecular Symposia*, 105:1-8.

Barbucci R, Lamponi S, Magnani A, and Renier D (1998). The influence of molecular weight on the biological activity of heparin like sulphated hyaluronic acids. *Biomaterials*, 19: 801-806.

Beauregard GP (1999). Synthesis and characterization of a biomimetic UHMWPE-based interpenetrating polymer network for use as an orthopedic biomaterial. Ph.D dissertation. Colorado State University, Fort Collins, Colorado.

Beauregard GP, Hu Y, Grainger DW, and James SP (2001). Silylation of poly-L-lysine hydrobromide (PLL-HBr) to improve dissolution in apolar organic solvents. *Journal of Applied Polymer Science*, 79: 2264-2271.

Beavers EM (1987). Lens with hydrophilic coating. US Patent 4663233.

Beavers EM and Lowry KM (1992). Non-fogging transparent coatings. US Patent 5148311.

Bellare A, Livinston BJ, and Cohen RE et al. (1996). Characterization of wear surface and bulk morphology of retrieved Hylamer acetabular cups. In *Transactions of the 5th World Biomaterial Conference*, 2: 982.

Bernard GW, Pilloni A, and Kang Mo et al. (2000). Osteogenesis in vitro and in vivo with hyaluronan and bone morphogenic protein-2. In *New Frontiers in Medical Science: Redefining Hyaluronan* (edited by Abatangelo G et al.). Elsevier Science B.V.: Amsterdam, the Netherlands, pp. 215-231.

Bettelheim FA (1971). Structure and hydration of mucopolysaccharides. In *Biophysical Properties of the Skin* (edited by Elden HR). John Wiley and Sons: New York, 1:303.

Biomatrix, Inc. (2002A). Viscosupplementation: a historical perspective. In *Hyaluronan 2000* (edited by Kennedy JF et al.). Woodhead Publishing Limited: Cambridge, England, 2: 385-389.

Biomatrix, Inc. (2002B). Viscoseparation: a historical perspective. In *Hyaluronan 2000* (edited by Kennedy JF et al.).Woodhead Publishing Limited: Cambridge, England, 2:3-5.

Biomatrix, Inc. (2002C). Viscourgery: a historical perspective. In *Hyaluronan 2000* (edited by Kennedy JF et al.). Woodhead Publishing Limited: Cambridge, England, 2: 461-465.

Biomatrix, Inc. (2002D). Viscoaugmentation: a historical perspective. In *Hyaluronan 2000* (edited by Kennedy JF et al.). Woodhead Publishing Limited: Cambridge, England, 2: 41-44.

Black J (1998). Handbook of Biomaterial Properties. Chapman and Hall: London.

Blamey J, Rajan S, Unsworth A, and Dawber R (1991). Soft layered prostheses for arthritic hip joints: a study of materials degradation. *Journal of Biomedical Engineering*, 13: 180-184.

Bragdon CR, O'Connor DO, and Weinberg EA et al. (1999). The effect of cycle rate on the wear of conventional and highly crosslinked UHMWPE acetabular components using the Boston AMTI hip simulator. In *Transactions of 25th Annual Meeting of the Society for Biomaterials*, pp. 211.

Breuing K, Eriksson E, Liu P, and Miller D (1991). Healing of partial thickness porcine wounds in a liquid environment. *Journal of Surgical Research*, 52: 50-58.

Brun P, Cortivo R, Radice M, and Abatangelo G (2000). Hyaluronan-based biomaterials in tissue engineering. In *New Frontiers in Medical Science: Redefining Hyaluronan* (edited by Abatangelo G et al.). Elsevier Science B.V.:Amsterdam, the Netherlands, pp.269-278.

Burns JW and Barry KJ (2000). Hyaluronan-based membrane for the prevention of postsurgical adhesions. In *Scarless Wound Healing* (edited by Garg HG et al.). Marcel Dekker, Inc.: New York, 307-325.

Busanelli L, Squarzoni S, and Brizio L et al. (1996). Wear in carbon fiber-reinforced polyethylene (poly-two) knee prostheses. *La Chirurgia Degli Organi Di Movimento*, 81: 263-67.

Campoccia D, Doherty P, and Radice M et al. (1998). Semisynthetic resorbable materials from hyaluronan esterification. *Bionmaterials*, 19:2101-2127.

Caplan AI (2003). Design parameters for functional tissue engineering. In *Functional Tissue Engineering* (edited by Guilak F et al.). Springer-Verlag: New York, pp.129-138.

Caravaggi C, Faglia E, and Paola LD et al (2000). Tissue engineering in the treatment of diabetic foot ulcers. In New Frontiers in Medical Science: Redefining Hyaluronan (edited by Abatangelo G et al.). Elsevier Science B.V.: Amsterdam, the Netherlands, 313-320.

Caravia L, Dowson D, and Fisher J (1993). A comparison of friction in hydrogel and polyurethane materials for cushion-form joints. *Journal of Materials Science: Materials in Medcine*, 4: 515-520.

Champion AR, Li S, and Saum K et al. (1994). The effect of crystallinity on the physical properties of UHMWPE. In *Transactions of the 40th Orthopedic Research Society*, 19: 585.

Charnley J (1968). Total prosthetic replacement of the hip. *Triangle*, 8: 211-216.

Chen J, Zhu F, and Pan H et al. (2000). Surface modification of ion implanted UHMWPE. *Nuclear Instruments and Methods in Physics Research*, B169: 26-30.

Connelly GM, Rimnac CM, and Wright TM et al. (1984). Fatigue crack propagation behavior of UHMWPE. *Journal of Orthopedic Research,* 2: 119-25.

Corkhill PH, Trevett AS, and Tighe BJ (1990). The potential of hydrogels as synthetic articular cartilage. In *Proceedings of the Institution of Mechanical Engineers (Part H)*, 204: 147-155.

Crescenzi V, Tomasi M, and Francescangeli A (1998). New routes to hyaluronan-based network and supramolecular assembles. In *the Chemistry, Biology and Medical Applications of Hyaluronan and its Derivatives* (edited by Laurent TC). Portland Press Ltd: London, pp.173-180.

Crescenzi V, Francescangeli A, Renier D, and Belline D (2001). New hyaluronate chemical derivatives, regioselectively C(6) oxidized products. *Macromolecules*, 34: 6367-6372.

Crescenzi V, Francescangeli A, Renier D, and Belline D (2002). New crosslinked and sulfated derivatives of partially deacetylated hyaluronan: synthesis and preliminary characterization. *Biopolymers*, 63: 1-9.

Crescenzi V, Francescangeli A, and Capitani D et al. (2003). Hyaluronan networking via Ugi's Condensation using lysine as crosslinker diamine. *Carbohydrate Polymers*, 53: 311-316.

Dahl LB, Laurent TC, and Smedsrød B (1988). Preparation of biologically intact radioiodinated hyaluronan of high specific radioactivity. *Analytical Biochemistry*, 175: 397-407.

Day AJ and Parkar AA (1998). The structure of the link module: a hyaluronan-binding domain. In *the Chemistry, Biology and Medical Applications of Hyaluronan and its Derivatives* (edited by Laurent TC). Portland Press Ltd: London, pp.141-147.

De Boer J, Van Den Berg HJ, and Pennings AJ (1984). Crosslinking of UHMWPE in the oriented state with dicumylperoxide. *Polymer*, 25: 513-519.

Defife KM, Shive MS, and Hagen KM et al. (1999). Effects of photochemically immobilized polymer coatings on protein adsorption, cell adhesion, and the foreign body reaction to silicon rubber. *Journal Of Biomedical Materials Research*, 44:298-307.

Della Valle F, Romeo A, and Lorenzi S (1988). Process for preparing salt of hyaluronic acid with a pharmaceutically active substance. US Patent 4736024.

Della Valle F and Romeo A (1989). Esters of hyaluronic acid. US Patent 4851521.

Deng M (1997). Properties of self-reinforced ultra high molecular weight polyethylene composites. *Biomaterials*, 18: 645-655.

Denlinger JL (1998). Hyaluronan and its derivatives as viscoelastics in medicine. In *the Chemistry, Biology and Medical Applications of Hyaluronan and its Derivatives* (edited by Laurent TC). Portland Press Ltd: London, pp.235-241.

de Nooy AEJ, Rori V, and Masci G et al. (2000). Synthesis and preliminary characterization of charged derivatives and hydrogels from scleroglucan. *Carbohydrate Research*, 324: 116-126.

Diamond MP and Moghissi KS (2000). Hyaluronan in the prevention of postsurgical adhesions. In *New Frontiers in Medical Science: Redefining Hyaluronan* (edited by Abatangelo G et al.). Elsevier Science B.V.: Amsterdam, the Netherlands, 333-344.

Dong H, Shi W and Li XY (2000). Plasma immersion ion implantation of UHMWPE. *Journal of Materials Science Letters*, 19: 1147-1149.

Dowson D (1966-67). Modes of lubrication in human joints. In *Proceedings of the Institution of Mechanical Engineers (Part 3J)*, 181: 45-55.

Dowson D (1995). A comparative study of the performance of metallic and ceramic femoral head components in total replacements hip joints. *Wear*, 190:171-183.

Eberhardt AW, Cole JA, and Lemons JE (2001). The effect of irradiation level and resin on fatigue crack resistance in UHMWPE. In *Transactions of 27th Annual Meeting of the Society for Biomaterials*, pp.480.

Eyerer P, Ellwanger R, and Federolf HA et al. (1990). Polyethylene. In *Concise Encyclopaedia of Medical and Dental Materials* (edited by Williams D and Cahn R). MIT Press: Cambridge.

Fan YL (1990). Hydrophilic lubricious coatings for medical applications. *Polymeric Materials (Part B): Science and Engineering*, 63: 709-716.

Fivia P, d'Agostino R, and Palumbo F (1997). Grafting of chemical groups onto polymers by means of RF plasma treatments: a technology for biomedical applications.

Journal de Physique IV France 7, Colloque C4, Supplément au Journal de Physique III d'octobre 1997, C4: 199-208.

Fivia P, Palumbo F, and d'Agostino R et al. (1998). Immobilization of heparin and highly-sulphated hyaluronic acid onto plasma-treated polyethylene. *Plasmas and Polymers*, 3:77-95.

Garg HG, Warren CD, and Siebert JW (2000). Chemistry of scarring. In *Scarless Wound Healing* (edited by Garg HG et al.). Marcel Dekker: New York, 1-21.

Glabe CG, Harty PK, and Rosen SD (1983). Preparation and properties of fluorescent polysaccharides. *Analytical Biochemistry*, 130: 287-294.

Glass JR, Dickerson KT, Stecker K, and Polarek JW (1996). Characterization of a hyaluronic acid-Arg-Gly-Asp peptide cell attachment matrix. *Biomaterials*, 17: 1101-1108.

Goldsmith AJ and Cliff SE (1998). Investigation into the biophasic properties of a hydrogel for use in a cushion form replacement joint. In *Transactions of the ASME*, 120:362-368.

Greer K and King R (2001). The mechanical and physical properties of four different crosslinked UHMWPE materials. In *Transactions of 27th Annual Meeting of the Society for Biomaterials*, pp.85.

Grigolo B, Roseti L, and Fiorini M et al. (2001). Transplantation of chondrocytes seeded on a hyaluronan derivative (Hyaff® –11) into cartilage defects in rabbits. *Biomaterials*, 22: 2417-2424.

Gsell R et al., Improved oxidation resistance of highly crosslinked UHMWPE for total knee arthroplasty. In *Transactions of 27th Annual Meeting of the Society for Biomaterials*, pp. 84.

Gul R (1997). *Improved UHMWPE for Use in Total Joint Replacement.* Ph.D Dissertation. Massachusetts Institute of Technology, Boston.

Gustafson S (1998). Hyaluronan in drug delivery. In *the Chemistry, Biology and Medical Applications of Hyaluronan and its Derivatives* (edited by Laurent TC). Portland Press Ltd: London, pp.291-303.

Harding K (2000). Clinical challenges and promises of HYAFF technology in wound healing. In *New Frontiers in Medical Science: Redefining Hyaluronan* (edited by Abatangelo G et al.). Elsevier Science B.V.: Amsterdam, the Nertherlands, pp.289-301.

Hallén L, Johansson C, Dahlqvist Å, and Laurent C (2000). The potential use of hyaluronan-based compounds in laryngeal augmentative surgery. In *New Frontiers in*

Medical Science: Redefining Hyaluronan (edited by Abatangelo G et al.). Elsevier Science B.V.: Amsterdam, the Nertherlands, pp.353-359.

Halpern G, Campbell C, Beavers EM, and Chen HY (1989). Method of hydrophilic coating of plastics. US Patent 4801475.

Halpern G, Campbell C, Beavers EM, and Chen HY (1990). Method of hydrophilic coating of plastics (contact Lens; coating of mucopolysaccharide film immobilized solution of aliphatic polyisocyanates). US Patent 4959074.

Heinegard D, Björnsson S, Mörgelin M, and Sommarin Y (1998). Hyaluronan-binding matrix proteins. In *the Chemistry, Biology and Medical Applications of Hyaluronan and its Derivatives* (edited by Laurent TC). Portland Press Ltd: London, pp.113-121.

Heisel C, Silva M and Schmalzried TP (2004). Bearing surface options for total hip replacement in young patients. *Instructional Course Lectures*, 53:49-65.

Hoekstra D (1999). Hyaluronan-modified surfaces for medical devices. *Medical Device & Diagnostic Industry*, 51-58.

Holland DA, Wild M, Konold P, and Windolf J (2000). Benzylester hyaluronic acid membranes: a delivery system for autologous keratinocyte cultures in the treatment of complicated chronic and acute wounds. In *New Frontiers in Medical Science: Redefining Hyaluronan* (edited by Abatangelo G et al.). Elsevier Science B.V.: Amsterdam, the Nertherlands, pp. 303-311.

Iocono JA and Krummel TM (2000). The role of hyaluronan in fetal repair: a review. In *New Frontiers in Medical Science: Redefining Hyaluronan* (edited by Abatangelo G et al.). Elsevier Science B.V.: Amsterdam, the Nertherlands, pp. 289-301.

Ikada Y and Uyama Y (1993). *Lubricating Polymer Surface*. Technomic Publishing Co., Inc.: Lancaster, Pennsylvania.

Jäger KE and Winkler UK (1979). Methyl ester of hyaluronate is unable to stimulate exolipase formation by serratia marcescens. *Journal of Bacreriology*, 139:1065-1067.

Jeanloz RW and Forchielli E (1950). Studies on hyaluronic acid and related substances, *The Journal of Biological Chemistry*, 18:495-511.

Jiang B, Drouet M, Milas M, and Rinaudo M (2000). Study on TEMO-mediated selective oxidation of hyaluronan and the effects of salt on the reaction kinetics. *Carbohydrate Research*, 327: 455-461.

Kawate K, Ohmura T, Hiyoshi N, and Nakajima H et al. (1999). Dynamic viscoelasticity of ultra-high-molecular-weight polyethylene after ethylene oxide gas or gamma-

irradiated sterilization. In *Joint Arthroplasty* (edited by Imura S, Wada M and Omaori H). Springer-Verlag: Tokyo, pp.87-96.

Kelly JM (2000). Ultra-high molecular weight polyethylene. In *Polymer Modification* (edited by Meister JJ). Marcel Dekker, Inc.: New York, pp.273-291.

King R, Kirkpatrick L, and Devanathan D et al. (1996). Long-term aging behavior of implant grades of polyethylene. In *Transactions of the 5th World Biomaterial Conference*, 2: 196.

King SR, Hickerson WL, Proctor KG, and Newsome AM (1991). Beneficial actions of exogenous hyaluronic acid on wound healing. *Surgery*, 109:76-84.

Klapperich CM, Komvopoulos K and Pruitt L (1999). Plasma surface modification of medical-grade UHMWPE for improved tribological properties. In *Materials Research Society Symposia Proceedings*, 550: 331-336.

Knapp JR, Kaplan EN, and Daniel JR (1977). Injectable collagen for soft tissue augmentation. *Plastic and Reconstructive Surgery*, 60:398-405.

Kurtz SM (1999). Advances in the processing, sterilization, and crosslinking of UHMWPE for total joint arthroplasty. *Biomaterials*, 20: 1659-1688.

Larsen NE and Balazs EA (1991). Drug delivery systems using hyaluronan and its derivatives. *Advanced Drug Delivery Reviews*, 7:279-293.

Larsen NE (1998). Management of adhesion formation and soft tissue augmentation with viscoelastics: hyaluronan derivatives. In *the Chemistry, Biology and Medical Applications of Hyaluronan and its Derivatives* (edited by Laurent TC). Portland Press Ltd: London, 267-281.

Laurent C (1998). The action of hyaluronan on repair processes in the middle ear. In *the Chemistry, Biology and Medical Applications of Hyaluronan and its Derivatives* (edited by Laurent TC). Portland Press Ltd: London, 283-289.

Laurent TC (1970). Structure of hyaluronic acid. In *Chemistry and Molecular Biology of the Intercellular Matrix* (edited by Balazs EA). Academic Press: London, 2: 703-728.

Laurent TC (1989). Introduction. In *the Biology of Hyaluronan, Ciba Foundation Symposium* (edited by Evered D et al.). John Wiley & Sons: Chichester, England, 143: 1-5.

Laurent TC (2003). The tree: hyaluronan research in the 20th century. In *Glycoforum-Science of Hyaluronan Today* (edited by Hascall VC). http://www.glycoforum.gr.jp/science/hyaluronan/hyaluronanE.html

Lee EH, Lewis MB, Blau PJ, and Mansur LK (1991). Improved surface properties of polymer materials by multiple ion beam treatment. *Journal of Materials Research*, 6: 610-628.

Lesley J (1988). Hyaluronan binding function of CD44. In *the Chemistry, Biology and Medical Applications of Hyaluronan and its Derivatives* (edited by Laurent TC). Portland Press Ltd: London, pp.123-133.

Lewis G (1997). Polyethylene wear in total hip and knee arthroplasties. *Jornal of Materials Research, 38:* 55-75.

Li S and Howard EG (1990). Characterization and description of enhanced UHMWPE for orthopedic bearing surfaces. In *Transactions of the Society of Biomaterials*, pp.190.

Li S and Howard EG (1991). Process for Manufacturing Ultra High Molecular Weight Shaped Articles, US Pat. 5037928.

Lowry KM and Beavers EM (1994). Resistance of hyaluronate coatings to hyaluronidase. *Journal of Biomedical Materials Research*, 28: 861-864.

Magnani A, Lamponi S, Rappuoli R, and Barbucci R (1998). Sulphated hyaluronic acids: a chemical and biological characterization. *Polymer International*, 46: 225-240.

Malson T and Lindqvist B (1998). Crosslinked hyaluronate gels, their use and method for producing them. US Patent 5783691.

Matton G, Anseeuw A, and DeKeyser F (1985). The history of injectable biomaterials and biology of collagen. *Aesthetic Plastic Surgery*, 9: 133-140.

McKellop HA, Campbell P, and Park SH (1995). The origin of submicron polyethylene wear debris in total hip arthroplasty. *Clinical Orthopedics*, 311: 3.

Mensitieri M, Ambrosio L, and Nicolais L et al. (1996). Viscoelastic properties modulation of a novel autocrosslinked hyaluronan acid polymer. *Journal of Materials Science: Materials in Medicine*, 7: 695-698.

Miyoshi T and Okamoto A (2002). Biocompatible gel of hyaluronan – medical applications. In Hyaluronan 2000 (edited by Kennedy JF et al.). Woodhead Publishing Limited: Cambridge, England, 2: 22-25.

Murashita T, Nakayoma T, Hirano T, and Ohashi S. Acceleration of granulation tissue ingrowth by hyaluronic acid in artificuial skin. *British Journal of Plastic Surgery*, 49: 58-63.

Muratoglu OK, Bragdon CR, and O'Connor DO et al. (1999). Unified wear model for highly crosslinked UHMWPE. *Biomaterials*, 20:1463-1470.

Narkis M, Raiter I Shkolnik S, and Siegmann A (1987). Structure and tensile behavior of irradiation- and peroxide-crosslinked polyethylenes. *Journal of Macromolecular Science (Part B)*: B26: 37-58.

Navsaria HA (2000). Biological rational for the application of hyaluronan in wound healing. In *New Frontiers in Medical Science: Redefining Hyaluronan* (edited by Abatangelo G et al.). Elsevier Science B.V.: Amsterdam, the Nertherlands, 279-288.

NIH Guide (1999). Deep Infections of Total Joint Replacements. Pa Number: PA-00-014. National Institute of Arthritis and Musculoskeletal and Skin Diseases, National Institute of Child Health and Human Development. Release Date: December 1, 1999.

Ogston AG (1970). The biological functions of the glycosaminoglycans. In *Chemistry and Molecular Biology of the Intercellular Matrix* (edited by Balazs EA). Academic Press: London, 3: 1231-1239.

Oonishi H, Clarke IC, Good VD, and Tsuji E et al. (1999). Low-wear effect of high-dose gamma-irradiated crosslinked polyethylene in total hip prostheses. In *Joint Arthroplasty* (edited by Imura S, Wada M and Omori H). Springer-Verlag: Tokyo, pp.97-118.

Pavesio A, Abantangelo G, and Borrione A et al. (2003). Hyaluronan-based scaffolds (Hyalograft® C) in the treatment of knee cartilage defects: preliminary clinical findings. In *Tissue Engineering of Cartilage and Bone, Novartis Foundation Symposium* (edited by Bock G et al.). John Wiley & Sons Ltd: Chichester, England, 249: 203-217.

Praemer A, Furner S and Rice D (1992). *Musculoskeletal Conditions in the United States*. American Academy of Orthopaedic Surgeons: Park Ridge, Illinois, pp. 125-141.

Prestwich GD, Marecak DM, and Marecek JF et al. (1998). Chemical modification of hyaluronan acid for drug delivery, biomaterials and biochemical probes. In *the Chemistry, Biology and Medical Applications of Hyaluronan and its Derivatives* (edited by Laurent TC). Portland Press Ltd: London, 43-65.

Prestwich GD (2003). Biomaterials from chemically-modified hyaluronan. In *Glycoforum-Science of Hyaluronan Today* (edited byHascall VC). http://www.glycoforum.gr.jp/science/hyaluronan/hyaluronanE.html

Pouyani T and Prestwich GD (1994). Functionalized derivatives of hyaluronic acid oligosaccharides: drug carriers and novel biomaterials. *Bioconjugate Chemistry*, 5:339-347.

Raja RH, Leboeuf RD, Stone GW, and Weigel PH (1984). Preparation of alkylamine and ^{125}I-radiolabeled derivatives of hyaluronic acid uniquely modified at the reducing end. *Analytical Biochemistry*, 139: 168-177.

Ramamurti BS (1995). Loci of movement of selected points on the femoral head during normal gait. In *Transactions of 21st Annual Meeting of the Society for Biomaterials*, pp347.

Rastrelli A, Beccaro M, and Biviano F et al. (1990). Hyaluronic acid esters, a new class of semisynthetic biopolymers: chemical and physico-chemical properties. In *Clinical Implant Materials* (edited by Heimke G et al.). Elsevier Science Publishers B.V.: Amsterdam, 9: 199-205.

Romanelli RR (2000). Recent Advances in Total Joint Replacements, Orthopaedic Center of Illinois, http://www.orthocenter.net/08orthoinfo/articles/Recent_Advances_In_Total_Joint_Replacements.htm

Rydell N and Balazs EA (1971). Effect of intra-articular injection of hyaluronic acid on the clinical symptoms and on granulation tissue formation. *Clinical Orthopedics*, 80:25-32.

Sakurai K, Ueno Y, and Okuyama T (1987). Crosslinked hyaluronic acid and its use. US Patent 4716224.

Savani RC, Bagli DJ, Harrison RE, and Turley EA (2000). The role of hyaluronan-receptor interactions in wound repair. In *Scarless Wound Healing* (edited by Garg HG) Marcel Dekker: New York, pp115-142.

Sawae Y, Murakami T, Higaki H, and Moriyama S (1996). Lubrication property of total knee prostheses with PVA hydrogel layer as artificial cartilage. *JSME International Journal(Series C)*, 39: 356-364.

Scott JE (1955). The reaction of long-chain quaternary ammonium salts with acidic polysaccharides. *Chemistry and Industry*, pp.168-169.

Scott JE (1960). Aliphatic ammonium salts in the assay of acidic polysaccharides from tissues. *Methods of Biochemical Analysis*, 8: 145-197.

Shen FW, McKellop HA, and Salovey R (1996). Irradiation of chemically crosslinked UHMWPE. *Journal of Polymer Science (Part B)*, 24: 1063-1077.

Shi W, Dong H, and Bell T (2003). Wear performance of ion implanted UHMWPE. In *Surface Engineering: A Joint Publication of the Institute of Metals and the Wolfson Institute for Surface Engineering*, 19: 279-283.

Skinner HB (1999). Ceramic bearing surfaces. *Clinical Orthopaedics and Related Research*, 1:83-91.

Smeds KA and Grinstaff MW (2001). Photocrosslinkable polysaccharides for in situ hydrogel formation. *Journal of Biomedical Materials Research*, 54:115-121.

Smith RC (1995). *Orthopedic Products (Part 1-3): Medical and Healthcare Marketplace Guide 1995.* Investment Dealers' Digest: New York.

Solchaga LA, Goldberg VM, and Caplan AI (2000). Hyaluronic acid-based biomaterials in tissue engineered cartilage repair. In *New Frontiers in Medical Science: Redefining Hyaluronan* (edited by Abatangelo G et al.). Elsevier Science B.V.: Amsterdam, pp.233-246.

Solchaga LA, Goldberg VM, and Caplan AI (2000). Hyaluronan and tissue engineering. In *Hyaluronan 2000* (edited by Kennedy JF et al.). Woodhead Publishing Limited: Cambridge, England, 2: 45-54.

Stein HL (1988). Ultra high molecular weight polyethylene (UHMWPE). In *Engineered Materials Handbook, Volume 2: Engineering Plastics*. ASM International: Materials Park, OH.

Sun DC, Park C, Dumbleton JH (1994). Material property comparison of surgical implant grade UHMWPE and "Enhanced" UHMWPE. In *Proceedings of 20th Annual Meeting of the Society of Biomaterials*. Boston, pp.102.
Tomihata K and Ikada Y (1997A). Preparation of crosslinked hyaluronic acid films of low water content. *Biomaterials*, 18: 189-195.

Tomihata K and Ikada Y (1997B). Crosslinking of hyaluronic acid with glutaraldehyde. *Journal of Polymer Science, Part A: Polymer Chemistry*, 35:3553-3559.

Tomihata K and Ikada Y (1997C). Crosslinking of hyaluronic acid with water-soluble carbodiimide. *Journal of Biomedical Materials Research*, 37: 243-251.

Toole BP, Munaim SI, Welles S, and Knudson CB (1989). Hyaluronate-cell interactions and growth factor regulation of hyaluronate synthesis during limb development. In *the Biology of Hyaluronan, Ciba Foundation Symposium* (edited by Evered D et al.), 143: 138-149.

Toole BP (1998). Hyaluronan-cell interactions in morphogenesis. In *the Chemistry, Biology and Medical Applications of Hyaluronan and its Derivatives* (edited by Laurent TC). Portland Press Ltd: London, pp.155-159.

Trieu HH, Haggard WO, and Parr JE et al. (1997). Accelerated fatigue wear of UHMWPE tibial components caused by radiation-induced oxidation. In *Transactions of 23rd Annual Meeting of the Society for Biomaterials*, pp. 44.

Unsworth A (1978). The effects of lubrication in hip joint prostheses. *Physics in Medicine and Biology*, 23: 253-268.

Unsworth A, Recent developments in the tribology of artificial joints. *Tribology International*, 28: 485-495.

Vercruysse KP, Marecak DM, Marecek JF, and Prestwich GD (1997). Synthesis and in vitro degradation of new polyvalent hydrazide crosslinked hydrogels of hyaluronic acid. *Bioconjugate Chemistry*, 8:686-694.

Walker PS (1993). Design of total knee arthroplasty. In *Surgery of the Knee* (edited by Insall J, Windsor R, and Scott W et al.), 2nd ed, Churchchill Livingstone: New York, pp.723-738.

Wang A, Essner A, and Polineni VK et al. (1998). Lubrication and wear of UHMWPE in total joint replacements. *Tribology International*, 31: 17-33.

Weigel PH, Frost SJ, LeBoeuf RD, and McGary CT (1989). The specific interaction between fibrin(ogen) and hyaluronan. *In the Biology of Hyaluronan, Ciba Foundation Symposium* (edited by Evered D et al.). John Wiley and Sons Ltd: Chichester, 143: 248-262.

Weiss C (1998). Viscoseparation and viscoprotection as therapeutic modalities in the musculoskeletal system. In *the Chemistry, Biology and Medical Applications of Hyaluronan and its Derivatives* (edited by Laurent TC). Portland Press Ltd: London, pp.255-265.

Weiss C (2000). Why viscoelasticity is important for the medical uses of hyaluronan and hylans. In *New Frontiers in Medical Science: Redefining Hyaluronan* (edited by Abatangelo G et al.). Elsevier Science B.V.: Amsterdam, pp.89-100.

Widmer MR and Spencer ND (2001). Influence of polymer surface chemistry on frictional properties under protein-lubrication conditions: implications for hip-implant design. *Tribology Letters* 10: 111-117.

Wiseman DM, Sherwood CH, Sadozai KK, and Bulpitt PC (2002). Preclinical animal studies on Incert® adhesion prevention gel. In *Hyaluronan 2000* (edited by Kennedy JF et al.). Woodhead Publishing Limited: Cambridge, England, 2: 17-20.

Wright TM, Rimnac CM, Faris PM and Bansal M (1988). Analysis of surface damage in retrieved carbon fiber-reinforced and plain polyethylene tibial components from posterior stabilized total knee replacements. *The Journal of Bone & Joint Surg*ery, 70: 1312-1319.

Wroblewski BM, Siney PD, Dowson D, and Collins SN (1996). Prospective clinical and joint simulator studies of a new total hip arthroplasty using alumina ceramic heads and crosslinked polyethylene cups. *The Journal of Bone & Joint Surgery B*, 78: 280-285.

Yates JR (1971). Mechanism of water uptake by skin. In *Biophysical Properties of the Skin* (edited by Elden HR). John Wiley and Sons: New York, 1:485.

Yerushalmi N, Arad A, and Margalit R (1994). Molecular and cellular studies of hyaluronic acid-modified liposome as bioadhesive carriers for topical drug delivery in wound healing. *Archives of Biochemistry and Biophysics*, 313: 267-273.

Yui N Ooya T and Sato I (2002). Chemically modified hyaluronic acid or salts thereof, and a process for producing thereof. US Patent Application, No. 20020143171.

Yun YH, Goetz DJ, Yellen P, and Chen W (2004). hyaluronan microspheres for sustained gene delivery and site-specific targeting. *Biomaterials*, 25: 147-157.

Zacchi V, Sorano C, and Cortivo R et al. (1998). In-vitro engineering of human skin-like tissue. *Journal of Biomedical Materials Research*, 40: 187-194.

Chapter 2

Silylation of Hyaluronan

2.1 Introduction

The term silylation means the replacement of the active hydrogen in organic compounds, such as H atoms in –OH, -COOH and NH_2, by a triorganosilyl moiety, especially the trimethylsilyl moiety ($-Si(CH_3)_3$) [Pierce, 1968; Birkofer et al., 1965]. This reaction is often used in organic chemistry to create volatile compounds for separation or gas chromatography analysis [Blakley, 1966; Langer et al., 1958], or to protect special groups during organic synthesis [Katsarava et al, 1994; Birkofer et al., 1965]. However, the silylation of polymers with high molecular weight has a very different purpose: producing organic-soluble derivatives [Harmon et al., 1973].

The three most commonly used silylation reagents are trimethylchlorosilane (TMCS), hexamethyldisilazane (HMDS), and N,O-bis(trimethylsilyl)acetamide (BSA). They are silyl donors in silylation, and their reactivity increases in the order: HMDS, TMCS and BSA. As the most powerful silyl donor, BSA is often used alone. TMCS can be used either alone or with bases [Pierce, 1968]. When used alone, TMCS requires a high silylation temperature to expel the by-product HCl and drive the reversible reaction to product. Pyridine and triethylamine are two bases frequently used with TMCS, but they form the base hydrochloride with the HCl released from the silylation, which is difficult

to remove from the non-volatile silylated polymer products [Harmon et al., 1973]. HMDS can be used alone, because its by-product, NH_3, is easily removed from the silylated product. However, the addition of a small amount of acidic catalyst usually increases the rate or degree of silylation by HMDS. TMCS is most commonly used with HMDS, although it is not a true catalyst [Pierce, 1968].

Proton-active groups of the parent compounds act as silyl acceptors in silylation, and the ease of their silylation decreases in the order: alcohols, phenols, carboxylic acids, amines, and amides [Pierce, 1968]. The mechanisms of silylation are complex, but they all involve nucleophilic attack on silicon atoms of the silyl donors by oxygen or nitrogen in the proton-active groups of the silyl acceptors. As a nucleophile, water is also a strong silyl acceptor. The silyl reagents are decomposed by water before they react with the compounds to be silylated. Therefore, silylation is a humidity-sensitive reaction, which should be performed in an anhydrous environment.

Despite the great success in silylation of compounds of small molecular weight, there has not been much research on silylating polymers, especially natural products such as polysaccharides, due to their high molecular weight, strong molecular interactions, steric hindrance, and natural attraction of water. In the following, the limited literature on silylation of polysaccharides is reviewed.

Cellulose is the most reported polysaccharide that has been successfully silylated. In the paper and textile industry, cellulose from different sources was silylated to improve its solubility in organic solvents [Harmon et al., 1973; Mormann et al., 1999], or to produce a melt-processable derivative [Cooper et al, 1981; Hermanutz, et al., 2001]. The silylation of cellulose with TMCS in the presence of pyridine was described for the first

time by Schuyten et al. [Schuyten et al., 1948; Klemm et al., 1998]. However, the trimethylsilylcellulose they prepared was insoluble in usual organic solvents. Later Harmon and De [1975] found this was because the higher chlorinated silane impurities (i.e. dimethyldichlorosilane and methyltrichlorosilane) had crosslinked the silyl cellulose. Using purified TMCS, they obtained a completely soluble trimethylsilyl-cellulose. They also used BSA to silylate cellulose in dimethylsulfoxide (DMSO), N-methylpyrrolidone (NMP), or other highly polar solvents. After heating at 150°C for 1 hour, a transparent tan-colored gel was obtained, which yielded a viscous solution upon addition of xylenes or benzene.

As a weak silyl donor, HMDS can also be used for the silylation of cellulose. Mormann et al. [1999] used HMDS in liquid ammonia to prepare a series of trimethylsilylcellulose compounds with predictable degrees of silylation (DS, see Section 2.2.3 for DS definition). The reaction was carried out at 80°C under the catalysis of saccharin. The DS was controlled by adjusting the molar ratio of OH groups of cellulose to trimethylsilyl groups of HMDS. The silyl celluloses with a DS above 1.6 are soluble in THF. Harmon et al. [1973] reported the silylation of cellulose, chitin, dextran and some other polysaccharides with HMDS in formamide at 70°C for 2 hours. It was found that only cellulose and dextran achieved high degrees of silylation, while the DS for the other polysaccharides was very low. The solubility of these derivatives in organic solvents, such as benzene, chloroform, and toluene increased with increasing DS.

The trimethylsilylcellulose prepared with appropriate processes was thermoplastic, and this could be processed into fibers via a melt spinning process. The use of a melt spinning process reduces the toxic emissions and heavy metal pollution associated with the

conventional wet spinning process. Cooper et al. [1981] prepared trimethylsilylcellulose, using HMDS and a catalytic amount of TMCS/pyridine in dimethylformamide (DMF). A thermoplastic material was obtained, which melted at 320-340°C (also the thermal decomposition range of celluloses) in the absence of oxygen, and could be melt spun into a fiber. Regenerated cellulose was obtained by treating the silylated cellulose fiber with a mild aqueous acid mixture (isopropanol/water/hydrochloric acid). Hermanutz et al. [2001] developed a new synthesis strategy to improve the melt processability of trimethylsilyl cellulose. They used bistrimethylsilylcarbamate (BSC) to silylate cellulose, producing a trimethylsilyl product with a melting temperature range of 250-260°C, which was below its decomposition temperature, making possible the decomposition-free thermoplastic processing of trimethylsilyl cellulose for the first time. The trimethylsilyl cellulose, prepared by Pawlowski et al. [1987; 1988] with HMDS for liquid-crystalline property study, also showed a melting range (245-270°C) below the decomposition temperature.

Compared with cellulose, chitin is more difficult to silylate. Silylation of chitin with HMDS in DMF resulted in only partial substitution (DS 0.6), while under the same condition cellulose gave a fully substituted product (DS 3.0) [Harmon et al., 1973]. However, when the silylation was carried out in pyridine with a mixture of HMDS and TMCS at 70°C, β-chitin achieved a completely silylated product [Kurita, 2001]. The resulting trimethylsilyl chitin was readily soluble in common solvents, such as acetone and pyridine and swelled considerably in other organic solvents.

Dextran was silylated by Ydens et al. [2000] to control the synthesis of poly(ε-caprolactone)-grafted dextran copolymers, a new group of biodegradable surfactants. The

number of the free hydroxyl groups of dextran, from which ring-opening polymerization of caprolactone started, was controlled by masking all other hydroxyl groups with trimethylsily groups. Dextran silylation was carried out in DMSO with the desired amount of HMDS. In some cases, a co-solvent, THF, was added to the reaction mixture to increase the degree of silylation (DS). A series of silyl dextrans with different DS were obtained, which are soluble in a variety of organic solvents, including toluene used for the ring-opening polymerization of caprolactone.

As a polysaccharide, the structure of hyaluronan is similar in some degree to that of the above mentioned cellulose, chitin and dextran (Figure 2.1). However, no reports of HA silylation have been found. In the present investigation, silylation of HA was explored to improve its solubility in non-polar organic solvents and the compatibility with UHMWPE. This is the key step for further introduction of HA into the UHMWPE porous preforms. Unlike cellulose, chitin and dextran, HA cannot be silylated directly. However, the complex between HA and the long aliphatic chain ammonium cation (reviewed in Section 1.2.6.1) was an effective silylation starting material. Silylated HA was also regenerated via hydrolysis. The thermal stability properties of the HA and its derivatives are also important because the micro-composites are molded.

2.2 Materials and Methods

2.2.1 Materials

Sodium hyaluronate (HyluMed®, medical grade, MW: 1.36×10^6 daltons) was purchased from Genzyme (Cambridge, MA) and stored at 2-8°C. Cetyltrimethyl-ammonium bromide (CTAB), cetylpyridinium chloride (CPC), hexamethyldisilazane

(HMDS, 99.9%), trimethylchlorosilane (TMCS, redistilled, 99+%, contains < 0.1% dimethyldichlorosilane), and N,O-bis(trimethylsilyl)acetamide (BSA) were obtained from Aldrich (Milwaukee, WI). HMDS, TMCS and BSA were stored at 4°C. Silylation grade dimethylsulfoxide (DMSO) was purchased from Pierce (Rockford, IL). Xylenes, dimethylformamide (DMF), pyridine and tetrahydrofuran (THF) were purchased from Fisher (Pittsburgh, PA), and were respectively dried by refluxing over Na, CaH_2, CaO and Na, and distilled just before use. All other common solvents used in this study were also purchased from Fisher, except ethanol (ACS/USP grade), which was purchased from Pharmco (Brookfield, CT). Deuterium oxide (D_2O, D 99.9%), chloroform-d ($CDCl_3$, D 99.8%) and dimethyl sulfoxide-D6 (D 99.9%) were purchased from Cambridge Isotope Laboratories, Inc. (Andover, MA). All chemicals were used as received unless specified.

2.2.2 Reactions

(1) Precipitation of HA with ammonium salts

Sodium hyaluronate (1.5 g) was dissolved in 600 ml of distilled water. CTAB (1.5 g) was dissolved in 300 ml of distilled water. The CTAB solution was slowly added to the HA solution with magnetic stirring. With the addition of CTAB, the solution mixture became more and more opaque. When close to the reaction end point, several more drops of CTAB made HA coagulate completely, while the supernatant became a clear solution. The white precipitate (HA-CTA) was centrifuged, washed with distilled water several times to remove CTAB residue, and then dried in a vacuum oven at 50°C for at least 24hours. The same method was used to precipitate HA with CPC from water to obtain an HA-CP complex.

(2) Silylation of HA-ammonium complexes

The above dry precipitate HA-CTA was cut into small pieces and charged into a 250 ml 3-neck flask, and then 50 ml of DMSO were added under dry N_2. The mixture was left overnight for swelling of HA-CTA, and then heated at 60°C for about 4 hours. Once all the HA-CTA particles had dissolved, 25 ml of HMDS were added to the above solution. HMDS did not dissolve in DMSO, so two liquid phases were formed. The silylation reaction was carried out at 55-75°C for a desired period of time, with stirring and under N_2 flow. In the resulting two-phases of light yellow solution, the upper HMDS layer contained silylated HA-CTA, which was separated from the bottom DMSO layer, vacuumed in 50°C water bath to remove HMDS, and then washed with xylenes five times, yielding light yellow silyl HA-CTA powder.

The above HA-CTA silylation method was also applied to HA-CP, but the product obtained from the upper HMDS layer was dark brown, not light yellow as the silyl HA-CTA.

(3) Regeneration of HA

Regeneration of HA from HA-CTA: HA-CTA (200 mg) was dissolved in 10 ml of 0.2M NaCl solution. HA was precipitated from the solution with 2-3 volumes of ethanol. The precipitate was then washed with ethanol several times to remove –CTA residue. To remove NaCl residue, the regenerated HA was dissolved in water and re-precipitated with 2-3 volumes of acetone. The resulting precipitate was collected and vacuumed at 50°C in an oven for 24 hours. The anhydrous, regenerated HA was a white bulk material.

Regeneration of HA from silyl HA-CTA: Silyl HA-CTA (200mg) was dissolved in 10 ml of 0.2M NaCl solution of water and ethanol (v/v 1:1). HA was precipitated with 1-2 volumes of ethanol. The precipitate was washed with ethanol several times to remove –CTA and $-Si(CH_3)_3$ residues. The NaCl residue was removed with the same method used for HA regeneration from HA-CTA.

2.2.3 Characterization Methods

Fourier Transform Infrared Spectroscopy (FT-IR): A Nicolet Magna-IR 760 spectrometer (E.S.P.) (Nicolet Instrument Corporation, WI) was used to record FT-IR spectra. Sample powder (1%, w/w) was ground and mixed with KBr, and pressed into pellets for analysis. Silyl HA-CTA was also dissolved in xylenes, hexane or other organic solvents with low boiling points, and cast into a film on an NaCl disk. Transmission absorption spectra were collected over a range of 600-4000 cm^{-1} at a resolution of 4 cm^{-1} with 128 scans.

X-Ray Photoelectron Spectroscopy (XPS): XPS analyses were performed on a PHI 5800 spectrometer (Physical Electronics, Inc., MN). The instrument was equipped with a monochromatic Al K_α (1486.6eV) X-ray source. A low energy (5 eV) electron gun was used for charge neutralization on the non-conducting samples. Measurements were taken with an electron takeoff angle of 45° from the surface normal (sampling depth ~ 50Å). Surface elemental compositions were determined from 0-1000 eV survey scans acquired with a pass energy of 100eV. High resolution spectra (C1s, N1s) were obtained at a pass energy of 25eV. Component peak analysis of high resolution spectra was performed

using XPSPeak 4.1 software. HA, HA-CTA and silyl HA-CTA samples were respectively dissolved in water, DMSO and xylenes, and then cast into films for analysis.

Nuclear Magnetic Resonance (NMR): ^{1}H and ^{13}C NMR spectra were recorded using a Varian Inova 300 NMR spectrometer (Varian, Inc., CA) operating at 300MHz. The number of scans for ^{1}H spectra was 32, while for ^{13}C spectra, the scan was continued until a satisfactory spectrum was obtained. HA, HA-CTA and silyl HA-CTA analysis samples were prepared respectively in deuterium oxide, dimethyl sulfoxide-D6 and chloroform-d. The concentration for ^{1}H spectra was approximately 25mg/ml, while that for ^{13}C was approximately 50mg/ml.

Silicon elemental analysis: Si elemental analysis was performed at Galbraith Laboratories (Knoxville, TN). The silicon content was determined using inductively coupled plasma optical emission spectroscopy (ICP-OES), after peroxide fusion in a Parr bomb.

Determination of the degree of silylation (DS): The DS was determined using three methods: weight gain (Δw), Si content (%Si), and FT-IR. The DS calculation formula from Δw and %Si were derived from those used for silyl cellulose [Schuyten et al., 1948; Goussé et al., 2002].

DS from weight gain: $$DS = \frac{\Delta w \times 662.846}{w_0 \times 72.184} \qquad (2.1)$$

DS from Si content: $$DS = \frac{\%Si \times 662.846}{28.06 - \%Si \times 72.184} \qquad (2.2)$$

In the above two equations, 662.846 represents the molecular weight of the HA-CTA disaccharide unit, 72.184 is the change of group weight from -H to $-Si(CH_3)_3$, w_0 is the weight of original HA-CTA ,and 28.06 is the atomic mass of Si.

For the FTIR method, the peak area (A) change of –OH groups was used to calculate the DS. In silylation, with the replacement of –OH by $-OSi(CH_3)_3$, the stretching vibration peak of –OH at approximate 3500 cm^{-1} decreases, and this decrease is proportional to the degree of silylation, so it can be used for the determination of DS. The vibration bands of C-O in alcohols and C-O-C in glycoside overlap at 1046-1150 cm^{-1} [Haxaire et al., 2003]. These peaks do not change during silylation and can be used as the internal reference to calculate the DS.

$$DS = 4 \times \frac{(A_{HA-CTA,3500} / A_{HA-CTA,1046-1150}) - (A_{silyl,3500} / A_{silyl,1046-1150})}{A_{HA-CTA,3500} / A_{HA-CTA,1046-1150}} \qquad (2.3)$$

Thermal degradation of HA: The molecular weight (MW) of HA was calculated based on viscosity measurement [Gura et al., 1998 & Laurent et al., 1960]. A 1.0 g/l HA solution in 0.2M NaCl was prepared and filtered through Whatman No.50 paper. The solution was divided into several 50-ml aliquots, put in sterile plastic tubes and degraded in an oil bath set at the temperature of interest. At the end of the desired exposure intervals, the tubes were removed, immediately immersed in ice water for 5 min, and then stored in a refrigerator at 4-8°C [Lowry and Beavers, 1994].

After degradation, the aliquots were diluted to concentrations of 0.8, 0.6, 0.4, and 0.2 g/l, respectively. The efflux time of 0.2M NaCl solution (t_0) and the HA solutions (t) was determined by using an Ubbelohde capillary viscometer (size: 1C, Cannon Instrument Co., PA) in a 25°C water bath. After equilibration at the test temperature for about 30 min, the flow times (t) of the solutions were measured and compared to pure solvent, t_0. Three observations were made for each sample and the averages were taken.

The relative viscosity of the HA solution is t/t_0, while the specific viscosity is $t/t_0 - 1$. By plotting (specific viscosity / HA concentration) vs. HA concentration, a straight line

was obtained, and its intercept is the intrinsic viscosity [η] of HA. The relationship between [η] and MW was described by the Mark-Houwink-Sakurada equation [Rodriguez, 1996]:

$$[\eta] = K\,Mw^{\alpha}$$

K and α are the constants related with solvent, temperature and polymer. For HA solution tested in 0.2M NaCl at 25°C, the following constants are used [E. Johnston, Genzyme, Personal Communication]:

$$K = 0.0228 ml/g$$

$$\alpha = 0.816.$$

Differential Scanning Calorimetry (DSC) and Thermal Gravimetric Analysis (TGA): The thermal properties of HA and its derivatives were determined using a Seiko DSC SCC 2200 differential scanning calorimeter (DSC) and Seiko TG SCC 5200 thermal gravimetric analysis (TGA) at a heating rate of 10°C/min in air. DSC data were recorded from the second scan to remove the effect of water and solvent residues. Prior to each test, the temperature was equilibrated at the starting point for 5 min.

2.3 Results and Discussion

2.3.1 Complexes of HA with Ammonium Salts

Complexes of HA with ammonium salts were used as the silylation starting materials after many attempts to silylate HA directly failed. Varied combinations of silylating agents (e.g., TMCS, BSA and HMDS) and solvents (e.g., THF, DMSO, DMF and pyridine) based on the silylation methods used for cellulose, chitin and dextran were also unsuccessfully applied to HA. HA is very hydrophilic. Tightly absorbed water is thought

to be a barrier resisting silylation. Toluene was used to boil HA and remove water via forming an azeotrope. Even after dehydration, HA still did not react with silylation agents. Therefore, the strong inter- and intra-molecular interactions (hydrogen bonds) and lack of solubility in silylation solvent were hypothesized to be the main reason that –OH groups on HA resist attack from silylation agents. Similar phenomena make silylation of cellulose very sluggish [Harmon & De, 1975].

The long aliphatic chains in quaternary ammonium cations were effective in disrupting the hydrogen bonds and increasing the solubility of HA in silylation solvents. HA can only dissolve in water, but its complexes with ammonium salts, such as HA-CP and HA-CTA (Figure 2.2), are soluble in highly polar solvents (e.g. DMSO & DMF). These complexes are actually the salts between hyaluronic acid and ammonium bases. The complexing reaction is shown in Figure 2.3a.

Compared with HA-CTA, HA-CP was more susceptible to the basic environment (releasing NH_3) during silylation, forming a dark brown product. This was confirmed by experiment. In a 50°C water bath and in the presence of NaOH, HA-CP solution became yellow and then brown until finally a dark brown product precipitated. Scott [1960] also mentioned the instability of the pyridinium rings of CPC at higher pH and temperature. Therefore, only HA-CTA was selected as the starting material for all remaining silylation reactions, was characterized in detail, and was used in manufacture of the HA-UHMWPE micro-composites (Chapter 3).

The difference between the native HA and HA-CTA structures was confirmed with FT-IR, XPS and NMR analysis. In the FT-IR spectra shown in Figure 2.4, absorption of hydrocarbon-associated bands in HA-CTA at 2926 and 2855 cm^{-1} increase markedly

compared to HA. The two bands are attributable to $-CH_3$ and $-CH_2$ stretching, respectively [Smith, 1998]. Introduction of a large amount of $-CH_3$ and $-CH_2$ groups into HA with CTA^+ cations results in the intensity increase of the two bands. The FT-IR vibration frequency of carbonyl –C=O groups in secondary amide –NHC=O (amide I) chemistry is sensitive to its environment, such as hydrogen bonding. The stronger the hydrogen bond, the lower the frequency of the amide I absorption [Griebenow et al., 1999]. In both HA and HA-CTA, hydrogen bonding is strong, so that amide I vibration appears at a lower frequency, overlapping with the carboxylate $-COO^-$ asymmetric stretch near 1620 cm^{-1} [Smith, 1998]. This vibration shifts to a much higher frequency in silylated HA-CTA and separates from the carboxylate $-COO^-$ vibration (see Section 2.3.2).

High-resolution N1s XPS spectra of HA and HA-CTA are shown in Figures 2.5a & b. Only one N1s XPS peak is seen at 399.8eV for native HA, associated with the only N atom present in the amide group (-CONH-) of HA [Moulder et al., 1992]. The N1s spectrum of HA-CTA can be best fit with two peaks (one at 399.8 eV, another at 402.8 eV) because quaternary ammonium nitrogen (CTA ammonium salt N^+) contributes to the new peak at 402.8 eV [Moulder et al., 1992]. The intensity of the two peak components should be the same theoretically, due to the 1:1 molar ratio between $-COO^-N^+Q$ and –CONH- in HA-CTA. This is confirmed by N1s XPS analysis below for silyl HA-CTA. However, the CTAB residue, which is not completely removed from HA-CTA, contributes a much stronger N^+ peak than the HA amide peak. The presence of the CTAB residue is also confirmed by trace Br present in HA-CTA (see XPS elemental analysis results shown in Table 3.3). The indicates overall that CTA presence is non-ideal and

non-stoichiometric based on excess XPS N1s signal from the quaternary nitrogen and bromide signal from CTAB.

C1s spectra for both HA and HA-CTA (Figure 2.6a & b) are best fit with 4 peaks based on the number of carbon-oxygen/nitrogen bonds: C0 (CHx, C-C; 285.0 eV, reference), C1 (C-O, C-N; 826.5 eV), C2 (O-C-O, C=O; 287.8 eV) and C3 (-O-C=O, -HN-C=O; 289.2 eV) [Favia et al., 1998]. The strongest peak component for HA is C1. This is consistent with the highest HA abundance of C-O. However, the most intense peak for HA-CTA is C0, indicating the presence of a large amount of CHx groups in HA-CTA. This further confirms the above FTIR analysis results.

The ^{1}H-NMR spectrum for HA-CTA (Figure 2.7b) shows completely different characteristics from that of HA (Figure 2.7a). In the ^{1}H-NMR spectrum of HA, the strongest resonance centered at 4.80 ppm is due to the protons of the solvent D_2O and the water absorbed by HA. Several other small peaks around 4.80 ppm correspond to the anomeric protons (2 H) and the hydroxyl protons (4 H) of the glucosidic units [Crescenzi et al., 2003; Nouvel et al., 2002; Günther, 1994]. The broad signals at 3-4 ppm are assigned to the non-anomeric protons (10 H) [Crescenzi et al., 2001]. The three methyl protons of CH_3CONH- are represented by a peak centered at 1.95 ppm. In the ^{1}H-NMR spectrum of HA-CTA, several new peaks appear with disappearance of the resonances of HA around 4.80 ppm and 1.95 ppm, and the shape and position of the signals at 3-4 ppm are also changed. The new triplet at 0.851 ppm is attributed to the methyl protons in the cetyl groups ($-CH_2(CH_2)_{14}CH_3$) of CTA, while the strong peak at 1.236 ppm is due to the methylene protons in cetyl groups ($-CH_2(CH_2)_{14}CH_3$), and the intensity ratio of these two peaks is 3.1: 26.54, very close to the theoretical value of 3:28. The broad resonance at

1.650 ppm could be assigned to the protons of the methyl or methylene groups connected to quaternary N^+ cation (-CTA^+). The multiplet centered at 2.50 ppm comprises the DMSO-d6 solvent peaks. The number of protons introduced with CTA is large compared to that in each HA disaccharide unit, so some peaks for the HA protons are too weak to be visible in the HA-CTA spectrum (actually, they are observable once the signal is amplified). Due to interaction with solvents, the same protons, especially in –OH and –NHx groups, may show different resonances in different solvents [Günther, 1994]. This might be the reason for the change of signals at 3-4 ppm.

The ^{13}C-NMR spectrum of HA-CTA is shown in Figure 2.8a. The strong multiplet centered at 40.207 ppm is due to solvent DMSO-d6. Peaks at 14.664, 22.801, 29.757, 31.989, and 52.809 ppm, respectively, represent the different carbons of –CTA (C1, C2, C4, C3 and C5) [Günther, 1994], and their corresponding relationships are shown in Figure 2.9. A desirable ^{13}C-NMR spectrum of HA was not obtained in this study due to the difficulty of making higher concentrations of HA, but it can be found elsewhere [Cowman et al., 1996; Crescenzi et al., 2003]. The reported carbon resonances for HA are not observed in ^{13}C-NMR spectrum of HA-CTA. This may be because these signals are too weak to be seen.

Since the HA-CTA complex is soluble in highly polar organic solvents, it can be used for the starting material of non-aqueous reactions, such as silylation. Furthermore, the complexed –CTA groups can easily be removed, as will be discussed in Section 2.3.5.

2.3.2 Silylation of HA-CTA

HA-CTA dissolved in DMSO, a good silylation solvent, forming a very viscous solution. Soluble HA-CTA reacted with typical silylation agents, such as BSA (N, O-bis(trimethylsilyl) acetamide), TMCS (trimethylchlorosilane) and HMDS. Based on the criteria of high or moderate reactivity and easy separation of product, HMDS was selected for the silylation agent. TMCS and BSA are more active than HMDS. However, removal of excess BSA and its by-products are difficult due to their high boiling temperature (BSA: 71-73°C/35 mm Hg; acetamide: 221°C). The higher-chlorinated silane impurities in TMCS, dimethyldichlorosilane ($(CH_3)_2SiCl_2$) and methyltrichlorosilane ($(CH_3)SiCl_3$), also caused crosslinking of the silylated polymer. The TMCS purification method suggested by Harmon and De [1975] was also attempted, but did not work. The low boiling point (125°C), gas by-product (NH_3) and easily separated products made HMDS a good choice of silyation agent in this study. HMDS is not soluble in DMSO. It forms a separate phase floating on DMSO. HA-CTA dissolved in DMSO reacts with HMDS at the interface. Vigorous stirring is therefore very important to keep the two phases interspersed sufficiently to assure completion of reaction.

In silylation, the –OH groups of HA-CTA were substituted by $-OSi(CH_3)_3$ groups (Figure 2.3b). FT-IR spectra shown in Figure 2.4 confirm the structural changes. The silyl HA-CTA spectrum shows four new pronounced peaks, characteristic of the absorption of $-OSi(CH_3)_3$ groups. The intense band at 1250 cm^{-1} is associated with symmetric bending of $Si-CH_3$ [Smith, 1998]. The two strong peaks at 847 and 758 cm^{-1} are assigned to rocking of $Si(CH_3)_3$. Another strong absorption at 879 cm^{-1} corresponds to

vibration of Si-OC [Zollfrank, 2001]. The appearance of a small peak at 2960 cm^{-1} represents the introduced -CH_3 groups from the trimethylsilyl residue. It is also noticed that the stretching band of –OH and amide –NH- in silyl HA-CTA around 3450 cm^{-1} is very weak compared with that in HA-CTA, while most of its intensity may come from the –NH- vibration. Two separate carbonyl –C=O stretch bands are seen at 1670 and 1611 cm^{-1} in silyl HA-CTA: one attributable to amide I, another due to carboxylate $–COO^-$. The two vibrations overlap in HA and HA-CTA. In silyl HA-CTA, the inter- and intra-molecular interaction is completely disrupted by the introduction of -$Si(CH_3)_3$, resulting in a hydrogen-bond free environment and causing the shift of the amide I band to a much higher frequency (1670cm^{-1}).

Like HA-CTA, the N1s XPS spectrum of silyl HA-CTA (Figure 2.5c) can also be split into two peaks: ammonium salt N^+ component and amide N component. Their peak areas are almost identical, indicating that the silylation reaction did not involve or alter the CTA groups complexed with HA carboxyl groups. The C1s signal of silyl HA-CTA (Figure 2.6c) shows an increased intensity of the C0 component (78.1%), compared to that of HA (66.3%). This is associated with the presence of large amounts of –$Si(CH_3)_3$ in silyl HA-CTA.

In the ^{1}H-NMR spectrum of silyl HA-CTA (Figure 2.7c), a new peak is observed at 0.162 ppm, the typical resonance of trimethylsilyl protons (–$Si(C\mathbf{H_3})_3$) [Günther, 1994]. Another new peak at 7.270 ppm is the solvent chloroform-d peak. Those two resonances at 0.851 and 1.236 ppm, present in the ^{1}H-NMR spectrum of HA-CTA and attributed to the methyl and methylene protons in the cetyl groups, still exist in the ^{1}H-NMR spectrum of silyl HA-CTA, and their intensity ratio does not change (3.31:27.91), confirming that

the –CTA groups were not involved in silylation. The intensity ratio of the trimethylsilyl proton peak at 0.162 ppm and the methylene proton peak at 1.236 ppm is 36:27.91, almost equal to 36:28, indicating four -Si(CH_3)$_3$ groups for each –CTA group ($CH_3(CH_2)_{14}CH_2(CH_3)_3N^+$). Thus, all four –OH groups of this HA-CTA sample silylated at 75°C for 24 hours have been replaced by -Si(CH_3)$_3$.

In comparison to the ^{13}C-NMR spectrum of HA-CTA, two new peaks appear in ^{13}C-NMR spectrum of silyl HA-CTA (Figure 2.8b). The triplet centered at 77.23 ppm represents the solvent chloroform-d. The signal around 0 ppm indicates the presence of -Si(CH_3)$_3$ [Günther, 1994; Monsef-Mirzai et al., 1998].

Silyl HA-CTA dissolved in hexane, xylenes, 1,2-dichloroethane and THF, depending on the degree of silylation (DS). Both the -CTA and trimethylsilyl groups –Si(CH_3)$_3$ introduced into HA through modification can be removed via hydrolysis, as will be discussed in Section 2.3.5.

2.3.3 The Effect of Silylation Conditions on DS

The effect of silylation temperature and time on the degree of silylation (DS) was investigated and results are shown in Table 2.1 and Figure 2.10. For the same sample, the DS values from the different calculation methods vary. Compared with the DS from weight gain, the DS from FT-IR is smaller, while that from Si content is higher, but they all exhibit the same trends with reaction conditions. Figure 2.10 indicates that a nearly complete silylation can be achieved at 75°C within 24 hours. This result is in agreement with the DS = 4 obtained from the ^{1}H-NMR analysis. However, at least 72 hours are required to reach the same DS for silylation at 55°C. The reactions at both temperatures

are fast before DS = 3, but after that they proceed slowly, especially when close to DS = 4.

It is necessary to discuss the relationship between the three DS calculation methods to find a convenient and accurate method to control the reaction. Because all silylated products were subject to vacuum at 50°C until they reached constant weight, the DS calculated from weight gain should be accurate. The FT-IR method can be easily used to test the DS during reaction. However, the DS values calculated from FT-IR are below that obtained with the weight gain method, due to the conflicting presence of the amide –NH vibration at 3500cm^{-1}. If the intensity from –NH- vibration is deducted, the denominator of equation 2.3 will become smaller and the DS will increase. The amide group does not change in the silylation due to the low reactivity [Pierce, 1968], and its contribution to the peak at 3500cm^{-1} should be constant. Therefore, the FT-IR method can be related to the more accurate weight gain method through a calibration [Mormann et al, 1999] (Figure 2.11). A linear correlation between the two DS values is obtained. With this calibration, the simpler FT-IR method can be used to determine the degree of silylation from very little product and in the process of reaction. The higher DS values from the Si content method may come from Si contamination ubiquitous in glass particles, vacuum grease and gloves.

The molar ratio of HMDS/-OH also affected the degree of silylation (Table 2.2). An increase in the ratio enhanced the silylation, but beyond 5:1, the effect leveled. To continue increasing the DS, a higher temperature may be required.

The above discussion provides evidence that the degree of the silylation can be controlled through adjusting the reaction temperature and time, and the HMDS/-OH

molar ratio. By doing this, silyl products with different solubility in organic solvents can be obtained to meet various solubility requirements.

2.3.4 Thermal Degradation of HA

From the review in Section 1.2.5, it is known that the properties of HA and its derivatives highly depend on HA molecular weight. In the silylation reaction, the HA-CTA was exposed to a high temperature. Whether the high silylation temperatures caused degradation of HA-CTA molecular chains was a concern. Intrinsic viscosity is the most common measure for polymer molecular weight, and was used in this study to assess this problem. The molecular weight (MW) was related to the intrinsic viscosity through the Mark-Houwink-Sakurada equation. The two constants (K and α) in the equation are polymer-solvent system dependent. Because of the lack of K and α values for HA-CTA in DMSO solution, HA in aqueous solution was utilized to examine the effect of temperature and time on degradation of HA. Under the same conditions, the degradation of HA in water should be greater that that of HA-CTA in DMSO due to the hydrolytic presence of water.

Two temperatures, 55°C and 75°C, were tested because all the HA-CTA reactions were performed within that temperature range. Aqueous degradation results are shown in Table 2.3. The molecular weight loss at 55°C up to 87 hours is less than 11.5%, and the loss at 75°C up to 48 hours less than 10.5%. Because the practical reaction time was much shorter and the silylation was carried out in an anhydrous environment, the actual degradation of HA-CTA molecular weight during silylation should be smaller than 5%.

Table 2.3 shows that the HA molecular weight before degradation is 1.0388×10^6 daltons, smaller than 1.36×10^6 daltons reported by the manufacturer (-23.6%). This may be due to the difference of measurement methods. Molecular weight measured by viscosity in this study is the viscosity average molecular weight (M_v), which lies between the number average molecular weight (M_n), measured by osmotic pressure, and the weight average molecular weight (M_w), measured by light scattering [Rodriguez, 1996].

A strange phenomenon is also found in examining these degradation data. The molecular weight of HA seems to significantly increase first and then decline at both test temperatures. This is in agreement with what Lowry and Beavers [1994] observed when examining the effect of temperature on the viscosity of HA. They explained the phenomenon with the viscoelastic behavior of HA. The viscosity of HA at a temperature above 25°C depends on the balance of two opposite factors. One is thermally induced polymer chain scission, and another is the increased molecular volume caused by further separation of chain segments at a higher temperature, which enhances the entanglement of HA molecules and leads to an increase in viscosity [Gura et al., 1998]. At the beginning of degradation, the latter factor dominates, causing an increased viscosity. However, as degradation continues, the latter factor is overtaken by the former, exhibiting typical degradation characteristics.

2.3.5 Regeneration of HA

To restore the hydrophilic, lubricious and other desired properties of HA, it is necessary to regenerate HA from its derivatives. The long chain aliphatic ammonium cation of HA-CTA was removed by precipitating HA with ethanol from its 0.2M NaCl

solution. The FT-IR spectrum of HA regenerated from HA-CTA is shown in Figure 2.12. The peaks (described in Section 2.3.1) characteristic of the absorption of –CTA groups disappear, and no difference is observed in this spectrum when compared with that of original HA (Figure 2.12), indicating the success in removing -CTA from HA-CTA.

There are some critical observations regarding the above regeneration procedure. First, the concentration of NaCl solution should not be higher than 0.2M, although HA-CTA more easily dissolves in more concentrated NaCl solution. Excess NaCl may also precipitate in ethanol together with HA. Second, acetone cannot be used to precipitate HA from HA-CTA solution, even though acetone is more effective in precipitating HA from water, because –CTA is not soluble in acetone.

The regeneration of HA from silyl HA-CTA appears complicated. Both trimethylsilyl and –CTA groups must be removed at the same time. It has been demonstrated that acid and water-miscible organic co-solvents promote hydrolysis of trimethylsilyl compounds [Pierce, 1968; Cooper et al. 1981]. No additional acid was used in this study, because it might cause degradation of the polymer, and distilled water itself is slightly acidic (pH 5.5-6). Silyl HA-CTA dissolved in ethanol, so ethanol was used as the co-solvent to enhance wetting of the hydrophobic silyl HA-CTA. The volume ratio of ethanol and water was determined through testing the solubility of silyl HA-CTA in a series of ethanol and water mixtures. It was found that silyl HA-CTA was soluble when the ethanol/water ratio is greater than 1:1, but too much ethanol might block the hydrolysis. Considering the requirements for removing both –CTA and $-Si(CH_3)_3$ groups, a 0.2M NaCl solution in ethanol and water (v/v 1:1) was selected to regenerate HA from silyl HA-CTA.

The FT-IR spectrum for the HA regenerated from silyl HA-CTA is also shown in Figure 2.12. All vibrational peaks associated with $-Si(CH_3)_3$ and –CTA vibrations are gone. The spectrum is the same as that for original HA, indicating the efficacy of the silyl HA-CTA hydrolysis method.

2.3.6 Handling and Thermal Properties of HA and Silyl HA-CTA

HA-CTA is a white bulk material. It must be cut into small pieces before use in silylation reaction. The polymer is soluble in DMSO and formamide, yielding a transparent viscous solution. It also dissolves in concentrated NaCl solution ($\geq$ 0.2M) via ion exchange. However, it is insoluble in acetone, ethanol, xylenes, pyridine, hexane, and other less polar solvents. The film cast from HA-CTA in DMSO solution was clear and flexible. Sharp creasing did not break it. When heated, like HA, HA-CTA does not melt before it decomposes in air around 175 °C (Figures 2.13 and 2.14). This was confirmed by the observation that HA-CTA gradually became brown when heated on a hot stage under a microscope, but did not melt. It also seems that the thermal stability of HA-CTA is inferior to that of its parent polymer HA ($T_d \sim 212°C$). This may be attributed to breakage of polymer hydrogen bonds and easier access of oxygen to the polymer chains.

Silyl HA-CTA is a colorless to slightly yellow powder depending on the degree of silylation. When the DS is low ($2.5 < DS \leq 3.2$), the silyl HA-CTA is colorless, and insoluble in xylenes, but soluble in THF, acetone, 1,2-dicholoroethane, etc. The solution-cast film is clear and also flexible. The silyl HA-CTA with DS > 3.2 is light yellow, and soluble in xylenes and hexane. Its film cast from xylenes solution is clear, but brittle. This is the product used for later UHMWPE porous preform treatment and characterized in

detail. The term "silyl HA-CTA" is used to represent the silyl HA-CTA with DS > 3.2 in the rest of this study unless otherwise defined.

Silyl HA-CTA is stable in air, unlike many other silylated compounds, such as silyl poly-L-lysine. Polymer samples left in ambient air for one year were still completely soluble in xylenes. At room temperature, silyl HA-CTA did not dissolve in water, but did swell after several days. When the water was heated to 40-50°C, the silyl HA-CTA particles were hydrolyzed and then dissolved within several days. Like HA and HA-CTA, silyl HA-CTA does not melt (Figure 2.13), and its decomposition starts (around 161 °C) at much lower temperatures than HA and HA-CTA. The low cleavage energy of the O-$Si(CH_3)_3$ group may be the reason.

2.4 Conclusions

The HA complex with aliphatic ammonium salts was soluble in highly polar organic solvents, and thus can be used as a reaction intermediate. HA was successfully silylated with HA-CTA as the starting material. Silylated HA was soluble in acetone, THF, 1,2-dichloroethane, xylenes and hexane, depending the silylation degree (DS). The degree of silylation could be controlled through modulation of the reaction temperature and time, and the silylation agent / -OH ratio.

HMDS was demonstrated to be an effective silylating agent, due to its easily separated product and gas by-product. The minimal degradation of HA molecules under silylation conditions was acceptable, because even in water solution the decrease of HA molecular weight was less than 12%.

Unlike many other silylated polymers, the silylated product of HA was very stable in air, and was not sensitive to humidity. Even after storage in air for one year, the silyl HA-CTA still dissolved in xylenes, forming a clear solution.

The silyl HA-CTA modification groups, including –CTA and $-Si(CH_3)_3$, could be removed through hydrolysis in aqueous NaCl and ethanol solutions. No difference was found between the regenerated HA and native HA, indicating that the silylation reaction did not affect the backbone of the HA molecular chains.

With the introduction of –CTA and silyl HA-CTA, the intermolecular interaction and the molecular order were disrupted, so the thermal stability of HA-CTA and silyl HA-CTA was inferior to native HA. This was especially true for silyl HA-CTA, due to the ready cleavage of $-Si(CH_3)_3$. The degradation temperature was much lower than that of native HA. Like native HA, HA-CTA and silyl HA-CTA did not melt before they degraded, so these two HA derivatives are not suitable for hot-melt processing.

2.5 Tables

Table 2.1 The effect of reaction temperature and time on DS

Silylation	DS from Weight Gain	DS from FTIR	Si Content (%)	DS from %Si
55°C×12h	2.58	2.13	10.64	3.46
55°C×24h	3.18	2.88		
55°C×48h	3.48	2.93		
55°C×72h	3.75	3.12	12.38	4.29
75°C×12h	2.97	2.81	11.93	4.07
75°C×24h	3.80	3.00		
75°C×36h	3.84	3.25		
75°C×48h	3.96	3.39	12.95	4.59

*The HMDS /OH molar ratio for all reactions was 10:1.

Table 2.2 The effect of HMDS/OH ratio on DS

HMDS/OH Molar Ratio	DS from FTIR*
1:1	1.67
5:1	2.62
10:1	2.88
30:1	2.92

*All silylation was carried out at 55°C for 24hours.

Table 2.3 Intrinsic viscosity and molecular weight of HA after thermal degradation

Degradation Condition	Intrinsic Viscosity (l/g)	MW ($\times 10^6$ daltons)	ΔMW (%)
Non-degradation	1.8511	1.0388	0
55°C×16h	1.9350	1.0968	5.6
55°C×48h	1.7859	0.9942	-4.3
55°C×87h	1.6757	0.9195	-11.5
75°C×16h	1.9053	1.0762	3.6
75°C×30h	1.6901	0.9292	-10.5
75°C×48h	1.7535	0.9721	-6.4

2.6 Figures

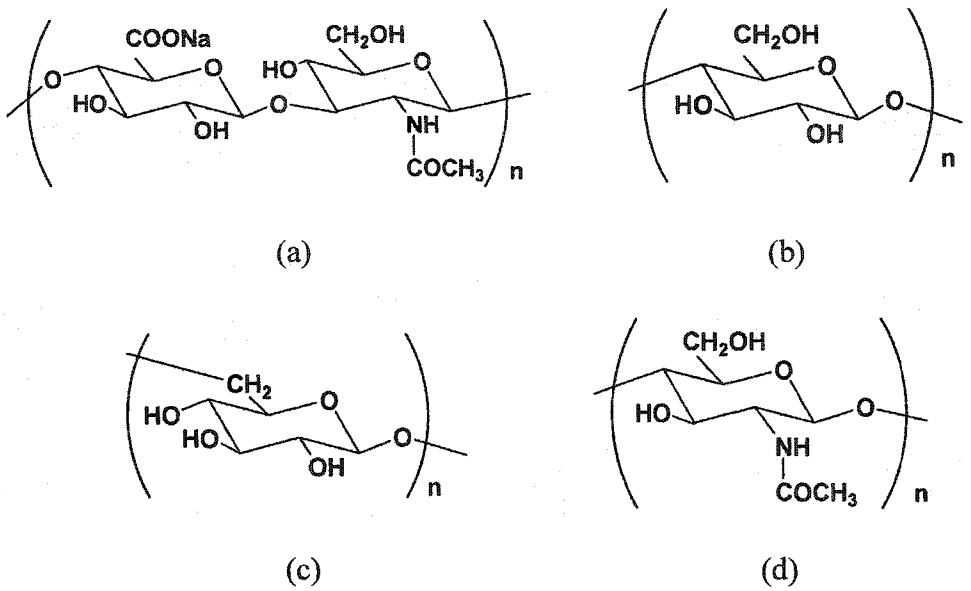

Figure 2.1 Structures of several polysaccharides: (a) hyaluronan; (b) cellulose; (c) dextran; (d) chitin

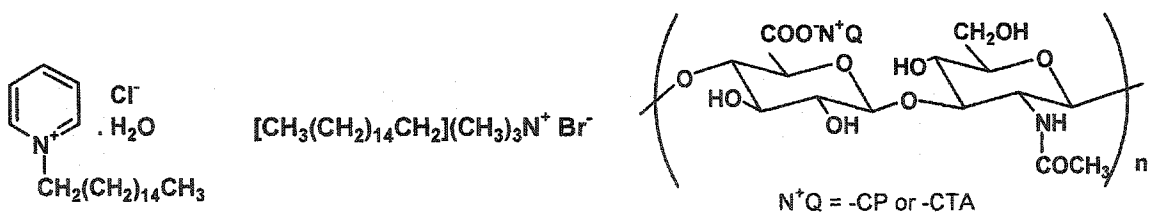

Figure 2.2 Formulas for (a) CPC; (b) CTAB; (c) HA-ammonium complex

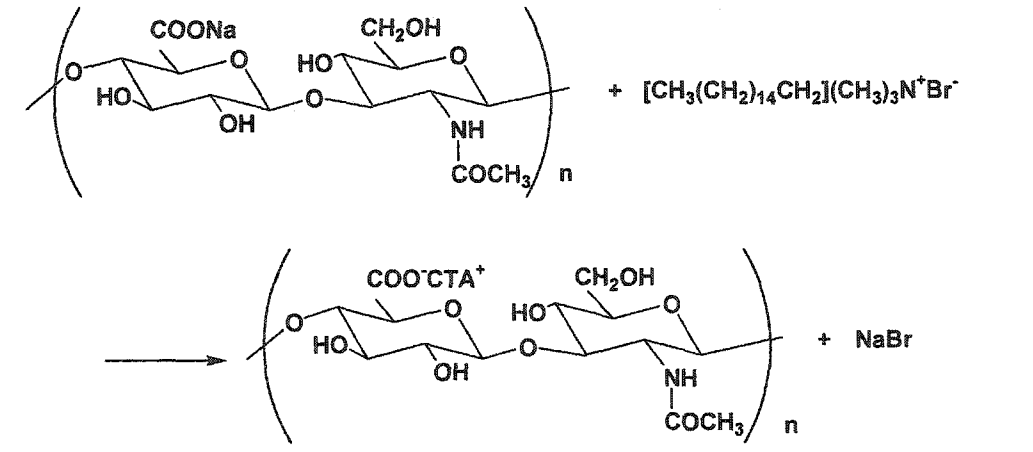

(a)

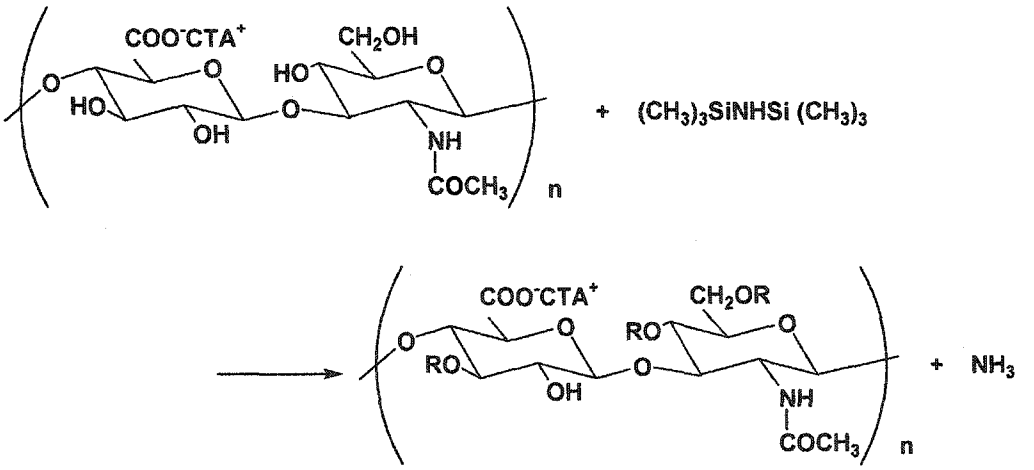

(b) R = -Si(CH3)3

Figure 2.3 Reactions: (a) precipitation of HA; (b) silylation of HA-CTA

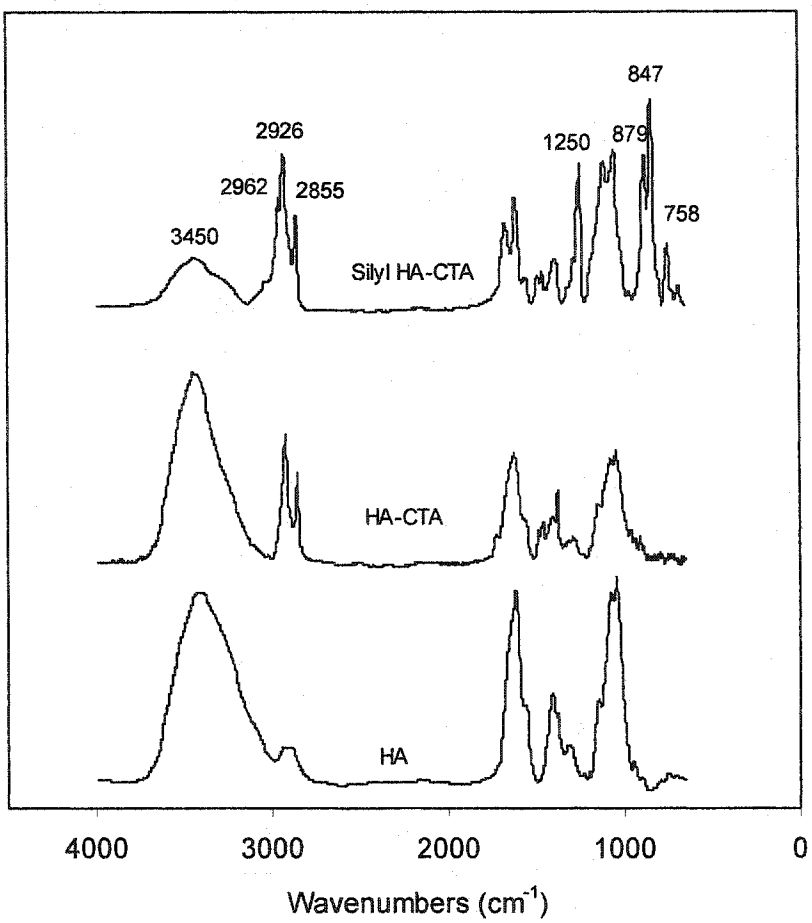

Figure 2.4 FT-IR spectra of HA, HA-CTA and silyl HA-CTA

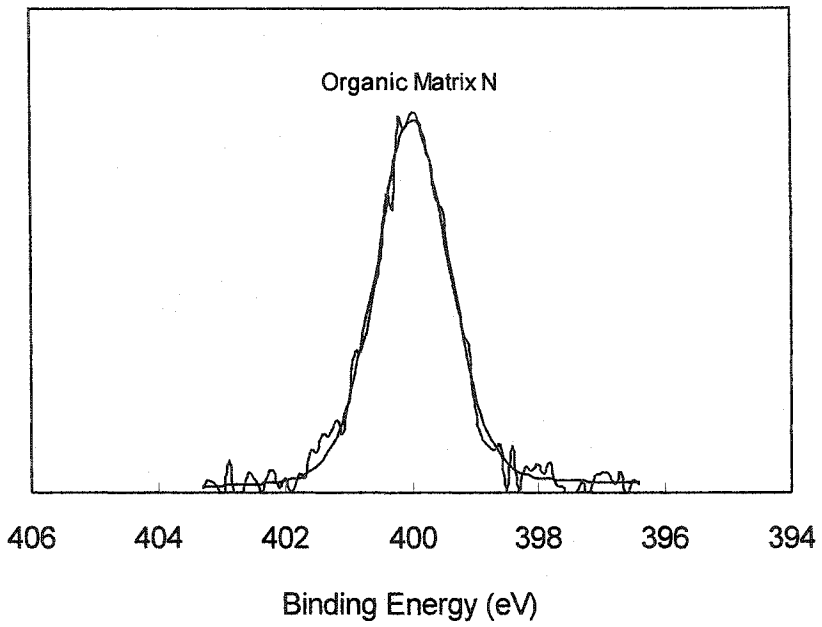

(a)

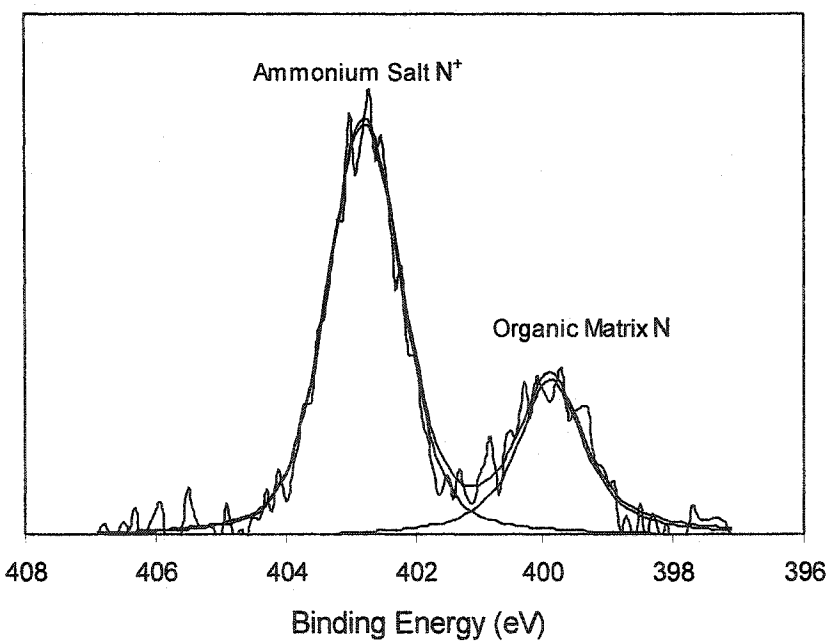

(b)

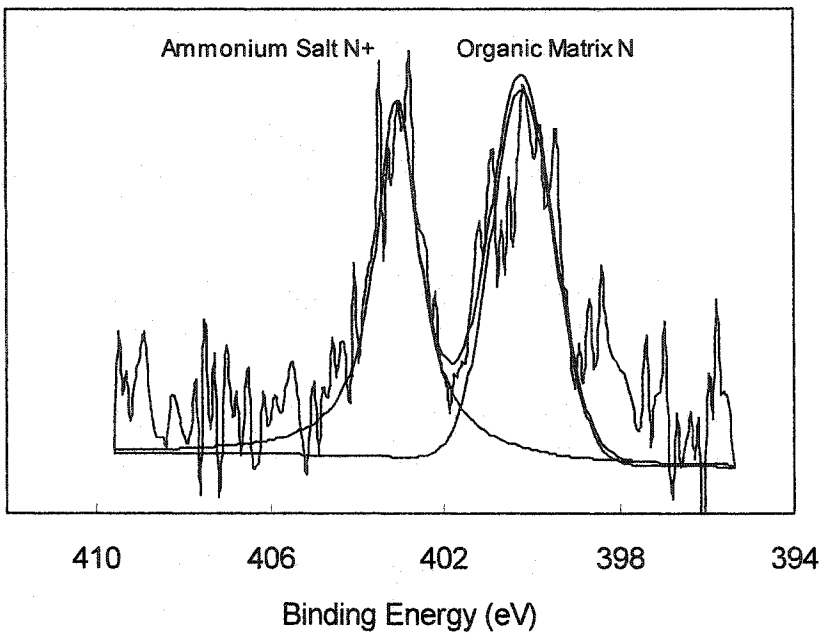

(c)

Figure 2.5 High-resolution XPS N1s spectra of (a) HA; (b) HA-CTA; (c) silyl HA-CTA

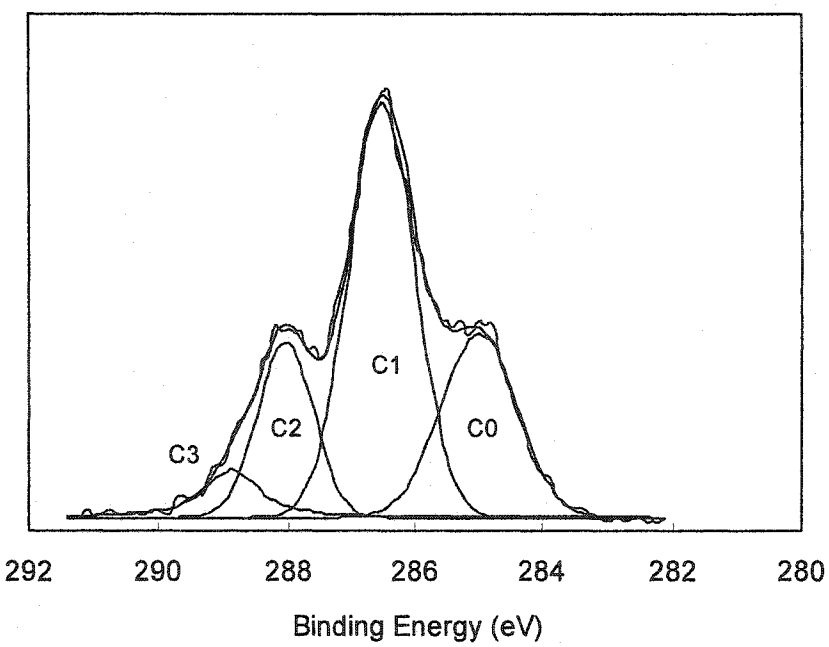

(a)

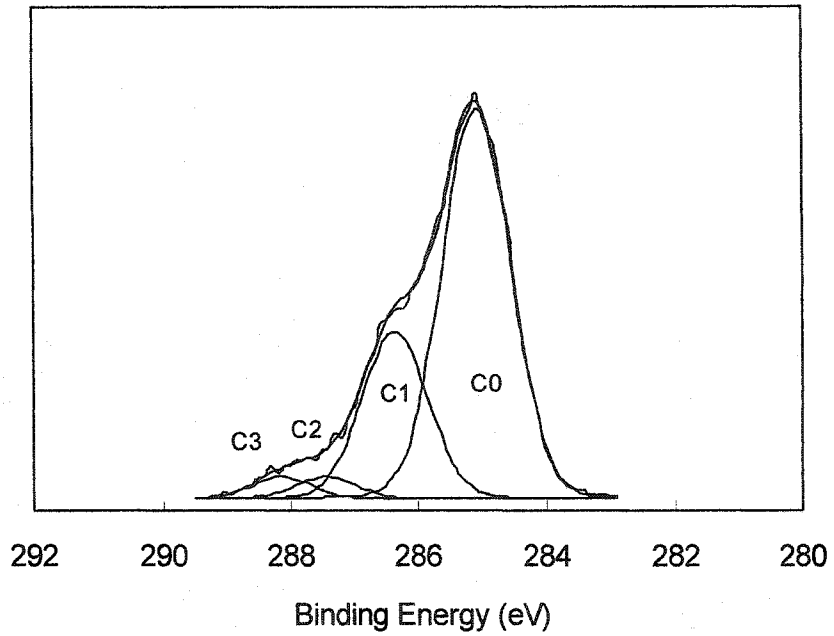

(b)

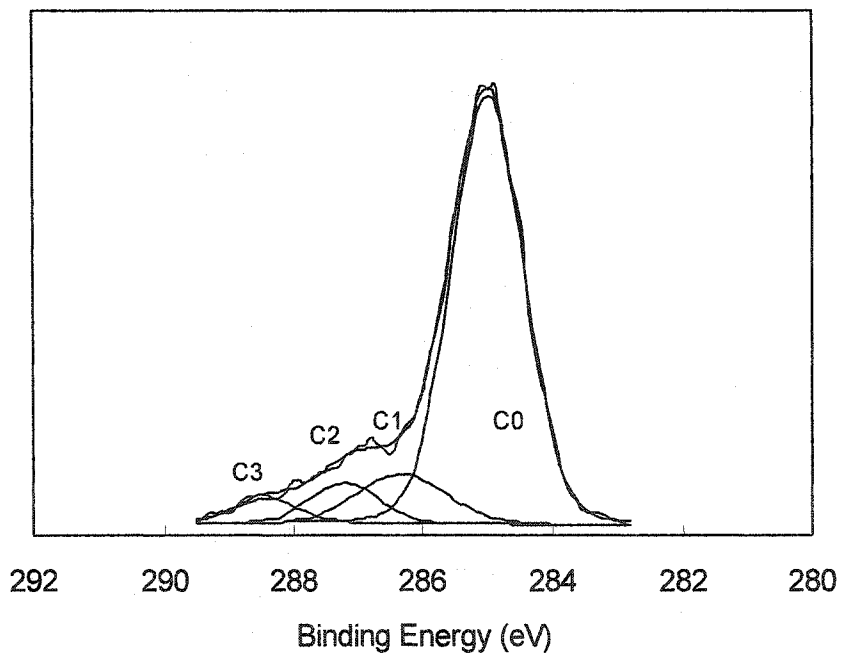

(c)

Figure 2.6 High-resolution XPS C1s spectra of (a) HA; (b) HA-CTA; (c) silyl HA-CTA

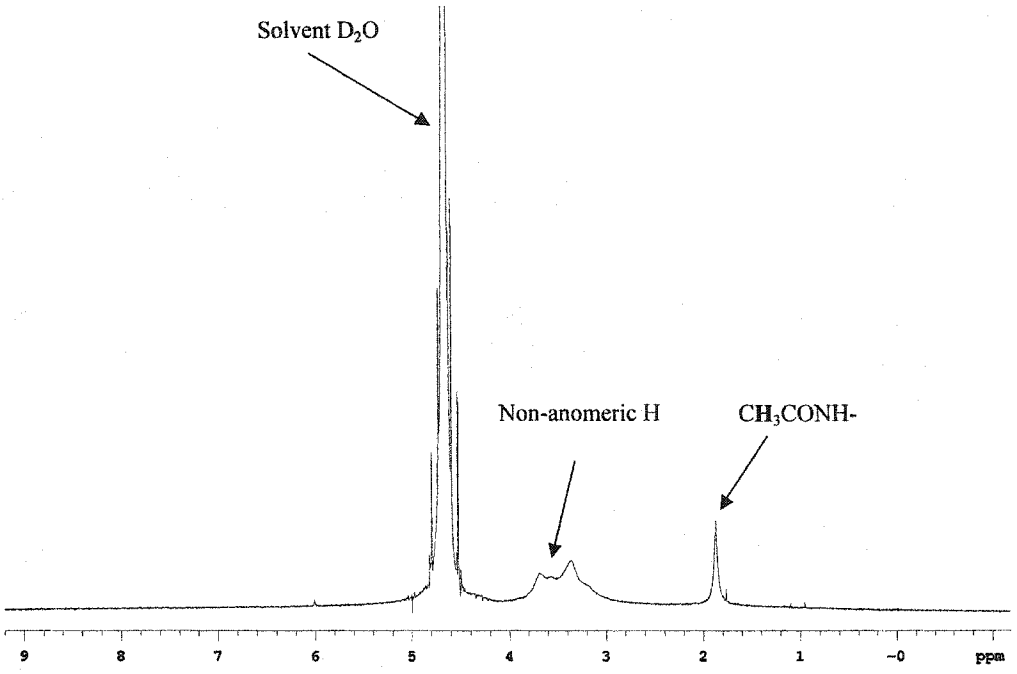

(a)

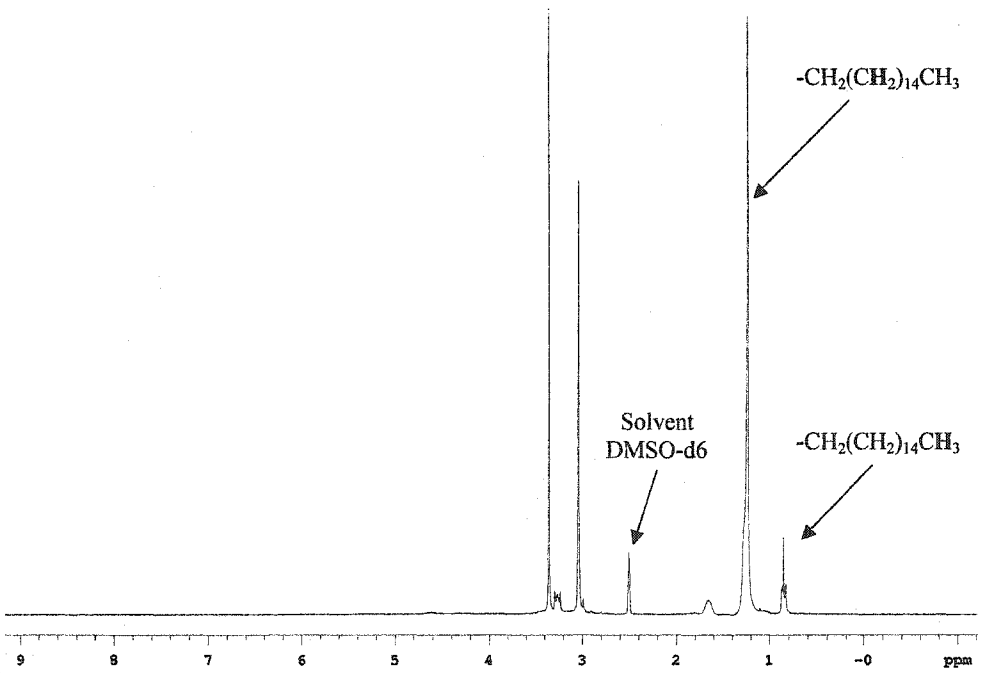

(b)

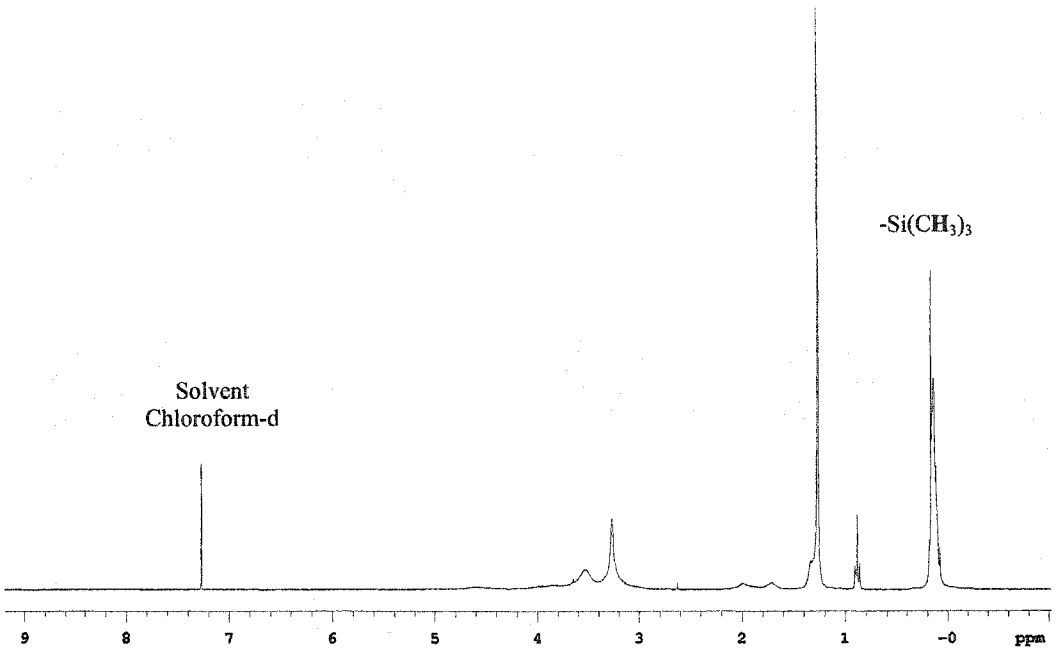

(c)

Figure 2.7 ^{1}H-NMR spectra of (a) HA; (b) HA-CTA; (c) silyl HA-CTA

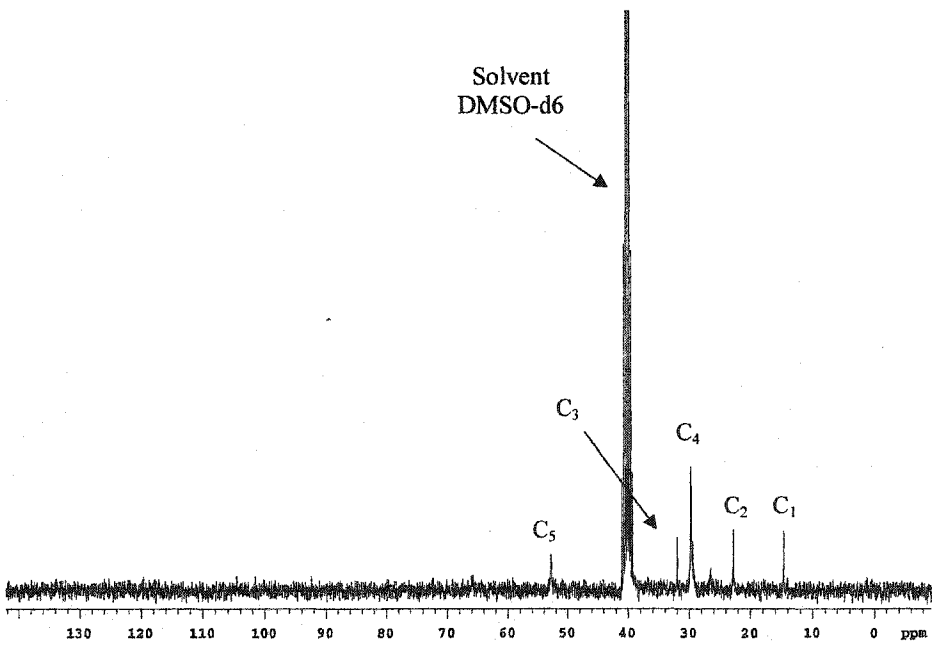

(a)

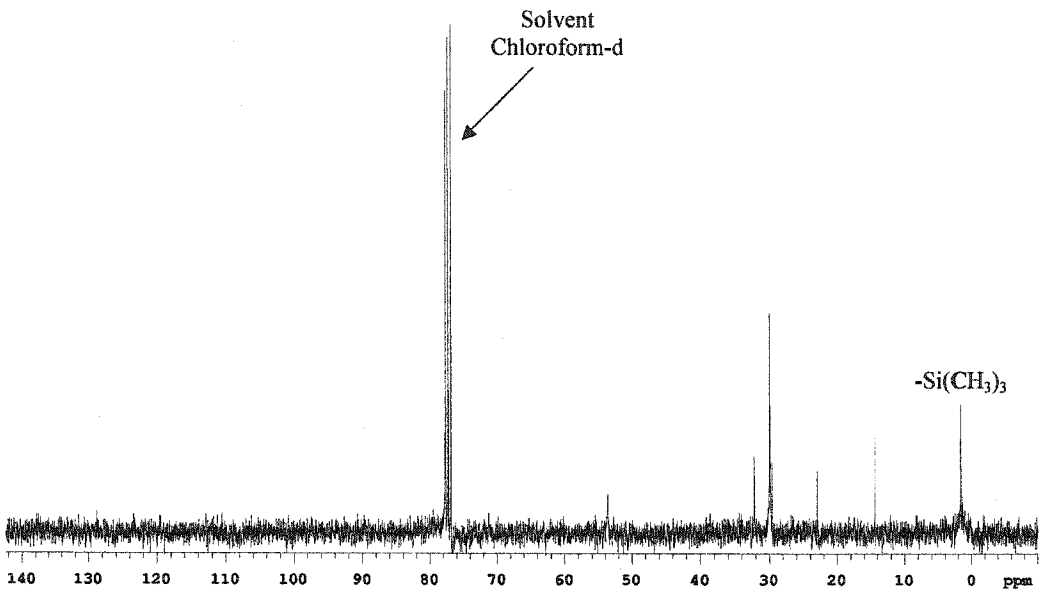

(b)

Figure 2.8 ^{13}C-NMR spectra of (a) HA; (b) HA-CTA; (c) silyl HA-CTA

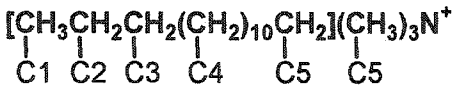

Figure 2.9 Schematic representation of –CTA group with the ^{13}C-NMR data

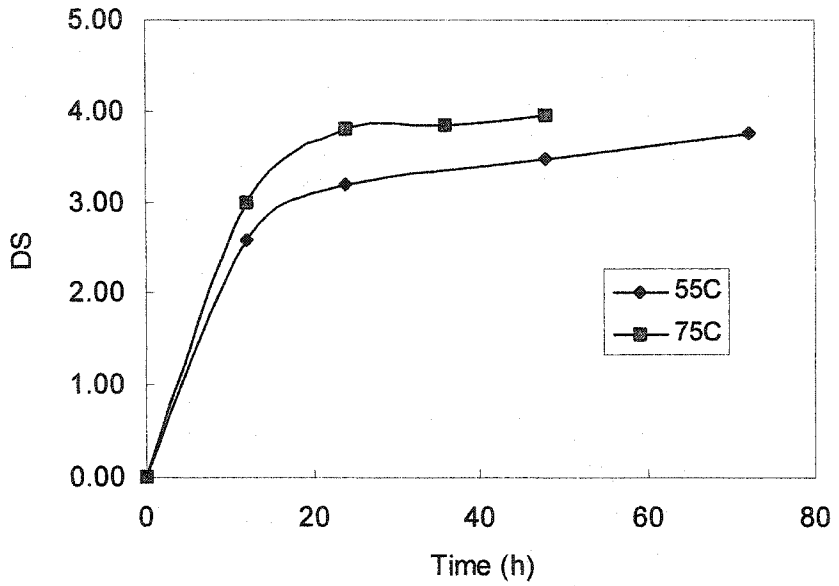

Figure 2.10 The effect of silylation temperature and time on the DS from weight gain

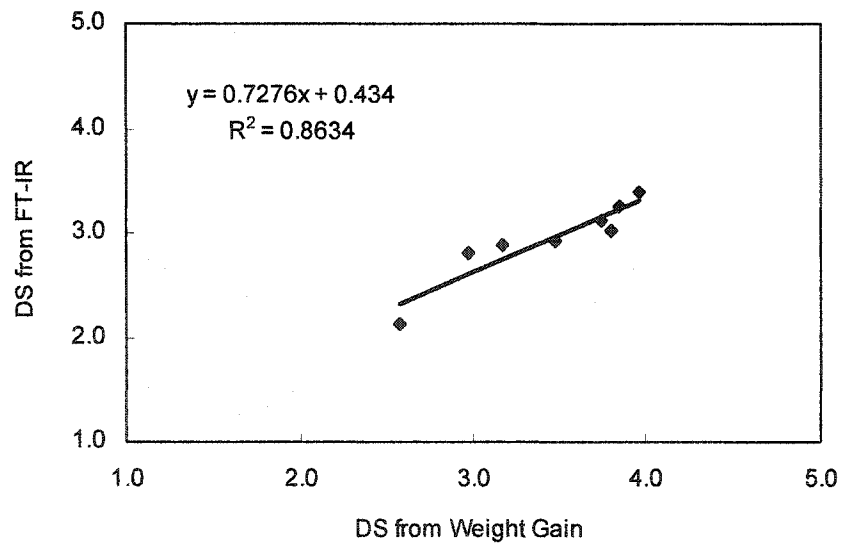

Figure 2.11 Calibration of the DS from FT-IR vs. the DS from weight gain

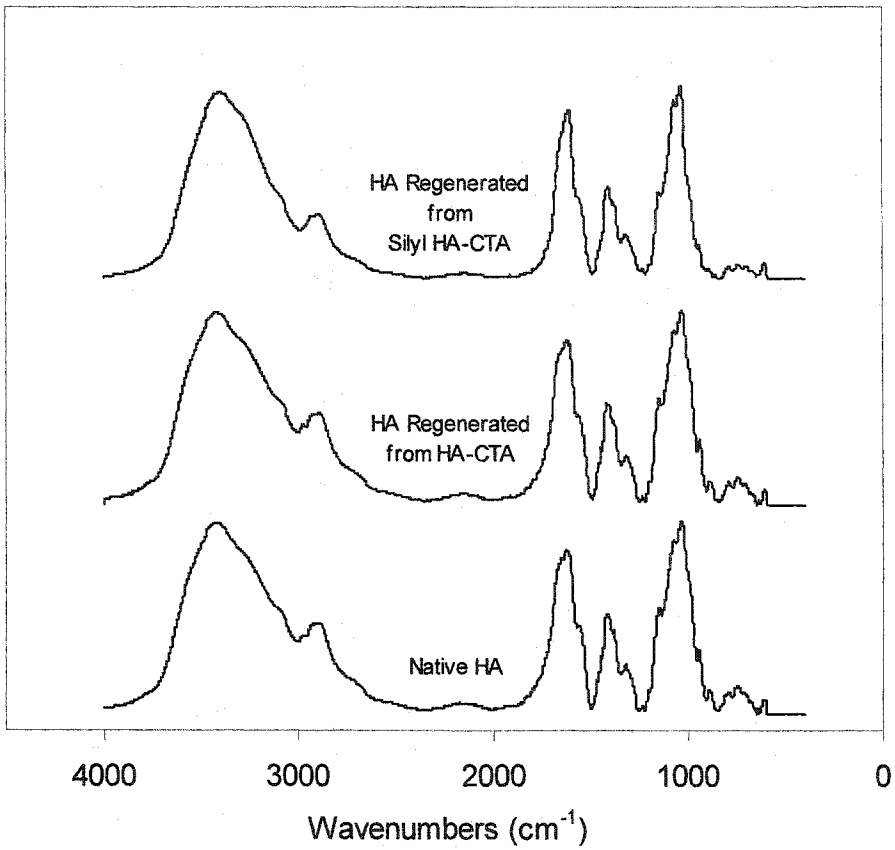

Figure 2.12 FT-IR spectra of HA regenerated from HA-CTA and silyl HA-CTA and native HA

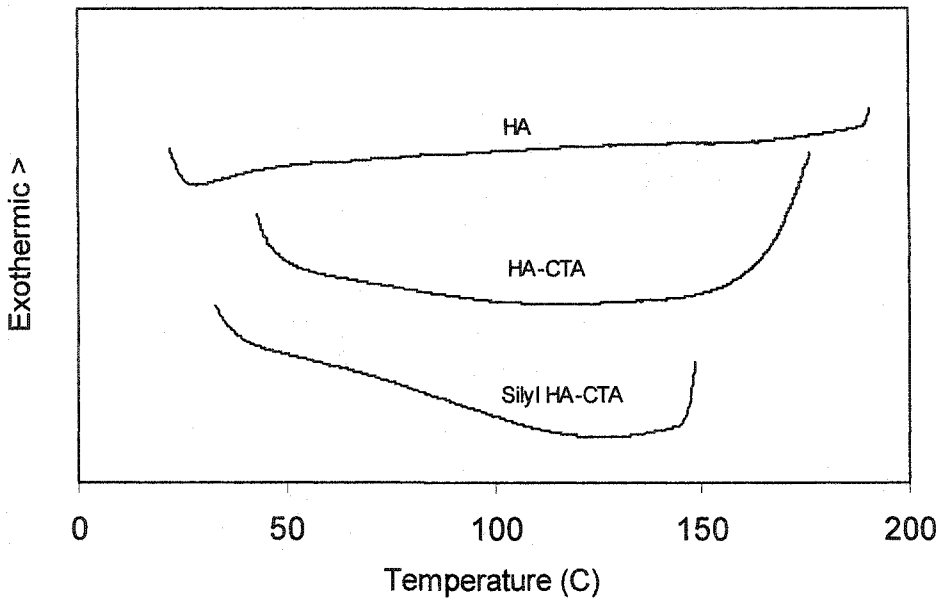

Figure 2.13 DSC thermograms of HA, HA-CTA and silyl HA-CTA

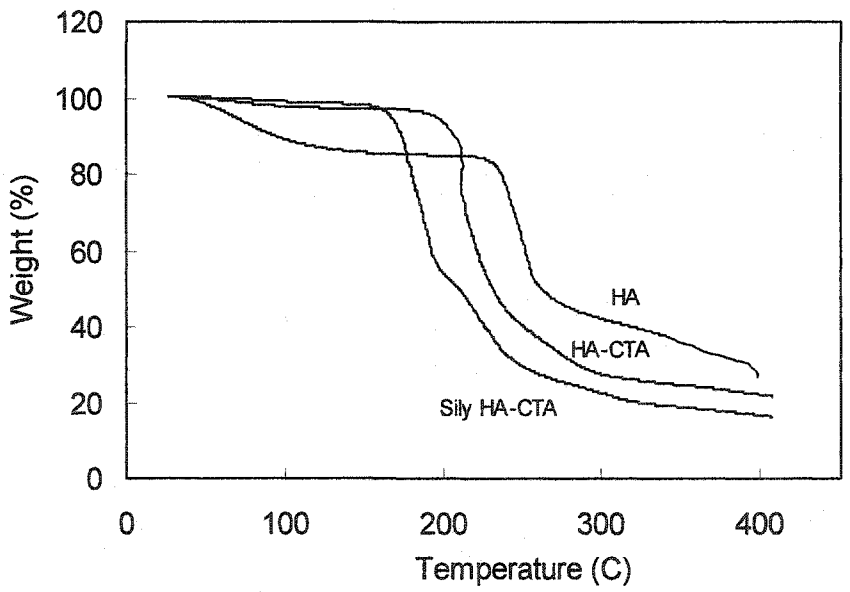

Figure 2.14 Thermal gravimetric analysis (TGA) of HA, HA-CTA and silyl HA-CTA

2.7 References

Birkofer L and Ritter (1965). The use of silylation in organic syntheses. *Angewandte Chemie, International Edition*, 4: 417-429.

Blakley ER (1966). Gas chromatography of phenolic acids. *Analytical Biochemistry*, 15: 350-354.

Cooper GK, Sandberg KR, and Hinck JF (1981). Trimethylsilyl cellulose as precursor to regenerated cellulose fiber. Journal of Applied Polymer Science, 26: 3828-3835.

Cowman MK, Hittner DM, and Feder-Davis J (1996). ^{13}C studies of hyaluronan: conformational sensitivity to varied environment. *Macromolecules*, 29:2894-2902.

Crescenzi V, Francescangeli A, Renier D, and Bellini D (2001). New hyaluronan chemical derivatives. Regioselectively C(6) oxidized products. *Macromolecules*, 34: 6367-6372.

Crescenzi V, Francescangeli A, and Taglienti A et al. (2003). Synthesis and partial characterization of hydrogels obtained via glutaraldehyde crosslinking of acetylated chitosan and of hyaluronan derivatives. *Biomacromolecules*, 4: 1045-1054.

Favia P, Palumbo F, and d'Agostino R et al. (1998). Immobilization of heparin and highly –sulphated hyaluronic acid onto plasma-treated polyethylene. *Plasma and Polymers*, 3: 77-96.

Goussé C, Chanzy H, and Excoffier G et al. (2002). Stable suspensions of partially silylated cellulose whiskers dispersed in organic solvents. *Polymer*, 43: 2645-2651.

Griebenow K, Santos AM, and Carrasquillo KG (1999). Secondary structure of proteins in the amorphous dehydrated state probed by FTIR spectroscopy. *The Internet Journal of Vibrational Spectroscopy,* Volume 3, Edition 1.
http://www.ijvs.com/volume3/edition1/section3a.htm

Gura E, Hückel M, and Müller PJ (1998). Specific degradation of hyaluronic acid and its rheological properties. *Polymer Degradation and Stability*, 59: 297-302.

Günther H (1994). *NMR Spectroscopy* (2nd edition). John Wiley & Sons: Chichester, England, pp. 23-25.

Harmon RE, De KK and Gupta SK (1973). New procedure for preparing trimethylsilyl derivatives of polysaccharides. *Carbohydrate Research*, 31: 407-409.

Harmon RE and De KK (1975). Silyl cellulose. In *Cellulose Technology Research, ACS Symposium Series 10* (edited by Turbak AF). American Chemical Society: Washington, D.C., pp.39-50.

Haxaire K, Maréchal Y, Milas M and Rinaudo M (2003). Hydration of polysaccharide hyaluronan observed by IR spectrometry. I. Preliminary experiments and band assignments. *Biopolymers*, 72:10-20.

Hermanutz F, Gähr F, and Pirngadi P et al. (2001). Process for producing silylated cellulose products for thermoplastic processing. *Chemical Fibers International*, 51:271-272.

Katsarava RD and Vygodskii YaS (1994). Silylation in the chemistry of polymers. *Polymer Yearbook*, 11:193-228.

Klemm D, Philipp B, and Heinze T et al. (1998). *Comprehensive Cellulose Chemistry.* Wiley-VCH: Weinheim, Germany, 2: 274-285.

Kurita K (2001). Controlled functionalization of the polysaccharide chitin. *Progress in Polymer Science*, 26: 1921-1971.

Langer SH, Connell S, and Wender I (1958). Preparation and properties of trimethylsilyl ethers and related compounds. *Journal of Organic Chemistry*, 23:50-58.

Laurent TC, Ryan M, and Pietruszkiewicz A (1960). Fractionation of hyaluronic acid. *Biochimica et Biophysica Acta*, 42: 476-485.

Lowry KM and Beavers EM (1994). Thermal stability of sodium hyaluronate in aqueous solution. Journal of Biomedical Materials Research, 28:1239-1244.

Monsef-Mirzai P, Manak H, and McWhinnie WR et al. (1998). Microwave driven trimethylsilylation of phenolformaldehyde resins: extent of reactions determined by ^{13}C and ^{29}Si n.m.r. *Fuel*, 77: 369-374.

Mormann W, Demeter J, and Wagner T (1999). Partial silylation of cellulose with predicatble degree of silylation-stoichiometric silylation with hexamethyldisilazane in ammonia. *Macromolecular Chemistry and Physics*, 200:693-697.

Moulder JF, Stickle WF, Sobol PE, and Bomben KD (1992). *Handbook of X-Ray Photoelectron Spectroscopy.* Physical Electronics Division: Eden Prairie, MN.

Nouvel C, Ydens I, and Degée P et al. (2002). Partial or total silylation of dextran with hexamethyldisilazane. *Polymer*, 43: 1735-1743.

Pawlowski WP, Gilbert RD, Fornes RE, and Purrington ST (1988). The liquid-crystalline properties of selected cellulose derivatives. *Journal of Polymer Science: Part B: Polymer Physics*, 26:1101-1110.

Pawlowski WP, Sankar SS, and Gilbert RD (1987). Synthesis and solid state ^{13}C-NMR studies of some cellulose derivatives. *Journal of Polymer Science: Part A: Polymer Chemistry*, 25: 3355-3362.

Pierce AE (1968). *Silylation of Organic Compounds*. Pierce Chemical Company: Rockford, IL, pp. 1-26.

Rodriguez F (1996). Viscous Flow. *In Principles of Polymer Systems (4th edition)*. Taylor & Francis: Washington, D. C., pp.225-289.

Schuyten HA, Weaver JW, Reid JD, and Jurgens JF (1948). *Journal of the American Chemical Society*, 70: 1919-1920.

Scott JE (1960). Aliphatic ammonium salts in the assay of acidic polysaccharides from tissues. *Methods of Biochemical Analysis*, 8: 145-197.

Smith B (1998). *Infrared Spectral Interpretation*. CRC Press: New York, pp.158-160.

Ydens I, Rutot D, and Degée P et al (2000). Controlled synthesis of poly(ε-caprolactone)-grafted dextran copolymers as potential environmentally friendly surfactants. *Macromolecules*, 33: 6713-6721.

Zollfrank C (2001). Silylation of solid beech wood. *Wood Science and Technology*, 35: 183-189.

Chapter 3

UHMWPE-Hyaluronan Micro-Composites

3.1 Introduction

A hydrophilic lubricious polymer surface is often conferred to medical devices made from hydrophobic resins through coating to increase biocompatibility, minimize friction and injury or inflammation of tissues, and reduce fouling [Ikada and Uyama, 1993]. Fan [1990] classified the hydrophilic coating processes into five categories based on the chemical nature of the resulting coatings: (1) simple dip or spray coating with hydrophilic polymers; (2) blending the hydrophilic polymer with the substrate; (3) chemically or physically forming an interpenetrating polymer network (IPN) with the substrate molecules; (4) hydrophilic polymers chemically bonded to the substrate or a tie coating; (5) surface grafting through in-situ polymerization of hydrophilic monomers. The first and second processes involve only physical coating operations; no chemical reactions occur. The third method may or may not have chemical reactions. Chemical reactions are definitely part of the fourth and fifth processes. With the introduction of chemical bonding in these processes, adhesion to the substrate and abrasion resistance increase, and the coatings become more and more durable.

Hyaluronan has been used to provide a biocompatible and lubricious surface through crosslinking or grafting, as has been described in Section 1.2.5.9. The interpenetrating

polymer networks of HA with other biomaterials were also discussed in Giusti and Callegaro's patent [1997]. However, these coatings or materials were not meant for load-bearing surface applications. For example, in total hip replacements, the compressive stress acting on the UHMWPE acetabular cups can be as high as 3000 psi [Hodge et al., 1986]. To withstand such severe conditions, hydrophilic polymer coatings must be firmly anchored on and within the UHMWPE matrix.

The hydrophilic UHMWPE surface created by Beauregard [1999] was formed from rooting poly-L-lysine into UHMWPE surface via formation of an interpenetrating network. However, the treatment was time-consuming, the depth of poly-L-lysine penetration was not controllable, the long-term swelling with xylenes solution at high temperature might cause matrix distortion, and the final lubricious layer was not uniform. UHMWPE preforms with a porous surface layer were used in the present study to solve these problems.

The preparation and application of porous UHMWPE films or sheets have been disclosed in several patents. Goethel et al. [1962] produced porous polyethylene articles by sintering the particles of polyethylene (MW: 10,000 to 1,000,000 g/mol) under heat and pressure without melting of the particles. Stein [1989] mixed polyethylene with a hydrocarbon wax first, and then heated it under pressure to a temperature above the melting point of UHMWPE for a period of time to allow particles to soften and contact with each other. The hydrocarbon wax was extracted from the fused mass to form porous articles. The method Duling et al. [1976] used to produce the UHMWPE porous articles was almost the same as Stein's. The only difference is that they heat the mixture first to a temperature above the melting point of the hydrocarbon before the final fusion heating.

These porous articles can be used as filters, diffusers, pen tips [Stein, 1989], and battery separators etc. [Navarrete et al. 2002]. They can also be used as preforms to produce molded articles that cannot be easily manufactured from the crude UHMWPE powder [Aoyama et al., 1989].

Silyl HA-CTA described in Chapter 2 is hydrophobic and can dissolve in xylenes at high DS, so a solution of it can easily diffuse into the pores of UHMWPE preforms within several minutes. After crosslinking the silyl HA-CTA in situ and then returning it to its unmodified state via hydrolysis, the treated porous performs are molded for the second time to consolidate the UHMWPE. The pores in UHMWPE preforms are inter-connected and tens of microns in size, so the finally molded material is called a micro-composite.

3.2 Materials and Methods

3.2.1 Materials

Silyl HA-CTA and silyl HA-CP were obtained through the methods described in Chapter 2. The original sodium hyaluronate (HyluMed®, medical grade, MW: 1.36×10^6 daltons) was purchased from Genzyme (Cambridge, MA). Toluidine Blue O (TBO), urea, dilaurate and 1,8-diisocyanotooctane (OMDI) were obtained from Aldrich (Milwaukee, WI). Desmodur N 3200 (1,6-hexamethylene diisocyanate based polyisocyanate) was provided by Bayer (Pittsburgh, PA). Xylenes, acetone and NaCl were purchased from Fisher (Pittsburgh, PA), and xylenes and acetone were dried by refluxing over Na and anhydrous $CaSO_4$, respectively, and distilled just before use. Ethanol (ACS/USP grade) was obtained from Pharmco (Brookfield, CT). All chemicals were used as received

unless specified. UHMWPE porous disk preforms (Φ 1.5″ and 4″) with different porosities were made from GUR 1020 resin, and were provided by DePuy Orthopaedics (Warsaw, Indiana). The pore size of the samples was approximately 1-20 microns. For other sample parameters, please see Table 3.1.

3.2.2 Fabrication

Preparation of crosslinked silyl HA-CTA powder: 5 ml of 50 mg/ml silyl HA-CTA xylenes solution were charged into a small vial, and 2 ml of 2% Desmodur N 3200 acetone solution were added under dry N_2. The solution mixture was shaken for a while, and left to stand at room temperature for one day. The precipitate was filtered from the solution, washed with acetone several times, and then vacuum dried at 50°C for 24 hours. The resulting powder was used for FT-IR and TG analysis.

UHMWPE-HA micro-composites: All the UHMWPE preforms were washed with acetone and ethanol, and then dried under vacuum before treatment. All the treated preforms were re-molded at DePuy Orthopaedics at 155-160°C. All the hydrolysis was performed at 45°C for 24 hours in 0.2M NaCl solution of water and ethanol (v/v 1:1), unless otherwise specified.

The first batch of samples was treated with silyl HA-CP solution (Table3.2). Two xylenes solutions (each 50 ml) of silyl HA-CP with 15mg/ml and 30mg/ml concentrations were prepared. 1,8-Diisocyanotooctane (OMDI, 0.75ml) and dibutyltin dilaurate (30 μl) were dissolved in 50 ml of acetone to make a crosslinking solution. Clean preforms were first soaked in 15mg/ml silyl HA-CP solution for 10 minutes, and vacuum dried at 50°C for 1 hour. The soaking was then repeated in 30 mg/ml solution.

After drying, the samples were dipped in the OMDI solution, and then crosslinked in a 50°C vacuum oven overnight. The treated samples were then re-molded by DePuy Orthopaedics and hydrolyzed.

All other batches of samples (i.e., batches 2-4, Table 3.1) were treated with silyl HA-CTA solution. For the 2nd batch of samples, the following solutions were first prepared: three xylenes solutions (each 50 ml) of silyl HA-CTA with 25, 50 and 75mg/ml concentrations, 50ml of 1% Desmodur N 3200 acetone crosslinking solution, and 50ml of a 0.5% native HA aqueous solution. The dry and clean preforms were respectively soaked in 25, 50 and 75mg/ml silyl HA-CTA solutions for about 10 minutes. Between soakings, each sample was vacuum dried at 50°C for 1 hour. After soakings and drying, all samples were dipped in Desmodur solution, and then crosslinked in a 50°C vacuum oven for 2 hours. The soaking and crosslinking procedure was then repeated once. All six samples were submitted to the above protocol, but the treatments varied in the following way: prior to re-molding, sample A (1 piece) was slightly crosslinked by γ-irradiation (30 KGy dose), while samples C (2 pieces) and D (1 piece) were hydrolyzed, and then sample D was soaked in HA solution for 10 minutes, dried and crosslinked as above. All the treated samples were also re-molded. Samples A and B (2 pieces) were hydrolyzed after molding.

For the 3rd batch of samples, the concentration of Desmodur N 3200 acetone solution was 5%, and the concentration of native HA solution was 1%. The silyl HA-CTA solutions were the same as those used for the 2nd batch. Samples were first soaked in 25 mg/ml silyl HA-CTA solution, and then crosslinked. The soaking and crosslinking operations were then repeated in 50 and 75 mg/ml silyl HA-CTA solutions. After

hydrolysis, but before re-molding, all samples were coated with 1% HA solution and crosslinked.

For the fourth batch of samples, 2% Desmodur N 3200 acetone solution and 50 mg/ml silyl HA-CTA xylene solution were prepared, while the HA solution was the same as that used for the 3rd batch. The samples were soaked in the silyl HA-CTA solution, and then crosslinked. Hydrolysis was carried out in 0.2 M NaCl solution of water and ethanol (v/v 1:1) for 40 hours, and the solution was changed every 10 hours. Ultrasonic water bath was employed to assist hydrolysis, but the total time was not beyond 2 hours. The hydrolyzed samples were dipped with HA solution and then crosslinked.

3.2.3 Characterization

Fourier transform infrared spectroscopy (FT-IR): The crosslinked silyl HA-CTA powder (1%, w/w) was ground and mixed with KBr, and pressed into pellets for analysis. The FT-IR instrument and measurement method were the same as that described in Section 2.2.3.

Thermal gravimetric analysis (TGA): The TG analysis of crosslinked silyl HA-CTA powder was performed on the same instrument used for HA and its other derivatives, but the heating rate was 5°C/min. The other test conditions were the same as described in Section 2.2.3.

X-ray photoelectron spectroscopy (XPS): Small pieces were cut from the surface layer of UHMWPE porous perform and micro-composite samples to fit the XPS sample

holder. The equipment, test conditions and analysis method were the same as that described in Section 2.2.3.

Visible spectroscopy: The visible absorbance of TBO solution was measured with a Cary 500 UV-Vis-NIR spectrometer (Varian Analytical Instruments, CA). A series of TBO standard solutions in 8M urea and 0.15 M NaCl (10, 20, 30, 40 and 50μM) were prepared to obtain a standard calibration curve by measuring the absorbance at 632nm. The micro-composite samples were flooded with TBO 0.1% in 8M urea and then rinsed with distilled water. After drying at room temperature, TBO dye bound to HA on the sample surface was eluted with 0.15M NaCl in 8M urea. Elution was performed dropwise, and continued until no more dye was visible in the runoff. The elutant was collected, and measured in volume. The visible absorbance of the elutant was obtained in Cary 500, and the concentration was calculated based on the standard curve. The surface density of HA was determined with the amount of dye over the surface area of the samples.

Aqueous Contact Angle Analysis: Static water contact angles were measured using the sessile drop method with a Krüss DSA 10 goniometer (KRŰSS GmbH, Hamburg). Before measurement, all samples were conditioned in distilled water for 4 hours. At ambient temperature, a water drop with a known volume (1 μL) was applied to the sample surface through the automatic dosing feature of DSA 10. The contact angles were determined with circle fitting profile after the video system imaged the water drop. At least five different locations on each sample surface were tested. To observe how the dry, uniform HA film hydrated with time, 3 μL of water drop was used, and the contact angles

were recorded at 1-minute interval until no data could be extracted from the system. At least 3-points were tested for each sample.

3.3 Results and Discussion

3.3.1 Crosslinking of Silyl HA-CTA

The FT-IR spectrum of crosslinked silyl HA-CTA is shown in Figure 3.1, and in comparison with HA-CTA and silyl HA-CTA. All peaks related with $Si(CH_3)_3$ vibrations (758, 847, 879 and 1250 cm^{-1}) disappear or decrease, indicating the removal of $Si(CH_3)_3$ groups during crosslinking. Increases in the intensity of peaks at 3450, 2926/2855 and 1463/1435 cm^{-1} respectively are related to the –NH- stretching of urethane, the stretching and bending of $–CH_2$ groups introduced with Desmodur N 3200. The absence of a strong peak near 2260 cm^{-1} demonstrates the complete conversion of –N=C=O into urethane during crosslinking [Smith, 1998]. The new peaks at 1768, 1524 and 772 cm^{-1} respectively are due to the C=O stretching, -NH- in-plane and out-of-plane bending of secondary urethane (-NH-COO-) [Hepburn, 1992; Bailey & Critchfield, 1981]. Amide I and II (–NHC=O) shift to 1691 and 1562 cm^{-1} from 1670 and 1558 cm^{-1} after silyl HA-CTA crosslinking.

Desmodur N 3200 is an aliphatic polyisocyanate resin based on hexamethylene diisocyanate (HDI). The reaction between Desmodur N 3200 and the un-silylated –OH residues of silyl HA-CTA should follow the regular reaction mechanism of isocyanates and alcohols to form urethane linkages, illustrated in Figure 3.2 [Rodriguez, 1996]. Gonda and Antalová [1991] have verified that the silylated N-containing nucleophiles could undergo nucleophilic addition to isocyanates similar to their non-silylated

counterparts. The reactivity of the silylated nucleophiles depends on the stability of the Si-N bonds, and in some cases they are more reactive than their non-silylated counterparts. Along similar lines of thought, the silylated O-containing nucleophiles (O-$Si(CH_3)_3$ of silyl HA-CTA) may also react with isocyanates. The disappearance or decrease of -$Si(CH_3)_3$ vibration related peaks and the appearance of urethane vibration related peaks in the FT-IR spectrum of crosslinked silyl HA-CTA demonstrated the crosslinking reaction occurring between O-$Si(CH_3)_3$ groups and isocyanates .

The TG curve of crosslinked silyl HA-CTA is shown in Figure 3.3. Compared with silyl HA-CTA, HA-CTA and HA, the thermal stability of crosslinked silyl HA-CTA is significantly increased. After hydrolysis and removal of –CTA groups, the crosslinked HA should be more heat resistant, and thus able to withstand the re-molding temperatures used on the UHMWPE preforms.

3.3.2 UHMWPE-HA Micro-Composites

The existence of HA on the surface of UHMWPE-HA micro-composites can be confirmed with XPS analysis and dye assay. Table 3.3 shows the XPS elemental analysis results of UHMWPE control, the various intermediates, and one of the micro-composites (sample D of the 2nd batch). Nitrogen, at similar levels to that found in HA, was found at the surface of the micro-composite, but none was detected in either the UHMWPE preform or molded control disk, demonstrating the presence of a thin layer of HA on the micro-composite surface. The amount of nitrogen beyond that found in HA might come from the -CTA residue, which could not be completely removed during hydrolysis. This may be due to the inability of enough water to enter the pores, the inability of the –CTA

groups to come out of the micro-pores, or from the urethane linkages. Both contamination and un-hydrolyzed -$Si(CH_3)_3$ residue might possibly be the source of the silicon detected in the micro-composite. However, it is most likely to be from contamination, such as vacuum grease and elastomer gloves, because even in the UHMWPE solid control, a significant amount of silicon was found.

The N1s spectrum of sample D is shown in Figure 3.4, which can be best fit with two peaks similar to HA-CTA and silyl HA-CTA: one at 399.8 eV, and one at 402.8 eV. However, the intensity of the peak at 402.8 eV is much smaller than that at 399.8 eV. Ammonium salt N^+ introduced with CTA contributes to the peak at 402.8 eV. A large decrease in the intensity of this peak means the removal of most –CTA groups during hydrolysis of the samples. To completely remove –CTA groups, the hydrolysis conditions must be improved, e.g., using ultrasound.

The C1s spectrum of the UHMWPE preforms (Figure 3.5a) can only be split into two components: C0 and C1. C0, from CH_2 and C-C of UHMWPE, is very strong, while C1 is very weak. The C1 peak may be due to residue of the pore-forming agent (poragen), e.g. polyethylene oxide, used by DePuy to make the porous performs. In the C1s spectrum of the micro-composite (Figure 3.5b), two new components, C2 and C3, are observed. They are respectively assigned to O-C-O and -O-C=O/-HN-C=O of HA, indicating the presence of HA on the surface of micro-composite.

The incorporation of HA on the micro-composite surface was also demonstrated by dye assay. TBO is a cationic dye, which can bind negatively charged groups on the polymer, such as sulfate groups on heparin and carboxyl groups on HA, so it is often used to visualize or quantify polysaccharide in coatings and tissue sections [Johnston, 2000].

After soaking in TBO solution for several minutes, the UHMWPE-HA micro-composite surface exhibited a dark to light purple color depending on the surface density of HA, which will be discussed in detail in the following Section. However, the UHMWPE preform and solid control were not dyed by the TBO solution. Although they have significant amounts of oxygen on their surfaces, they remained un-dyed, indicating that their oxygen is not that in carboxylate groups ($-COO^-$).

3.3.3 The Effect of Treatment Conditions on the Surface Properties of Micro-Composites

The surface properties of UHMWPE-HA micro-composites were characterized by aqueous contact angles and measuring the surface density of bound HA. The binding between TBO and HA is a simple ion exchange equilibrium process, so strong salts, such as NaCl, can be used to remove TBO from the dyed sample surface. TBO has a strong absorption at 632 nm in 8 M urea solution (Figure 3.6), so the solution was used with NaCl to elute bound TBO from the dyed surfaces. The standard calibration curve (Figure 3.7) shows a good linear relationship between the visible absorbance and TBO concentrations within 50 μM. In 8M urea solution, TBO binds carboxyl group at a 1:1 molar ratio [Johnston, 2000], while each HA repeat disaccharide unit has just one carboxyl group, so TBO amount diluted from the sample surface can be directly used to calculate the surface density ($nmol/cm^2$) of bound HA.

The first batch of samples was treated with silyl HA-CP. The decomposition of pyridinium groups during silylation resulted in a brown product, so the treated UHMWPE samples were also brown. The contact angles for all the HA-CP/UHMWPE

micro-composite samples were around 75°, not a large reduction compared with 91.2° of the control. Thus, the treatment was not successful perhaps because the decomposition of pyridinium groups affects the HA structure. However, this trial still provided some beneficial information. For example, it was observed that the overflow of UHMWPE during molding might mask the silyl HA-CP on the surface, resulting in a non-significant decrease in contact angles, compared to the control sample.

For the remaining batches (2-4), silyl HA-CTA was used instead of silyl HA-CP to avoid the pyridinium decomposition problem. The silyl HA-CTA was pale yellow, so the treated UHMWPE preforms remained white. In the 2nd batch, the effects of pre-irradiation and hydrolysis before or after re-molding on the micro-composite surface properties were investigated. The results of HA surface density and contact angle for the second batch are listed in Table 3.4. The relationship between the contact angle and HA surface density is apparent: with increasing HA surface density, contact angles decrease.

Samples C and D, hydrolyzed *before* final molding, exhibited significantly lower contact angles than samples A and B (Figure 3.8), hydrolyzed *after* final molding. The regenerated, crosslinked HA within C and D preform pores after hydrolysis had good high temperature resistance and high hydrophilicity. This prevented HA from degrading and UHMWPE from overflowing and masking HA on the surface during re-molding. Thus, the HA surface density of C and D was much higher than that of A and B. Although sample D is not significantly lower in contact angle than sample C, it appears that coating with an HA solution after hydrolysis, and subsequent crosslinking of the coating, increases the surface density of HA. If an HA solution with higher concentration were used, the effect may become significant.

Pre-irradiation was used to crosslink sample A in an attempt to limit the overflow of the UHMWPE during molding, but it also caused severe degradation of the silyl HA-CTA in the preform. Silylation itself also reduced the thermal resistance of HA: the decomposition temperature of silyl HA-CTA was very close to the molding temperature, so samples A and B exhibited discoloration and degradation. Furthermore, the trimethylsilyl residues trapped within the samples could not be removed with hydrolysis after molding. Therefore, the treatment conditions for samples C and D are superior to those for samples A and B. Furthermore, it may be that the D treatment conditions are better than those used in C.

However, visual observation and dye assay of the HA film on the surface of samples C and D indicated the films were not uniform, so process modification was necessary to improve surface HA film uniformity. Methods that can increase HA surface density include crosslinking after each soaking with silyl HA-CTA solution, increasing the HA concentration of the final soaking, and using a higher porosity perform. The effects of these methods were examined in the latter two batches of samples.

Compared to the 2nd batch, process changes in the 3rd batch included: (1) preforms with 20% and 40% porosity, (2) crosslinking silyl HA-CTA after each soaking, (3) 5% crosslinking solution instead of previous 1%, (4) 1% HA solution instead of previous 0.5%. The 5% crosslinking concentration was selected based on an enzyme degradation experiment, described in more detail in Chapter 4. Several small pieces of 20% porosity UHMWPE porous preforms were treated with the same process used for the 2nd batch, but four different crosslinking concentrations were used, including 0.2%, 1%, 2% and 5%. It was found that the samples crosslinked with 2% and 5% Desmodur solution still

had a uniform HA film after degradation in a high concentration hyaluronidase solution, which was comparable to that before degradation. However, for those samples crosslinked with 0.2% and 1% Desmodur solution, the HA film was not so uniform, and peeled off in small local regions.

Aqueous contact angles of the 3rd batch are shown in Figure 3.9. No significant differences are found between all the samples through ANOVA and student's T-test. The results for this batch of samples are not desirable, as expected, and are inferior to the results for the 2nd batch. One possible reason was the high crosslinker concentration, which might consume too many –OH groups, decreasing the surface density of polar groups. The multiple soaking and crosslinking operations also resulted in a very high silyl HA-CTA content in the porous samples (Table 3.5), especially in the 40% porosity samples. It was very difficult to completely hydrolyze so much silyl HA-CTA within very small pores. The molecular weight of the silyl HA-CTA repeat unit (951.6) is more than two times that of the HA repeat unit (401.3), so after complete hydrolysis, the weight change of the samples should decrease to less than half of that after soaking and crosslinking. However, data in Table 3.5 show that the weight after hydrolysis is much larger than expected, indicating an incomplete hydrolysis. The silyl HA-CTA residue was compatible with UHMWPE, and was easily covered by flowing UHMWPE during re-molding. This may be the reason that the 40% porosity samples have more scattered contact angles, while the 20% porosity samples have a more uniform film of HA. In addition, the un-hydrolyzed silyl HA-CTA easily decomposed at the molding temperature, and became brown. This can be demonstrated by the much more severe local brownness in the 40% porosity samples. Too much HA might also prevent the full

consolidation of UHMWPE, resulting in a poorly consolidated final product. Visual observation indicated the 1.5″ 40% porosity sample had nominally good consolidation, but the 4.0″ 40% porosity sample was so poorly consolidated that it cannot be used for tensile testing. Based on the above analysis, it can be seen that lower silyl HA-CTA content within the porous preform and high HA content on the surface are necessary to obtain a material with good comprehensive properties.

To solve the above problems, the following changes were performed in the 4th batch: (1) soaking and crosslinking just once, (2) 2% crosslinker solution, (3) application of ultrasound during hydrolysis (2 hours), (4) soaking with HA solution twice and crosslinking. The samples treated with the new method have a moderate silyl HA-CTA and high surface HA content (Table 3.5). After soaking in water, the surfaces of all samples were completely wetted by water, a uniform water-swollen layer formed at the surface. The water drop immediately spread on the surface, indicating the formation of a uniform layer of HA film on the micro-composite surface. The wetted surface could not be used for contact angle measurements due to the rapid spreading of the water drops, so a dry surface was used to observe the hydration of the surface HA film. At the same time, the two 1.5″ disks from the 3rd batch were also tested after soaking with HA solution and crosslinking again (3'-1# for re-treated 20% porosity 1.5″ disk, 3'-2# for re-treated 40% porosity 1.5″ disk). A uniform HA film was also formed on the two disk surfaces after re-treatment. 4-1# and 4–2# in Figure 3.10 respectively represented those two 1.5″ 40% porosity disks of the 4th batch. The water drop used in this contact angle testing was 3 μL. It is observed that with the hydration of HA film, the contact angles of the micro-composites rapidly decrease from the initial almost hydrophobic state until the water drop

evaporated. From the trend of the curves, it may be inferred that within 15-20 minutes, water drops should completely spread in a saturated water-vapor environment, and the HA film on the treated samples can be completely hydrated. However, for the control sample, the decrease of contact angles with time and evaporation was very slow, and equilibrated around 65°.

3.4 Conclusions

XPS analysis and TBO dye assay demonstrated the presence of HA on the surface of the micro-composite. In comparison with the control, the contact angles of the appropriately treated micro-composites significantly decreased, and the degree of decrease was related to the surface density of HA. The higher the surface density of HA, the lower the contact angles of the micro-composites.

Hydrolysis before re-molding was necessary due to the inferior thermal stability of the silyl HA-CTA. The hydrolyzed and crosslinked HA was much more stable, and was able to withstand the re-molding temperature without discolor. This was confirmed by samples C and D of the 2^{nd} batch and by all the samples of the 4^{th} batch. Furthermore, the hydrolyzed HA-CTA was hydrophilic and not compatible with the UHMWPE, so it was effective in preventing the overflow of UHMWPE and keeping the HA exposed at the material surface.

It was also found that the concentration of the Desmodur crosslinking solution must be moderate to obtain a lubricious and stable HA film. High crosslinker concentration consumed too many polar groups, causing higher contact angles, while too low crosslinker concentration led to a sparse HA network, which was not strong enough to

resist enzymatic-degradation. The 2% Desmodur solution seemed a good compromise between these extremes.

Unexpectedly, the high silyl HA-CTA content within the porous preforms that resulted from multiple soaking and crosslinking operations did not achieve a uniform HA film and very low contact angles. Furthermore, too much silyl HA-CTA in the preforms was difficult to completely hydrolyze and adversely affected the consolidation of the micro-composites. In direct contrast, a small to moderate silyl HA-CTA content and high surface HA content were desirable. This was demonstrated by the formation of a uniform layer of HA film on the samples of the 4^{th} batch. By soaking and crosslinking the preforms only once and using a high concentration HA solution for the final soaking, an appropriate amount of silyl HA-CTA and a large amount of surface HA were obtained. Short periods of ultrasonic treatment were helpful in completely removing the modified groups during hydrolysis.

3.5 Tables

Table 3.1 Parameters of UHMWPE porous preforms

Batch Number	Porosity (%)	Porous Structure	Number of Samples	Diameter (in)	Thickness of Solid Layer (in)	Thickness of Porous Layer (in)
1st	30-35	Through	3	1.5	0	0.25
		Top layer	3	1.5	0.5	0.1
	40	Through	3	1.5	0	0.3
2nd	20	Through	6	1.5	0	0.125
3rd	20	Through	1	4.0	0	0.15
		Top layer	1	1.5	0.75	0.15
	40	Through	2	4.0	0	0.2
		Top layer	1	1.5	0.75	0.2
4th	40	Through	1	4.0	0	0.2
		Top layer	1	4.0	0.09	0.05
			1	4.0	0.06	0.1
			3	1.5	0.75	0.2

Table 3.2 Summary of different sample treatments

Sample	Conc. of silyl HA	Conc. of Crosslinker	Soaking & crosslinking	Hydrolysis	Soaking with HA	Conc. of HA
1st batch	Silyl HA-CP I - 15 mg/ml II - 30 mg/ml	15μl/ml OMDI + 4% dilaurate	I→ II→ OMDI	After molding	No	N/A
2nd batch	Silyl HA-CTA I - 25 mg/ml II - 50 mg/ml III - 75 mg/ml	Desmodur 1%	I→ II→III →Desm. Two cycles			
A				Pre-radiation & After molding	No	N/A
B				After molding	No	N/A
C				Before molding	No	N/A
D				Before molding	Yes	0.5%
3rd batch	Silyl HA-CTA I - 25 mg/ml II - 50 mg/ml III - 75 mg/ml	Desmodur 5%	I→Desm. → II→Desm.→ III→Desm.	Before molding	Yes	1%
4th batch	Silyl HA-CTA I – 50mg/ml	Desmodur 2%	I→Desm.	Before molding	Yes	1%

Table 3.3 XPS elemental analysis results

Sample	C (%)	O (%)	N (%)	Si(%)	Na(%)	Cl(%)	F(%)	Br (%)
HA	57.8	35.9	3.2	0	3.0	0	0	0
HA-CTA	80.8	12.9	4.3	0	0	0.4	0	1.7
Silyl HA-CTA	65.6	20.4	2.7	11.4	0	0	0	0
UHMWPE Preform	97.2	2.8	0	0	0	0	0	0
Molded UHMWPE (Control)	77.9	14.0	0	6.6	0	1.0	0.5	0
Sample D	71.8	22.4	3.7	2.1	0	0	0	0

Table 3.4 Surface Properties of the 2nd of batch of micro-composite samples

Sample	Surface density of HA (nmol/cm^2)	Aqueous Contact Angle (°)
Control	0	91.20 ± 1.64
A	3.76	72.01 ± 11.53
B	6.31	46.15 ± 5.53
C	34.01	32.44 ± 3.18
D	36.17	26.77 ± 6.28

Table 3.5 Weight changes ($\Delta w/w_0$*) of UHMWPE preforms during treatment

Sample	Weight Change (%)		
	After soaking and crosslinking	After hydrolysis	After coating with HA
2nd batch			
A	4.74		
B	5.55		
C	5.06	0.35	
D	5.00	0.40	1.54
3rd batch			
1.5″-20% porosity	2.97	2.27	2.68
1.5″-40% porosity	8.50	6.35	8.00
4.0″-20% porosity	1.98	1.46	1.64
4.0″-40% porosity	15.94	11.02	13.6
4th batch			
1.5″-40% porosity-1#	6.36	1.10	3.31
1.5″-40% porosity-2#	3.88	1.12	2.51
4.0″-40% porosity-1/4	8.66	1.63	5.03
4.0″-40% porosity-1/2	6.10	0.81	3.39
4.0″-40% porosity-through	5.60	0.83	1.80

Δw: weight change in comparison with the original weight of UHMWPE performs (w_0).

3.6 Figures

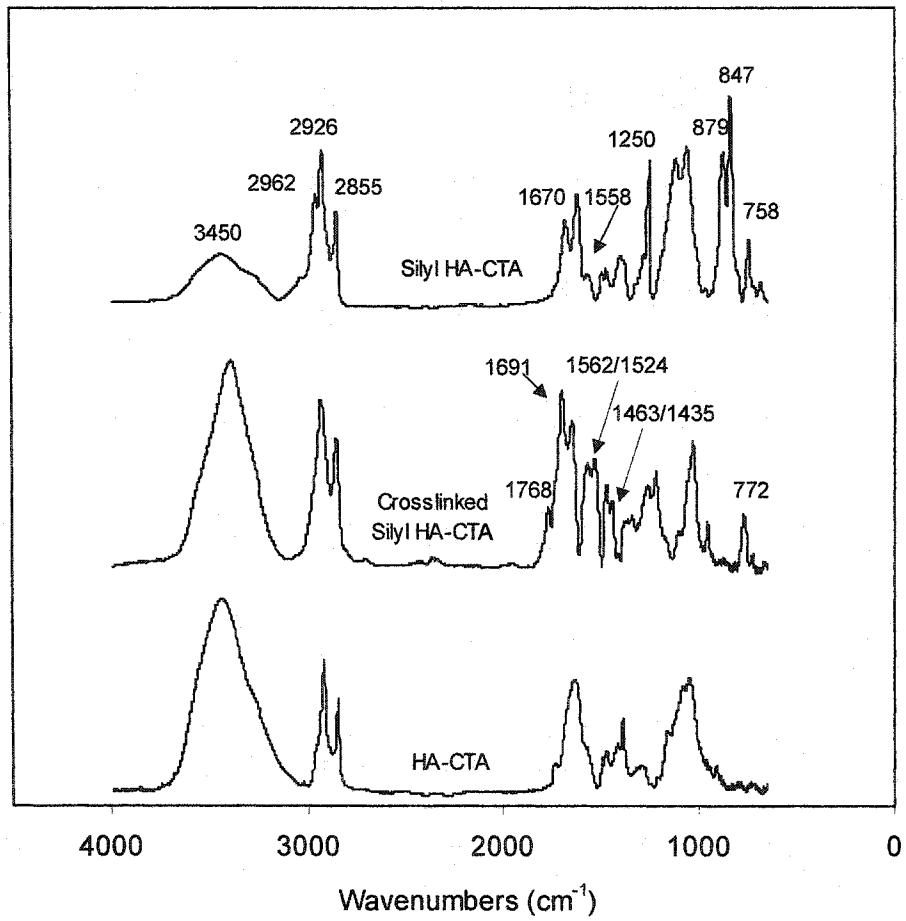

Figure 3.1 FT-IR spectra of crosslinked and original silyl HA-CTA, and HA-CTA

Figure 3.2 Reaction between isocyanates and alcohols

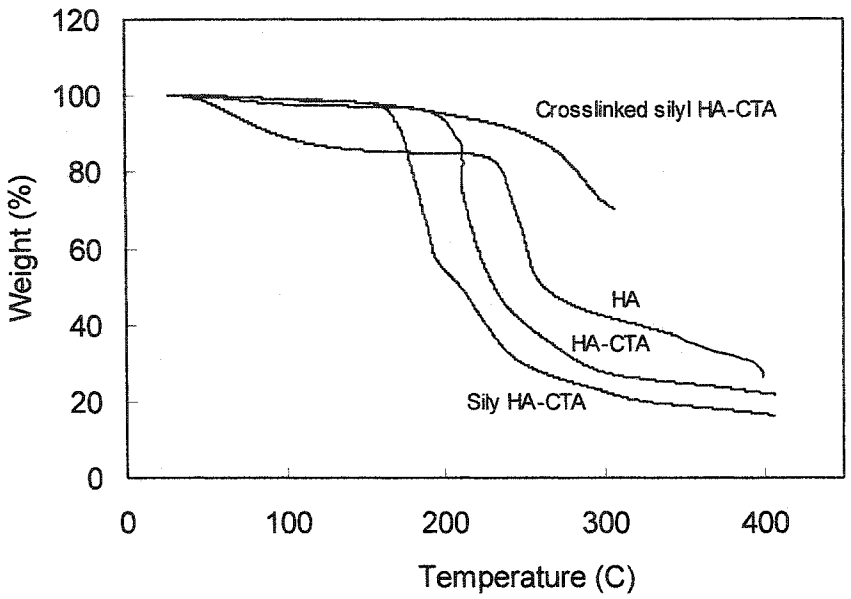

Figure 3.3 TGA of crosslinked and original silyl HA-CTA, and HA-CTA

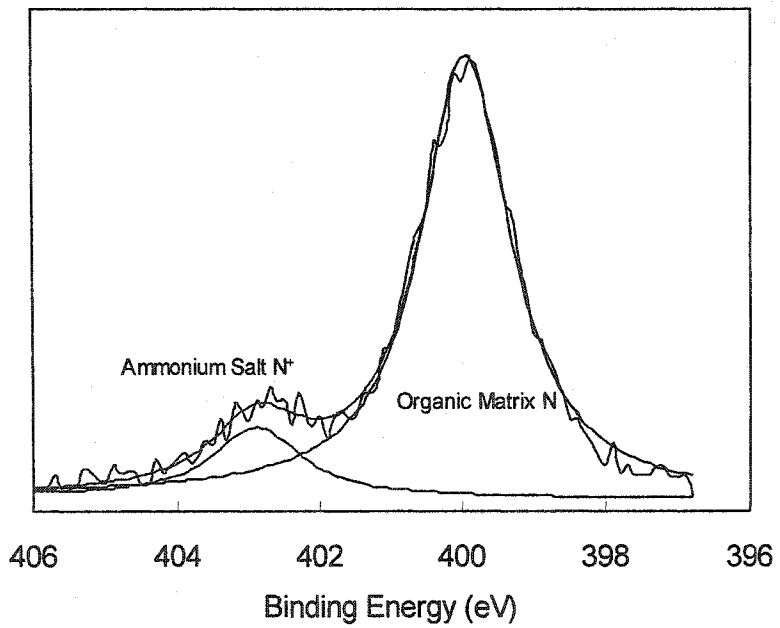

Figure 3.4 XPS N1s spectrum of micro-composite surface (sample D)

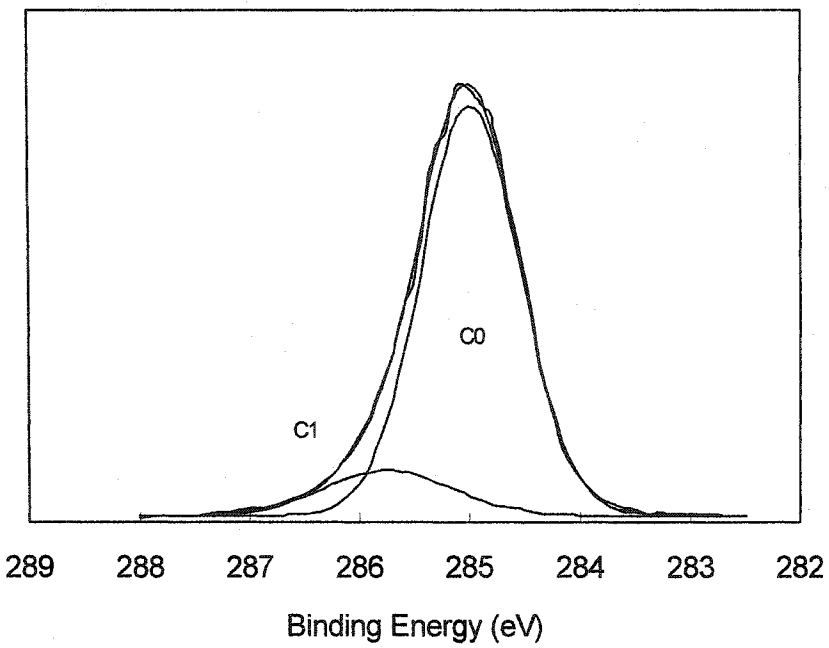

(a)

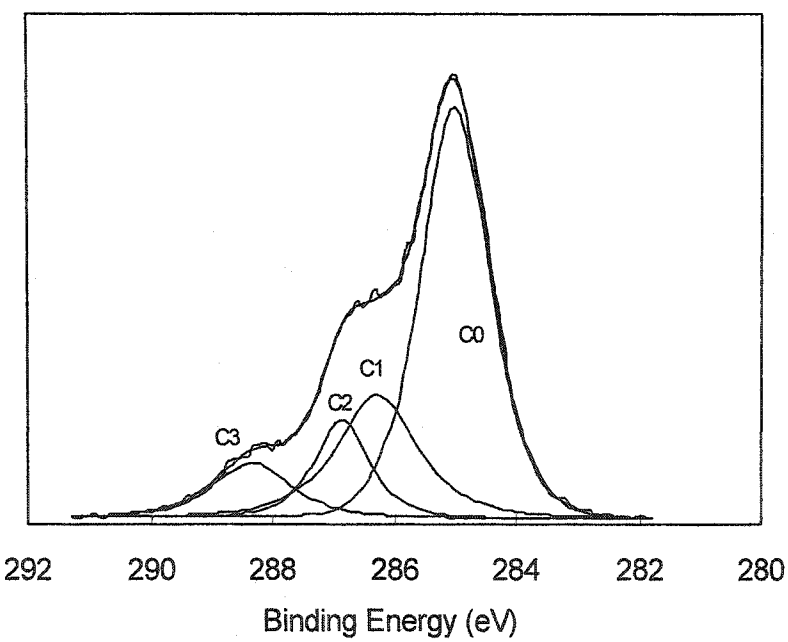

(b)

Figure 3.5 XPS C1s spectra of (a) UHMWPE perform and (b) micro-composite surface (sample D)

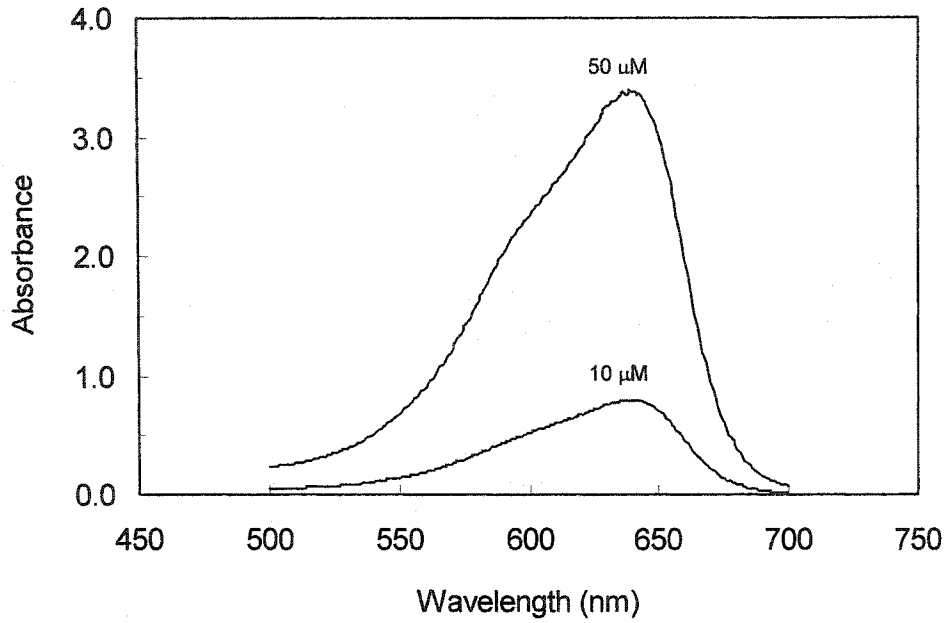

Figure 3.6 Visible absorbance spectra of 10 µM and 50 µM TBO in 0.2M NaCl and 8M urea solution

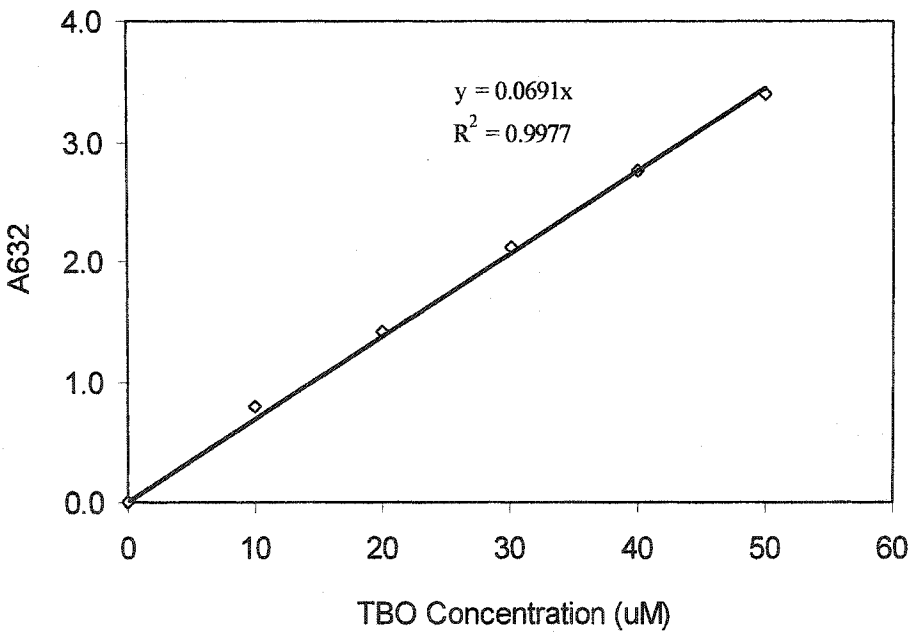

Figure 3.7 TBO Standard curve in 0.2M NaCl and 8M urea solution

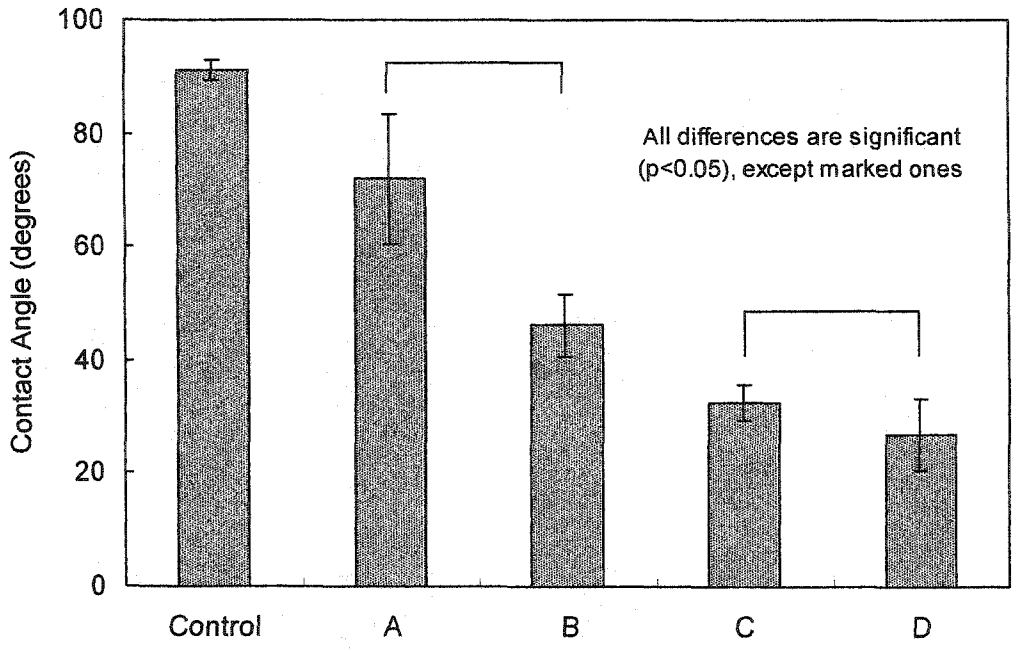

Figure 3.8 Aqueous contact angles of the 2nd batch

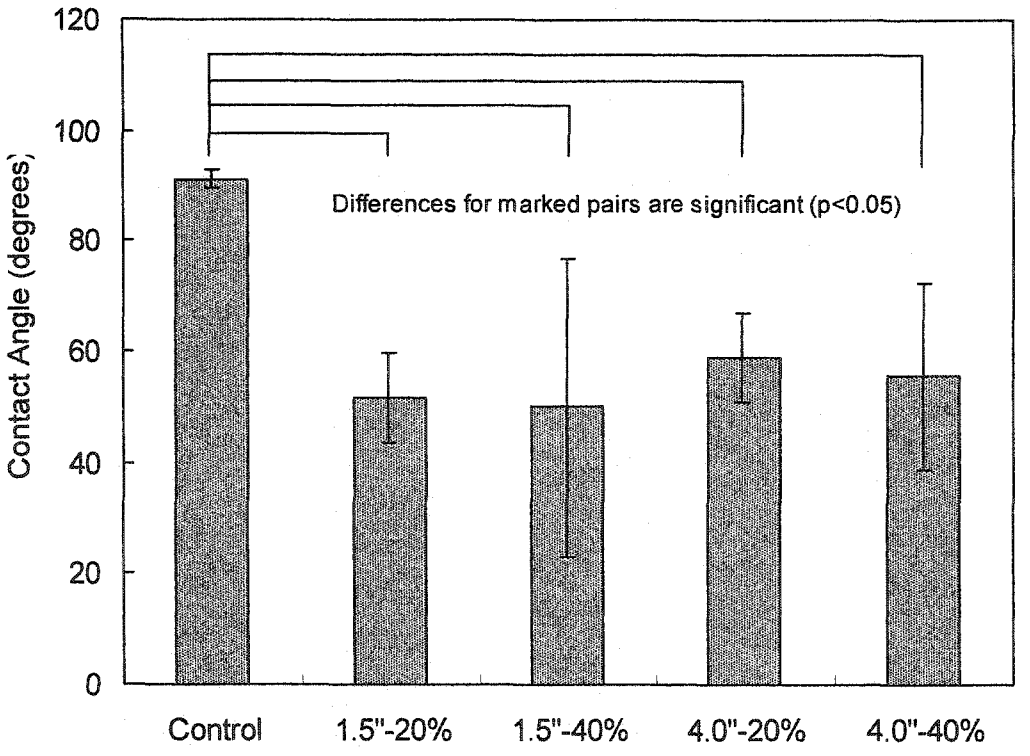

Figure 3.9 Aqueous contact angles of the 3rd batch

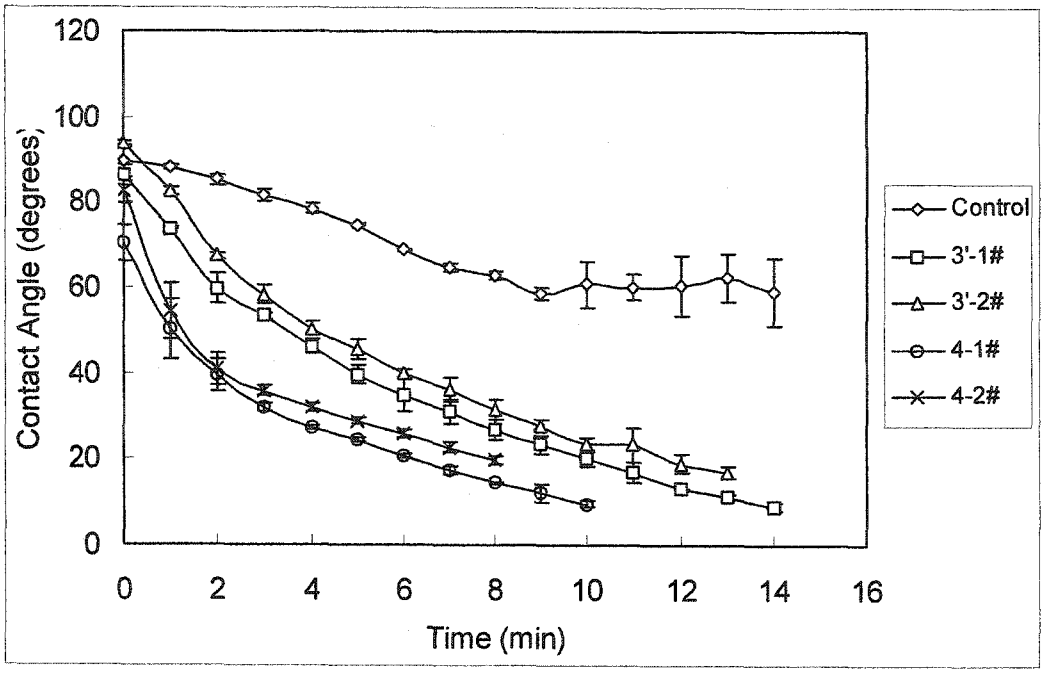

Figure 3.10 Kinetics of aqueous hydration of micro-composite surface

3.7 References

Aoyama T, Imai T, Hattori J, and Uehara M (1989). Method for preparing molded articles of ultra-high molecular weight polyethylene. US Patent 4876049.

Bailey FE (Jr.) and Critchfield FE (1981). A reaction sequence model for flexible urethane foam. In *Urethane Chemistry and Applications, ACS Symposium Series 172* (edited by Edwards KN). American Chemical Society: Washington, D.C., pp.127-148.

Beauregard GP (1999). Synthesis and characterization of a biomimetic UHMWPE-based interpenetrating polymer network for use as an orthopedic biomaterial. Ph.D dissertation. Colorado State University, Fort Collins, Colorado.

Goethel H, Sterkrade O, and Jacob E et al. (1962). Process for the production of porous polyethylene bodies. US Patent 3024208.

Duling IN, Merges JC (Jr.) (1976). Method of making porous objects of ultra high molecular polyethylene. US Patent 3954927.

Fan YL (1990). Hydrophilic lubricious coatings for medical applications. *Polymeric Materials (Part B): Science and Engineering*, 63: 709-716.

Giusti P and Callegaro L (1997). Biomaterial comprising hyaluronic acid and derivatives thereof in interpenetrating polymer networks. US Patent 5644049.

Gonda J and Antalová Z (1991). Reactions of isothiocyanates and isocyanates with some silylated nitrogen-containing nucleophiles. Collection of Czechoslovak Chemical Communications, 56: 685-694.

Hepburn C (1992). *Polyurethane Elastomers* (2nd ed). Elsevier Applied Science: New York, NY, pp.312-319.

Hodge WA, Fijan RS, and Carlson KL et al. (1986). Contact pressures in the human hip joint measured in vivo. In *Proceedings of the National Academy of Sciences of the United States of America*, 83: 2879-2883.

Ikada Y and Uyama Y (1993). *Lubricating Polymer Surface*. Technomic Publishing Co., Inc.: Lancaster, Pennsylvania.

Johnston JB (2000). A simple, nondestructive assay for bound hyaluronan. *Journal of Biomedical Materials Research*, 53:188-191.

Navarrete J, Chapman AJ, Parikh CJ and Toomey RT (2002). Use of lignins in thermoplastics. US Patent 6485867.

Rodriguez F (1996). Viscous Flow. *In Principles of Polymer Systems (4th edition)*. Taylor & Francis: Washington, D. C., pp.225-289.

Smith B (1998). *Infrared Spectral Interpretation*. CRC Press: New York, pp.158-160.

Stein HL (1989). Composition and process for making porous articles from ultra high molecular weight polyethylene. US Patent 4880843.

Chapter 4

Properties of UHMWPE-Hyaluronan Micro-Composites

4.1 Introduction

A uniform layer of HA film has been achieved on the surface of the UHMWPE micro-composites. Film stability in a physiological environment, and how the presence of HA affects the mechanical and tribological properties of UHMWPE will be examined in this chapter.

In the physiological environment, the turn-over of hyaluronan is very rapid. Its half-life in circulation in a human is 2.5-5.5 minutes [Laurent and Fraser, 1986], indicating that about 25% of the plasma HA content is eliminated every minute [Fraser and Laurent, 1989]. Although significant HA degradation in synovial cells has not been observed, and labeled HA injected into the joint has a similar high molecular weight in the residue synovial fluid [Fraser and Laurent, 1989], Bollet and his coworkers [1963] have demonstrated the presence of hyaluronidases, enzymes that degrade hyaluronic acid, in synovial fluid and its activity against hyaluronan. Three different types of hyaluronidases are classified according to the sites of cleavage. Testicular hyaluronidases are endo-β-N-acetylhexosaminidases with tetrasaccharides and hexasaccharides as the major end products. Bacterial hyaluronidases are also endo-β-N-acetylhexosaminidases, but operate by a beta elimination reaction, yielding disaccharide products. Leech hyaluronidases are

endo-β-glucuronidases, generating tetrasaccharide and hexasaccharide end products [Stern and Csóka, 2002; Laurent, 1970].

Lowry and Beavers [1994] used hyaluronidase Type I-S from bovine testes to investigate the resistance of their hyaluronate coatings to enzyme degradation. The HA top-coat covalently bound to an acrylic tie-coat on polymethylmethacrylate samples survived without damage after exposure to three levels of hyaluronidase in phosphate buffer (2.5, 15 and 150 units/ml) for up to 28 months.

HA is expected to have a plasticization effect on UHMWPE in the HA micro-composites, but the decreases in strength and modulus should not be too large due to the low content of HA within the micro-composites. Prior investigations demonstrated that the presence of hydrophilic poly-L-lysine in the surface layer of UHMWPE significantly decreased the modulus, strength and creep resistance of UHMWPE, significantly increased its elongation to failure, but did not significantly affect the fatigue properties of UHMWPE. However, the decrease in material properties was within the ASTM acceptable range [Rentfrow, 1999; Zhang et al., 2001A].

The HA films were also expected to significantly increase the lubricity of UHMWPE, and thus improve its wear resistance. Due to the micro-composite nature of the surface layer, the HA film was expected to have good mechanical integrity and thus reduce wear throughout a long term (i.e., at least one million cycles) wear test. See Chapter 1 for a more complete literature review and motivation.

4.2 Materials and Methods

4.2.1 Materials and Fabrication

All preforms and micro-composites used for characterization were molded at DePuy Orthopedics and are listed in Table 4.1 with batch numbers and treatments described in Tables 3.1 and 3.2. GUR 1020 UHMWPE powder was used to create all samples. The treatment processes have been described in detail in Section 3.2.1.

Hyaluronidase lyophilized powder (Type I-S from bovine testes, 608 units/mg solid) was purchased from Sigma (St. Louis, MO), and was stored at less than 0°C. Monobasic sodium phosphate (anhydrous, minimum 99.0%), dibasic sodium phosphate (anhydrous) and sodium chloride solid used to make phosphate buffer saline were the cell culture tested and insect cell culture tested products of Sigma. Ethanol (ACS/USP grade) was obtained from Pharmco (Brookfield, CT). Toluidine Blue O (TBO) and urea were obtained from Aldrich (Milwaukee, WI). Sodium chloride (certified A.C.S.) used for dye elution was purchased from Fisher (Pittsburgh, PA).

4.2.2 Characterization

Enzyme Degradation: To examine the effect of crosslinker concentration on the stability of crosslinked HA, 12 small squares were cut from 20% porosity preforms of the 2nd batch, and treated with process D described in Section 3.2.3. For stability investigation of the micro-composites, 5 squares (2.0 cm × 1.0 cm) each were cut from 20% porosity and 40% porosity disks of the 3rd batch, and 3 squares (2.0 cm × 1.0 cm) and 1 arc sample were cut from sample D of the 2nd batch. See Table 3.1 and 3.2 for details of the batch and treatment methods.

All micro-composite samples were first dyed with 0.1% TBO solution (in 8M urea) to examine the HA surface density before degradation. After flooding with TBO solution for several minutes, rinsing with distilled water, and drying at room temperature, TBO dye bound to HA on the sample surface was eluted with 0.15 M NaCl solution (in 8M urea). Elution was performed dropwise, and continued until no more dye was visible in the runoff. The eluant was collected, and measured in volume. The visible absorbance of the eluant and the surface density of HA were determined with the same methods described in Section 3.2.3. To ensure that all TBO molecules were removed, micro-composite samples were soaked in 0.4 M NaCl solution for several days, and the solution was changed every day. Before enzyme degradation, all porous and micro-composite samples were soaked in distilled water overnight and then sterilized with ethanol.

Phosphate buffer saline (PBS) was prepared based on the method described in U.S. Pharmacopeia for hyaluronidase injection [1990]. 1.25g of monobasic sodium phosphate, 0.5 g of anhydrous dibasic sodium phosphate and 4.1 g of NaCl were dissolved in water to make 500ml of solution. The buffer solution, glassware and all supplies used for enzyme solution preparation were autoclave sterilized before use.

Enzyme solutions (60 ml) with two different hyaluronidase levels were prepared with PBS: 15 unit/ml and 150 unit/ml. Falcon® sterile polypropylene tubes with 15 ml capacity were used to contain the test samples and 10 ml of enzyme solutions. All the tubes were tightly capped, and placed in a 37 ± 0.5°C water bath for the desired exposure intervals. After washing with water and soaking in ethanol, the enzymatically degraded samples were dyed with 0.1% TBO solution (in 8M urea), and the surface density of HA after degradation was determined.

The activity of the hyaluronidase enzyme during the experiment was checked by viscosity reduction of a freshly prepared 0.1% HA aqueous solution [Lowry and Beavers, 1994; Bollet et al., 1963]. Viscosity of this HA solution treated with the enzyme was measured at 37°C with an Ubbelohde capillary viscometer, and was compared to that of the un-treated HA control solution. The viscometer and measurement method were the same as that described in section 2.2.3. At the exposure time of interest, 4.5 ml of enzyme solution was pipetted from the tubes containing the micro-composite samples, and put into the viscometer. 2.5 ml of HA solution and 8 ml of phosphate buffer solution were added respectively, and mixed with the enzyme solution by rocking the viscometer. After equilibrating at 37 °C for 30 min, the flow time of the solution was measured. The same measurement was made on 2.5 ml of HA solution diluted with 12.5 ml PBS, without enzyme treatment.

Tensile Tests: Dumbbell-shaped tensile samples were punched from the 4″ molded UHMWPE disks at DePuy Orthopedics according to ASTM Standard D638-99 Sample Type V. Five samples were punched from each disk. Two of them were used for the modulus test, while the remaining three were used for the measurement of yield strength, tensile strength and elongation to failure. The tests were performed according to ASTM Standard D638-99 on a servohydraulic biaxial mechanical testing system (Bionix, model 809, MTS Corporation, Eden Prarie, MN) with a low force uniaxial (tension/ compression) load cell (Model 661.19E-01, 1000 lb.). All the samples were conditioned with distilled water for 24 hours before testing.

UHMWPE has a high elongation to failure, so modulus and elongation to failure are difficult to accurately measure at the same time. Thus, two different tests were carried

out: one for modulus determination, and another for strength and elongation-to-failure determination. The tests were performed according to ASTM Standard D638-99. In the modulus test, an extensometer (model 632.31F-24) with a 10 mm gage length was used to measure the sample deformation accurately. The crosshead speed was 0.5 inch/min, and the data acquisition rate was 10 Hz. Within 1% strain, the stress-strain curve was linear. If not at coordinate origin, the starting point of the curve was shifted to (0,0). A linear regression was performed on the curve, resulting in a linear equation with a zero intercept. The slope of the equation was the modulus. The R^2 values for all the samples were generally near 0.98. This method of calculating modulus was similar to that used by Rentfrow [1999] and Bennett [1995] for the Hospital for Special Surgery (HSS) reference UHMWPE.

In the elongation-to-failure test, sample deformation was recorded by a video camera. The initial gage length of approximately 0.4 inches was marked on each sample with black marker and was measured with a caliper. The crosshead speed was the same as that used in the modulus test, 0.5 inch/min, but the data acquisition rate was decreased to 5 Hz. The distance change between the two marks during testing was recorded with the video camera, and the digitized video was then analyzed using Peak Motus 32 software (Englewood, CO). A 40 mm × 40 mm standard square was used to calibrate the digitized video frames. A ruler was also attached to the crosshead sample grip in case the mark went out of the camera view. The yield strength was calculated from the first maximum stress in the engineering stress-strain curve, and the tensile strength was calculated from the absolute maximum stress before sample failure. Thus, if the engineering stress did not

increase after yield, the yield and tensile strengths were equal. The elongation-to-failure was determined by capturing the data of the last frame just before failure.

All tensile data were analyzed using Data Analysis Tool of MS Excel. Comparisons were made between groups using a one-way ANOVA. The differences were significant when p values were less than 0.05 ($p<0.05$).

Wear Tests: Wear testing was performed at Zimmer, Inc. (Warsaw, Indiana). Four pins (ϕ 0.356″ × 0.375″) were machined from each ϕ 1.5″ disk listed in Table 4.1 (control, 3′-1#, 3′-2#, 4-1# and 4-2#--see Chapter III for batch/treatments descriptions). The "control" (i.e., UHMWPE molding control) was a sample put through the same molding processes as the micro-composites but without the addition of HA. It was ϕ 1.5″ 40% porosity preform of the 4th batch without treatment that was then re-molded to full density under the same conditions as the treated samples. Samples 3′-1#, 3′-2#, 4-1# and 4-2# were the same disks used for the aqueous hydration test of the micro-composite surface shown in Figure 3.10. Three of these pins were used for wear test, while the fourth was used as a load soak control. Both conventional and highly crosslinked UHMWPE pins machined from extruded GUR 1050 bar stock were used as UHMWPE bulk controls (solid controls). They were provided by Zimmer (Warsaw, IN). The conventional polyethylene ("ConvPE") and the treated samples were not sterilized. The crosslinked polyethylene ("XLPE") was irradiated (to crosslink it) to 100±5 kGy with an electron beam. Before testing, the surface profiles for all the pins were analyzed with a 3D Imaging Surface Structure Analyzer (NewView 200, ZYGO Corporation, Middlefield, CT). The pin-on-flat (POF) wear test machine used was Zimmer's custom-built 12-station device, capable of crossing motion paths, but can only apply a static load during testing (i.e., it is not

capable of a typical gait cycle of fluctuating load). All pins were conditioned in distilled water for 8 hours before testing. The wear test was performed at room temperature at 1.0 Hz for 1.0 million cycles. The lubricant was undiluted bovine calf serum with sodium azide as an antibacterial agent. EDTA was used to bind the calcium in the lubricant, preventing the formation of calcium phosphate on the tested sample surfaces. Superfinished (Ra: 0.053 ± 0.020 μin) CoCrMo alloy disks were employed as the wear counterface. A constant load of 100 lb was applied to each UHMWPE pin. The wear path was a square (15 mm × 15 mm) with a total length of 60 mm. The test conditions are also summarized in Table 4.2. Amounts of wear (weight loss) were determined by measuring weight changes of samples after every quarter million cycles and were the average of three pin samples. Wear rate values reported here are the change of weight loss values normalized with the number of cycles. Prior to weighing, all pins were cleaned in an ultrasonic bath of de-ionized water and rinsed with isopropyl alcohol to extract absorbed water. The load soak control was used to check the weight increase of wear pins caused by fluid uptake. The loading conditions for the soak control samples were the same as those used for wear samples (i.e., 100 lb), but no motion was applied to them. The height changes of these load soak control samples with time were also monitored during testing, and a creep curve was obtained.

All data were analyzed using Data Analysis Tool of MS Excel. Comparisons were made between groups using a one-way ANOVA. The differences were significant when p values were less than 0.05 ($p<0.05$).

4.3 Results and Discussion

4.3.1 Enzyme Degradation

To select an appropriate crosslinker concentration for the micro-composites, the enzyme degradation experiment was first performed on porous preforms treated with the same process as that used for sample D, but in this case preforms were not re-molded. Four Desmodur (i.e., the crosslinker) acetone solutions, 0.2%, 1%, 2% and 5% concentrations, were used to crosslink the treated UHMWPE performs. After being exposed, respectively, to 15 and 150 units/ml hyaluronidase in PBS at 37°C for one month, the samples were dyed with TBO solution, and the results were compared to the similarly treated preforms that had not been enzymatically degraded. Preforms crosslinked with 2% and 5% Desmodur solutions had a uniform purple surface, indicating that a uniform layer of HA film remained even after degradation at two enzyme levels. However, the dyed surface of those samples crosslinked with the 0.2% and 1% Desmodur solutions was no longer uniform in color, showing evidence of slight degradation in some regions. Based on this observation, the 5% Desmodur solution was chosen for crosslinking the 3rd batch of micro-composites.

The enzyme activity after the degradation experiment was also checked with viscosity reduction of a 0.1% HA control solution. The average flow time of HA diluted with five volumes of PBS was 1 min and 59.58 s at 37°C. The HA treated with 150 units/ml enzyme solution had a flow time of 31.54 s, very close to that of water (approximately 28 s). This significant decrease in HA molecular weight indicated that the hyaluronidase was still active after one month of incubation in a 37°C water bath and continuous contact with the polymer samples. Lowry and Beavers [1994] also reported that hyaluronidase

activity could be retained for up to one year at 37°C, so a decrease in enzyme activity should not pose a problem for the short term (i.e., one month) experiments.

Micro-composite samples were also tested with two enzyme levels. The HA surface density for all samples before and after degradation is listed in Table 4.3. No significant decreases in HA density were found, with the exception of sample no.3 from the 40%-through batch after 30 days in the 150 units/ml solution, and sample no.5 from the 20%-through batch after 30 days in the 15 units/ml solution. The significant decreases in HA surface density for these two samples may be an anomaly or, more likely, are false results due to measurement errors, because even those samples crosslinked with only a 1% crosslinker solution (sample D) did not show a significant decrease in HA surface density after 30 days in enzyme solution. Furthermore, visual observations provide no evidence of degradation on these samples. All samples, including the supposedly-degraded samples, were still lubricious, water-wettable, and showed no staining difference when compared to non-enzymatically treated samples.

The crosslinked HA within the UHMWPE performs is much more resistant to hyaluronidase attack than free, native HA solublized in water. The enzyme level that could reduce the viscosity of HA solution to almost that of water, had few effects on the crosslinked HA, especially the more highly crosslinked samples. Lowry and Beavers [1994] attributed this to the inability of the immobilized HA to participate in an enzyme-substrate conformation requirement. Formation of micro-composites with a hydrophobic material (UHMWPE) also increases the resistance of HA to degradation by enzymes. The 1% Desmodur crosslinked porous samples could not retain the uniformity of its HA film after degradation, but the HA film of the micro-composite (sample D) crosslinked with

the same solution showed very good stability. This is likely due to the fact that the HA in the micro-composites is rooted into the UHMWPE, reducing its conformational mobility and leaving fewer HA "loose ends" [Lowry and Beavers, 1994] that could be attacked by enzyme.

The enzyme concentrations used in this study are the same as those used by Lowry and Beavers [1994] in their coatings. The two enzyme levels, 15units/ml and 150 units/ml, were respectively 6 times and 60 times the hyaluronidase concentration present in human serum [Delpech et al., 1987]. Bollet et al. [1963] demonstrated the presence and activity of hyaluronidase in synovial fluid, but did not provide its level. However, from their results, hyaluronidase activity in synovial fluid is seen to be much lower than that in human serum. This is consistent with what Fraser and Laurent [1989] found: labeled HA injected into the joint has a similar high molecular weight in the draining lymph and residual synovial fluid. Therefore, the enzyme degradation environment used here should be much more severe that the human synovial fluid environment. Lowry and Beavers' [1994] grafted HA coatings could stand 28 months of hyaluronidase degradation without damage, so it can be inferred that the HA film is crosslinked and is deeply rooted into UHMWPE surface, providing much better enzymatic stability.

4.3.2 Tensile Properties

The tensile test results for the porous control and the micro-composites are summarized in Table 4.4, wherein they are compared to the reference UHMWPE and the ASTM standard requirements. The modulus and yield strength values for the control and micro-composites are acceptable, but the ultimate strength and elongation to failure

values are much lower than the ASTM requirements and reference materials. The samples molded from the porous preforms (both control and microcomposite) were so brittle that they could not be "strain-hardened" [Askeland, 1994], and thus could not produce an ultimate strength higher than the yield strength. However, this is clearly not the result of HA introduction, because the control from the re-molded 40% porous preforms (without HA treatment) also exhibit significantly decreased elongation-to-failure values. Before testing these molded samples, two HSS (Hospital for Special Surgery) UHMWPE tensile samples were tested and the measured properties fell within the normal range as previously reported [Rentfrow, 1999]. Thus, the observed embrittlement was not caused by the test method either.

The high elongation-to-failure (i.e., ductility) of thermoplastic polymers is due to entanglement of their long molecular chains. For semi-crystalline polymers, the molecular chains extending from crystalline regions into the amorphous regions act as tie chains. It is the disentanglement of these tie chains under tensile stress that results in large plastic deformation before the polymer fails [Askeland, 1994]. Factors, such as crosslinking induced oxidation, high crystallinity, incomplete consolidation etc., that decrease chain length and/or entanglement, can also reduce the elongation-to-failure of the polymer. Incomplete consolidation of the UHMWPE powder particles is likely the major cause of the observed sample embrittlement. To prevent HA from degrading, all samples, including the control, were re-molded at 160°C (melting point of UHMWPE: 135.6 ± 4°C [Bennett, 1995]), rather than at 205 °C which is often used to mold UHMWPE powder. The low molding temperature and large sample size (4 inch diameter) might reduce the heat energy and heat transfer, resulting in insufficient

UHMWPE flow and particle fusion. In the poorly consolidated UHMWPE, the molecules within two adjacent particles would not sufficiently entangle with each other, resulting in a low elongation-to-failure. This poor consolidation theory is supported by observations of the sections microtomed from the fracture surface showing more pronounced particle boundaries (i.e., less fusion) than normally observed in molded UHMWPE. Furthermore, solid portions of 40%-half and –quarter samples which were well consolidated in a separate 205°C molding cycle before preform manufacture showed an elongation similar to that of HSS UHMWPE (i.e., the video system allowed quantification of elongation-to-failure for each portion of the sample cross section separately as the preform layer broke much earlier than the solid layer). This also supported the theory that poor consolidation during the final molding cycle of the preforms resulted in low elongation-to-failures. The 40%-through samples have the best elongation-to-failure values, indicating that its consolidation was better than all the other samples. These samples also provide evidence that the HA microcomposite treatment does not degrade the mechanical properties of UHMWPE.

Although the properties of these samples are not desirable due to the inappropriate re-molding conditions, the effect of HA on micro-composite properties can been seen from the analysis of these properties. A graphical summary of the modulus for all samples is shown in Figure 4.1. Comparisons were made among samples using a one-way ANOVA, but no significant differences were found, indicating that the introduction of HA did not significantly change the modulus of UHMWPE. According to the rule of mixtures for composites [Askeland, 1994], the contribution of HA to the modulus of micro-composite is proportional to its volume fraction. The maximum weight fraction of HA is 5.03% in

the 40%-quarter samples, so the volume fraction of HA is small, and thus its contribution to the micro-composite bulk modulus is negligible.

The yield strength and tensile strength results are shown in Figures 4.2 and 4.3. The tensile strengths of the control, 20%-through and 40%-through samples were equal to their yield strengths because these samples could not be "strain hardened". However, the 40%-half and -quarter samples have a tensile strength higher than the yield strength due to the presence of a well-molded solid layer. In Figure 4.2, except for the marked pairs, all the comparisons are significantly different. The yield and tensile strength of the 20%-through sample is the lowest, and is even significantly lower than that of the 40%-through sample. This was unexpected, but might be explained by the fact that the HA content within 20%-through is 1.46%, higher than that within 40%-through (0.83%). Also the pore-forming-agent residue (i.e., poragen), which could not be completely removed from the preform due to the low porosity, might also contribute to the decrease in yield strength. There are no significant differences among the yield and tensile strength results of the three 40% porosity micro-composites, so the effect of porous layer thickness cannot be seen here. Although significantly lower in yield strength than the control, the maximum decrease for the three micro-composites is only 13.5%. In Figures 4.2 and 4.3, the effect of the porous layer thickness on the yield and tensile strength is apparent, although it is not significant. As the thickness of the porous layer increases, the tensile strength decreases.

Elongation-to-failure results in Figure 4.4 show that the 20%-through samples are still inferior to all other samples, demonstrating the effect of the pore-forming-agent residue. The elongation-to-failure for all the 40% porosity samples is significantly higher than that

of the control. This is the inverse of the strength results, indicating that the presence of HA in the micro-composites slightly, but significantly, decreases the strength and increases the elongation-to-failure of UHMWPE. This phenomenon is similar to that observed in poly-L-lysine-modified UHMWPE [Rentfrow, 1999]. A remarkable thing is that the 40%-through micro-composite has a much higher elongation than all other samples, indicating its comparatively good consolidation quality.

4.3.3 Tribological Properties

Wear results for both UHMWPE controls and micro-composites are summarized in Table 4.5 and Figures 4.5, 4.6 and 4.7. The results of sample 3′-2# are not included because all the pins from 3′-2# disk fractured at the interface between the top micro-composite layer and the bottom UHMWPE layer. There are four possible reasons for this failure: (1) the wear test fixture gripped these pins during wear testing right near the interface between the HA-UHMWPE micro-composite layer and underlying bulk UHMWPE (unlike the other samples which were gripped well below this interface), resulting in high stress concentrations at that interface; (2) the weight gain of this UHMWPE porous preform after hydrolysis was very high (6.35% compared to 2.27% for 3′-2#, 1.10% for 4-1# and 1.12 for 4-2#, see Table 4.6), indicating there was more crosslinked HA present within the micro-pores of this preform than in the other samples, resulting in mechanical properties inferior to the other samples as described in Section 3.3.3 and confirmed in the tensile testing; (3) the extra HA within the micro-composite might absorb large amounts of water during wear testing (compared to the other samples), causing large deformation of micro-composite layer and high stress at the

interface; (4) defects at the interface from the molding processed might also have contributed to the failures.

The wear and wear rates of crosslinked UHMWPE are very low and significantly lower than all other materials, as expected. The UHMWPE molding control (i.e., control) has both higher wear and wear rate than the conventional UHMWPE (i.e., ConvPE) control, although the differences are not significant at 0.75 and 1.00 million cycles for wear and at 0.50, 0.75 and 1.00 million cycles for wear rate (see Tables 4.7 and 4.8). The surface roughness of the mold control is significantly lower than ConvPE (shown in Table 4.9 and Figure 4.8) (molded UHMWPE surfaces are smoother than machined ones). This demonstrates that material properties are more important than surface roughness in determining the wear resistance. Two possible reasons for the higher wear and wear rate of the mold control are its lower molecular weight and inferior mechanical properties. The mold control was made from GUR 1020 with an average molecular weight of 3.5×10^6 g/mol [Kurtz et al, 1999], and re-molded at a temperature that could not produce complete consolidation of UHMWPE particles (as discussed in Section 4.3.2), causing inferior mechanical properties. ConvPE came from extruded GUR 1050 bar stock with an average molecular weight of $5.5\sim6.0 \times 10^6$ g/mol [Kurtz et al, 1999] and good consolidation. Kurtz et al. [1999] discussed the effects of molecular weight on the wear and mechanical behavior of UHMWPE, and found that wear resistance increased as the average molecular weight increased.

Figures 4.5 and 4.6 show that the average wear of all micro-composites is lower than that of both mold and conventional polyethylene controls, and all the differences in wear between 4-1# and both controls are significant. Sample 4-2# has a significantly lower

wear than the mold control at cycles up to 0.75 million, and than ConvPE at 0.25 million cycles. For sample 3′-1#, the wear differences from both controls are significant at cycles up to 0.75 million. Wear rates are the slopes of the wear lines in Figure 4.5, and are also shown in Figure 4.7 and Table 4.8. The wear rate of sample 4-1# is significantly lower than ConvPE at cycles up to 0.75 million, and than the mold control at 0.25 and 0.5 million cycles. Samples 4-2# has a significantly lower wear rate than ConvPE only at 0.25 million cycles, and than the mold control at 0.25 and 0.5 million cycles. For sample 3′-1#, its wear rate is lower than both controls at 0.25 and 0.5 million cycles, but the difference is significant only at 0.25 million cycles. After 0.5 million cycles, the wear rates of 3′-1# increase sharply and are significantly higher than both ConvPE and mold controls. In summary, sample 4-1# is the most wear resistant, and the next is 4-2#. Sample 3′-1# has a good wear resistance before 0.5 million cycles, but poorer wear resistance after that.

No significant differences in surface roughness were found among all the micro-composite samples, as shown in Table 4.9. Thus, the large differences in their wear properties might be due to HA amounts on the surface and the film quality. Sample 4-1# has a higher weight increase than 4-2# after the final HA coating (Table 4.6), indicating larger amounts of HA present on the surface, so more HA molecules are involved in the lubrication, and the HA cushion swollen with water is thicker and more effective in separating two articulating surfaces. For sample 3′-1#, the very low wear and wear rates before 0.5 million cycles are attributed to large amounts of HA on its surface. The extra HA film coated on the surface after consolidation may not be tightly adherent to the

sample surface, so is more easily rubbed away, causing an abrupt increase in the wear rate after 0.5 million cycles.

It is also found that the wear curves are almost straight lines for both mold and conventional polyethylene controls, so their wear rates are nearly constant. However, for the micro-composites, wear rates slightly increase with the number of cycles. This may be due to the exposure of some UHMWPE regions to the articulating surface with the removal of HA film. Of course, determining whether the wear of micro-composites occurred only within the HA layer or within both HA and UHMWPE requires further study on the wear surface and the wear debris collected from the lubricant. To avoid the wear of HA itself and further increase the wear resistance, crosslinking should be optimized and controlled to form a more robust and durable HA surface layer. However, a favorable balance between HA crosslinking density and surface lubricity are required. If the crosslinking is too dense, the crosslinking will consume too many polar groups, reducing boundary lubrication.

Incomplete preform consolidation due to low-temperature re-molding may also adversely affect wear properties for all micro-composites, as it did to the mold control. Wear resistance of micro-composites is expected to increase with improved treatment and molding processes.

Data for load soaked controls are listed in Table 4.10. The weight increases of all samples due to liquid absorption during wear testing are very small compared to the magnitude of weight loss from wear, so are considered negligible. Figure 4.9 shows the creep curves for all the load soaks. The creep of all micro-composite samples are

comparable to that of the conventional polyethylene, indicating the presence of HA did not significantly change the creep resistance of UHMWPE.

4.4 Conclusions

Unlike free HA in water solution, HA introduced into the micro-composites was resistant to attack by hyaluronidase. The micro-composite surface was still as water wettable, lubricious, and stainable by TBO as the original material after 1 month of exposure to enzyme levels 6-60 times the concentration of hyaluronidase in human serum.

The presence of HA significantly decreased the strength and increased the elongation-to-failure of the micro-composites, as observed in the previous study on UHMWPE-PLL IPNs, demonstrating the plasticization effect of HA on micro-composites. However, because the decrease in strength was less than 15%, it is considered acceptable. The increase in the elongation-to-failure of one microcomposite was remarkable, indicating that with much better consolidation, the micro-composites have properties only slightly inferior to control UHWMPE. The thickness of the porous layer also affected the strength. Lastly, the tensile strength decreases with porous layer thickness increases.

The HA-UHMWPE micro-composites did significantly lower both the wear and wear rate for UHMWPE, and the decreases were very significant (at 1.0 million cycles, the maximum decrease in wear was 42%, while in wear rate was 27%) when the sample treatment was appropriate. Material properties and surface chemistry appear to be more important than surface roughness in determining the wear properties of these materials. Although the surface roughness of the mold control was significantly lower than that of

ConvPE, its wear and wear rates were higher than that of ConvPE, due to its lower molecular weight and incomplete consolidation compared to ConvPE. Low HA content within micro-composites, abundant HA on the surface, sufficient crosslinking and good film adhesion are required to achieve significant lubrication and improve wear resistance.

4.5 Tables

Table 4.1 Samples used for characterization

Characterization	Samples	Treatment
Enzyme Degradation		
20%-preform	Porous preforms, 20% all porous	2nd batch, treatment D
Sample D	1.5″ disk, 20% all porous	2nd batch, treatment D
20%-through	4.0″ disk, 20% all porous	3rd batch, treatment
40%-through	4.0″ disk, 40% all porous	3rd batch, treatment
Tensile Tests		
Control	4.0″ disk, 40% all porous	4th batch, no treatment
20%-through	4.0″ disk, 20% all porous	3rd batch, treatment
40%-through	4.0″ disk, 40% all porous	4th batch, treatment
40%-half	4.0″ disk, 40% half porous	4th batch, treatment
40%-quater	4.0″ disk, 40% quarter porous	4th batch, treatment
Wear Tests		
Control	1.5″ disk, 40% top 3 cm porous	4th batch, no treatment
3′-1# (20%)	1.5″ disk, 20% top 3 cm porous	3rd batch, treatment
3′-2# (40%)	1.5″ disk, 40% top 3 cm porous	3rd batch, treatment
4-1# (40%)	1.5″ disk, 40% top 3 cm porous	4th batch, treatment
4-2# (40%)	1.5″ disk, 40% top 3 cm porous	4th batch, treatment

Table 4.2 Pin-on-flat wear test conditions

Parameters	Conditions
Machine	Zimmer's custom-built pin-on-disk machine
Counterface	CoCrMo alloy 2A-74 (Ra = 0.053 ± 0.020 μin)
Wear Path	Square waveform with each side 15 mm
Motion	Hydraulic control
Frequency	1.0 Hz
Load	Constant and pneumatic control, 100 lbf / pin
Nominal stress	1000 psi (6.9 MPa)
Path length	60 mm
Temperature	Room temperature
Lubricant	Undiluted bovine calf serum + EDTA & sodium azide
Number of cycles	1 million
Sliding distance	60 km
Sliding speed	6 cm/s

Table 4.3 HA surface density (nmol/cm^2) of micro-composites before and after degradation by hyaluronidase

Sample	Before degradation	Enzyme 150 units/ml			Enzyme 15 units/ml	
		10 days	20 days	30 days	10 days	30 days
40%-through						
1	164.0	170.0				
2	68.55		83.72			
3	59.68			46.96		
4	78.55				93.79	
5	70.35					87.84
20%-through						
1	38.44	33.26				
2	42.99		35.83			
3	36.29			31.13		
4	21.70				27.36	
5	33.38					22.30
Sample D						
1	37.44	32.53				
2	41.82			44.46		
3	31.99				41.60	
4	39.50					41.53

Table 4.4 Mechanical properties of the UHMWPE control and micro-composites

Sample	Modulus (MPa)	Yield Strength (MPa)	Ultimate Strength (MPa)	Elongation-to-Failure (%)
Control	786.59±118.92	21.90±0.30	21.9±0.31	68.66±8.82
20%-through	725.37±166.4	15.91±0.87	15.91±0.87	50.00±14.54
40%-through	824.14±59.46	19.56±3.16	19.56±3.16	279±73.61
40%-half pores	736.12±19.37	20.33±0.32	21.06±4.92	82.94±5.48
40%-quater pores	797.84±6.89	18.94±1.33	21.51±2.41	70.29±58.49
Reference UHMWPE*	944.74	23.27	48.57	384
Requirements of AST M F648-98	N/A	19	27	250

* Data from the paper by Bennett et al. [1996].

Table 4.5 Wear properties of the UHMWPE controls and micro-composites

	XLPE	ConvPE	Control	3'-1#	4-1#	4-2#
Wear (mg)						
0.25 million cycles	0.05±0.00	1.37±0.03	1.72±0.17	0.34±0.11	0.68±0.23	0.77±0.31
0.50 million cycles	0.09±0.01	2.98±0.08	3.56±0.31	1.59±0.34	1.64±0.45	2.12±0.54
0.75 million cycles	0.14±0.02	4.74±0.20	5.25±0.62	3.95±0.46	2.81±0.77	3.52±0.79
1.00 million cycles	0.18±0.01	6.59±0.36	7.17±1.09	6.45±0.54	4.21±1.07	5.31±1.06
Wear Rate (mg/million cycles)						
0.25 million cycles	0.19±0.01	5.50±0.12	6.87±0.68	1.37±0.44	2.72±0.92	3.07±1.22
0.50 million cycles	0.15±0.03	6.41±0.42	7.37±0.69	4.99±1.58	3.85±0.88	5.40±0.98
0.75 million cycles	0.21±0.07	7.04±0.49	6.74±1.28	9.45±0.48	4.65±1.29	5.62±1.00
1.00 million cycles	0.17±0.05	7.40±0.94	7.71±2.14	9.97±0.43	5.61±1.07	7.15±1.09

Table 4.6 The weight change of micro-composite wear disks during treatment

	3'-1#	3'-2#	4-1#	4-2#
Weight gain after hydrolysis	2.27%	6.35%	1.10%	1.12%
Weight gain after coating	5.40%	9.75%	3.31%	2.51%

Table 4.7 Statistical analysis of weight loss

	ConvPE	Control	3'-1#	4-1#	4-2#
P-value in comparison to ConvPE					
0.25 million cycles		0.0265	0.00009	0.0062	0.0264
0.50 million cycles		0.0342	0.0024	0.0074	0.0564
0.75 million cycles		0.2460	0.0530	0.0141	0.0614
1.00 million cycles		0.2784	0.7266	0.0195	0.1183
P-value in comparison to control					
0.25 million cycles	0.0265		0.0003	0.0032	0.0092
0.50 million cycles	0.0342		0.0018	0.0037	0.0163
0.75 million cycles	0.2460		0.0434	0.0131	0.0409
1.00 million cycles	0.2784		0.3577	0.0265	0.1001

Table 4.8 Statistical analysis of wear rate

	ConvPE	Control	3′-1#	4-1#	4-2#
P-value in comparison to ConvPE					
0.25 million cycles		0.0265	0.00009	0.0067	0.0266
0.50 million cycles		0.1105	0.2068	0.0104	0.1747
0.75 million cycles		0.7244	0.0036	0.0402	0.0923
1.00 million cycles		0.8277	0.0126	0.0949	0.7758
P-value in comparison to control					
0.25 million cycles	0.0265		0.0003	0.0033	0.0093
0.50 million cycles	0.1105		0.0752	0.0055	0.0464
0.75 million cycles	0.7244		0.0268	0.1183	0.2999
1.00 million cycles	0.8277		0.1472	0.2018	0.7036

Table 4.9 Surface roughness (μin) and statistical analysis results (p-values)

	XLPE	ConvPE	Control	3′-1#	3′-2#	4-1#
Ra (μin)	17.35±2.39	34.07±5.91	5.85±0.67	25.93±6.57	45.06±27.10	24.55±7.17
vs ConvPE	0.0015					
vs Control	0.00008	0.00005				
vs 3′-1#	0.0178	0.0676	0.0002			
vs 3′-2#	0.1036	0.4821	0.0345	0.2381		
vs 4-1#	0.0785	0.0653	0.0011	0.7392	0.2138	
vs 4-2#	0.0177	0.8092	0.0017	0.1574	0.5632	0.1325

Table 4.10 Weight changes (mg) of the load soaks

Sample	At 72 hours	At 110 hours
XLPE	0.00004	N/A
ConvPE	-0.00002	0.02000
Control	-0.00005	-0.05500
3'-1#	0.00068	N/A
4-1#	0.00003	0.10000
4-2#	0.00001	N/A

4.6 Figures

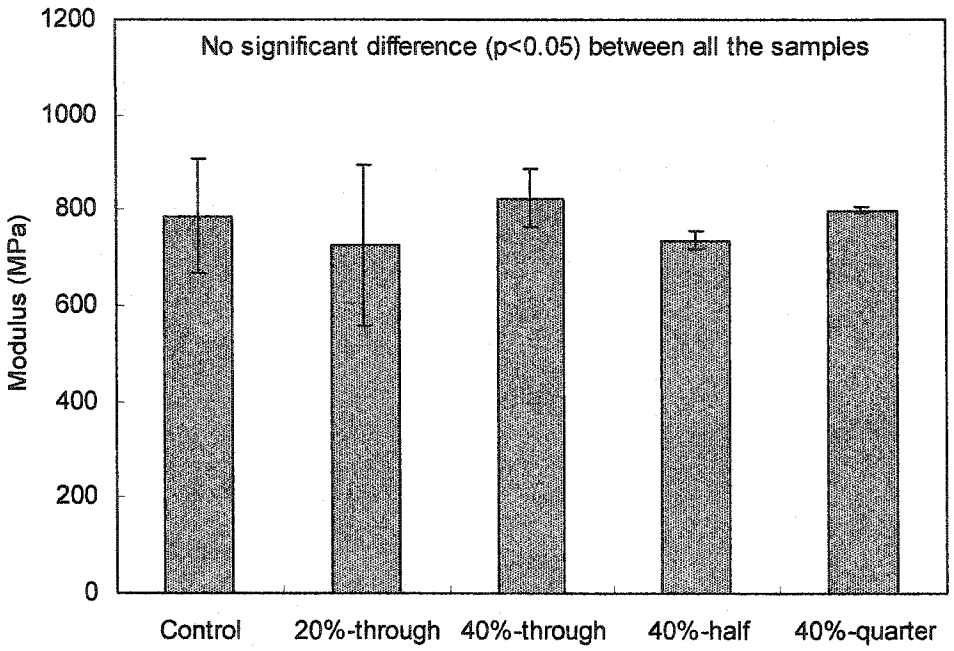

Figure 4.1 Modulus of elasticity for the control and micro-composites

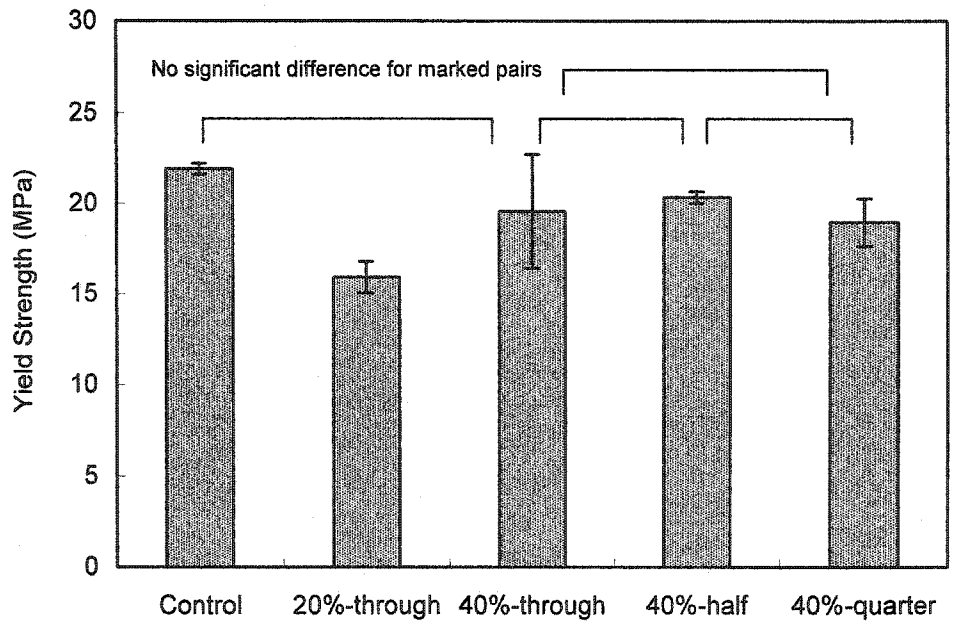

Figure 4.2 Yield strength for the control and micro-composites

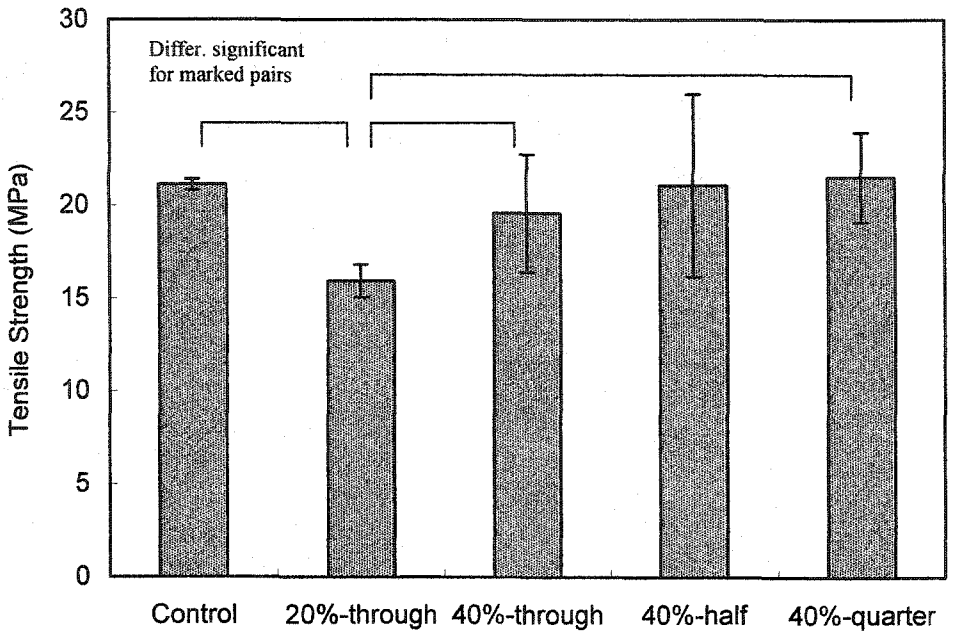

Figure 4.3 Tensile strength for the control and micro-composites

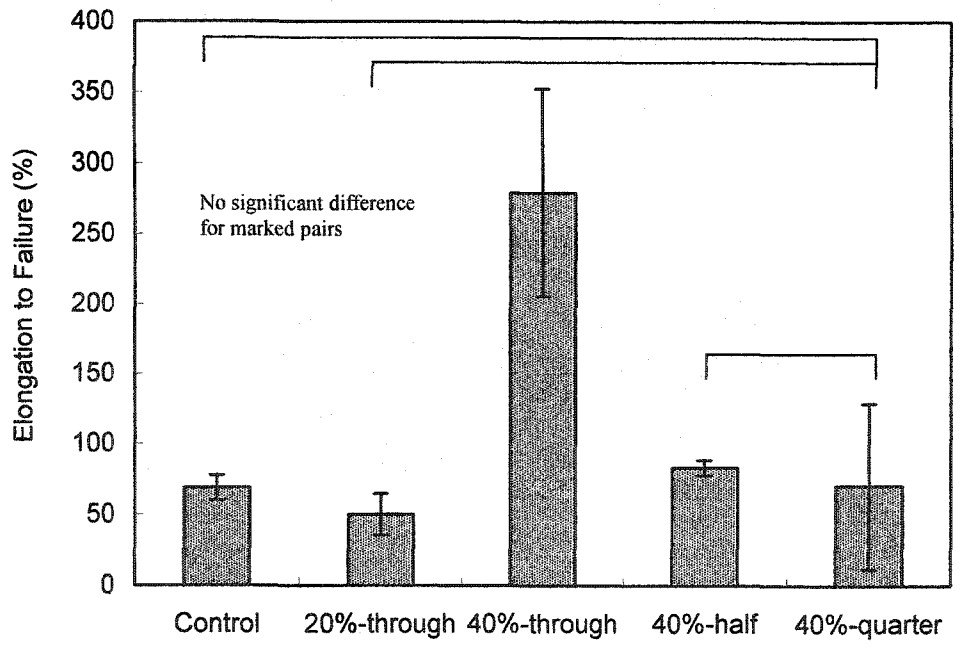

Figure 4.4 Elongation to failure for the control and micro-composites

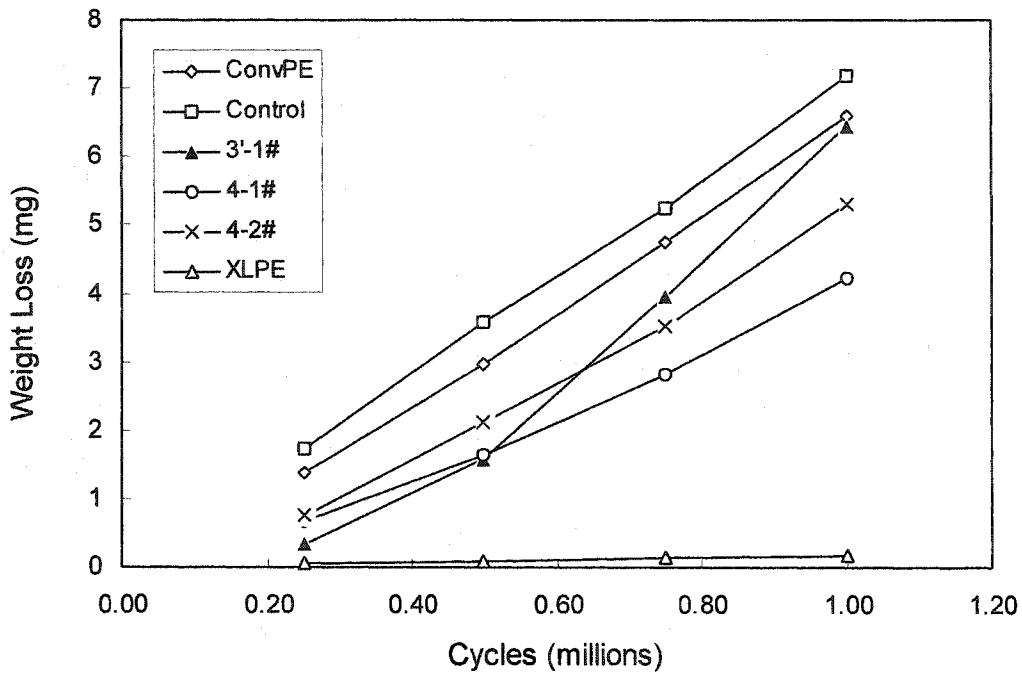

Figure 4.5 Average weight loss for UHMWPE controls and micro-composites at cycles up to 1.0 million.

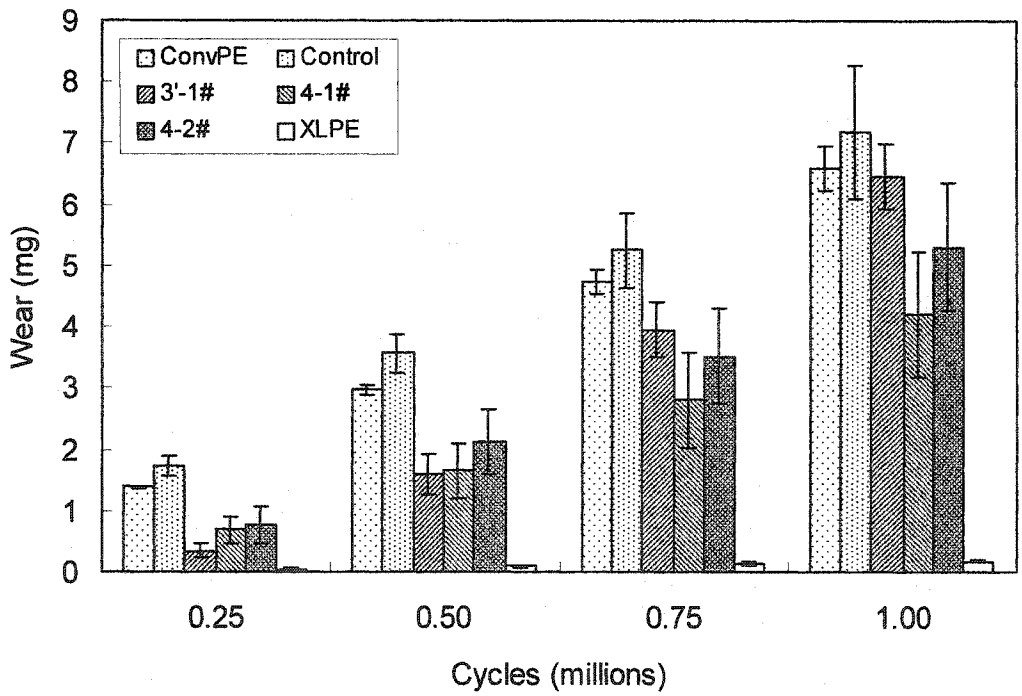

Figure 4.6 Wear results for UHMWPE controls and micro-composites

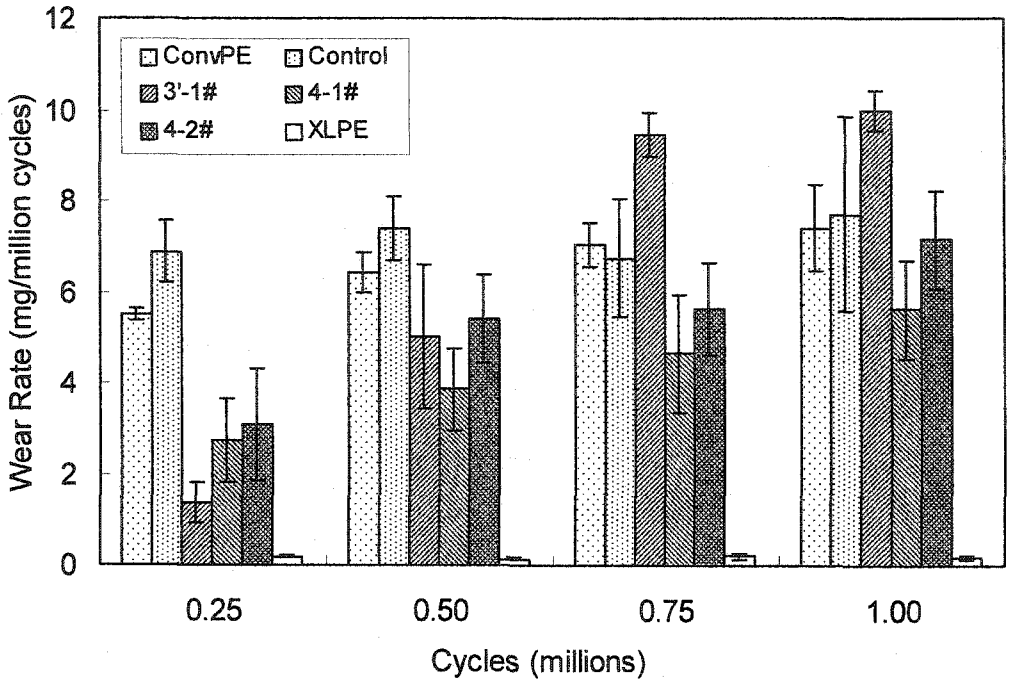

Figure 4.7 Wear rate for UHMWPE controls and micro-composites

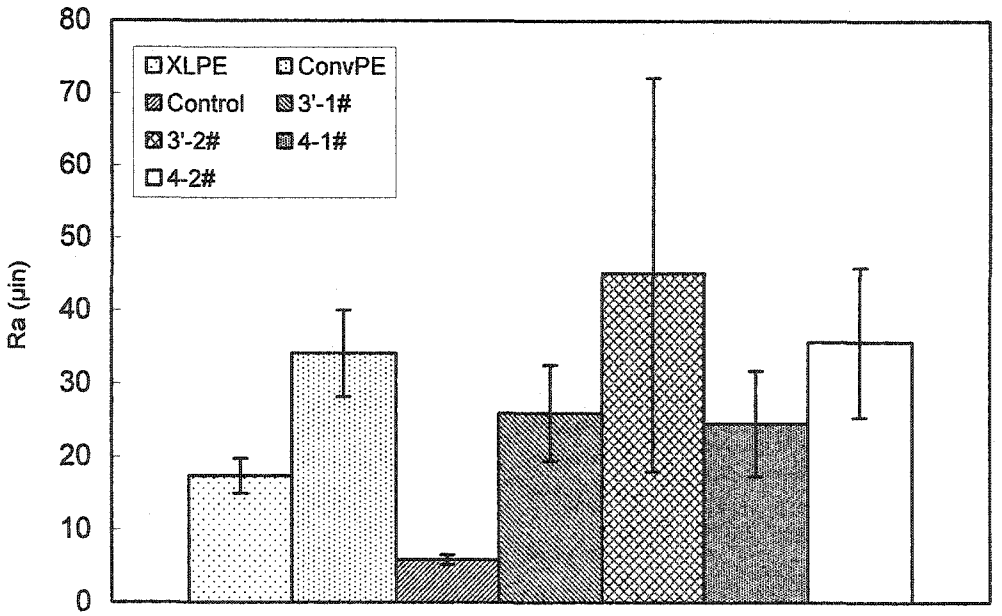

Figure 4.8 Surface roughness for all the wear test samples

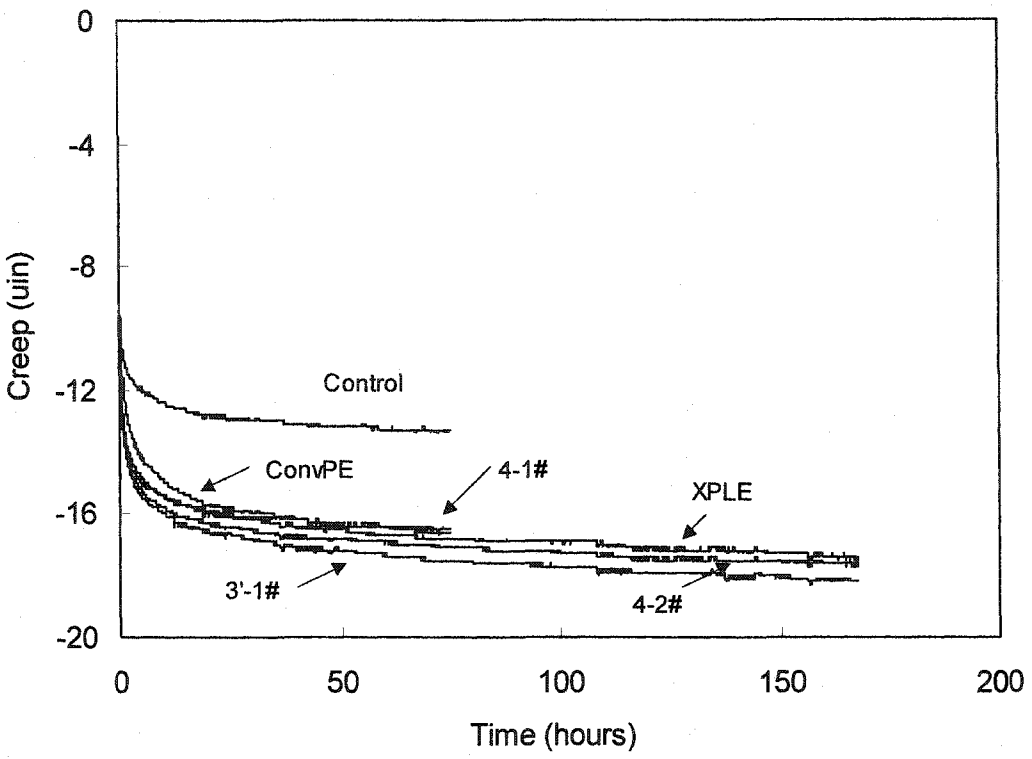

Figure 4.9 Creep curves for the load soak controls

4.7 References

Askeland DR (1994). The Science and Engineering of Materials (3rd ed.). PWS publishing Company: Boston, pp.175- 199 & 467-522.

Bennett AP (1995). HSS/Poly Hi Solidur/Hoeschst Reference UHMWPE: Protocol for Quality Control. Hospital for Special Surgery, New York, NY.

Bennett AP, Wright TM and Li S (1996). Global reference UHMWPE: characterization and comparison to commercial UHMWPE. In *42nd Annual meeting of Orthopaedic Research Society*, Atlanta, Georgia, pp.472.

Bollet AJ, Bonner WM (Jr.), and Nance JL (1963). The presence of hyaluronidase in various mammalian tissues. *The Journal of Biological Chemistry*, 238: 3522-3527.

Delpech B, Bertrand P, and Chauzy C (1987). An indirect enzymoimmunological assay for hyaluronidase. *Journal of Immunological Methods*, 104: 223-229.

Fraser JRE and Laurent TC (1989). Turnover and metabolism of hyaluronan. In The Biology of Hyaluronan, *Ciba Foundation Symposium 143*. John Wiley & Sons: Chichester, 41-53.

Kurtz SM, Muratoglu OK, Evans M and Edidin AA (1999). Advances in the processing, sterilization, and crosslinking of UHMWPE for total joint arthroplasty. *Biomaterials*, 20: 1659-1688.

Laurent TC (1970). Structure of hyaluronic acid. In *Chemistry and Molecular Biology of the Intercellular Matrix* (edited by Balazs EA). Academic Press: London, 2: 703-728.

Laurent TC and Fraser JRE (1986). The properties and turnover of hyaluronan. In *Functions of the proteoglycans, Ciba Foundation Symposium 124*. John Wiley & Sons: Chichester, pp.9-24.

Lowry KM and Beavers EM (1994). Resistance of hyaluronate coatings to hyaluronidase. *Journal of Biomedical Materials Research*, 28: 861-864.

Rentfrow E (1999). Mechanical and physical characterization of a novel surface treatment on ultra-high molecular weight polyethylene. Master Thesis. Colorado State University, Fort Collins, Colorado.

Stern R and Csóka AB (2003). Mammalian hyaluronidases. In *Glycoforum-Science of Hyaluronan Today* (edited by Hascall VC). http://www.glycoforum.gr.jp/science/hyaluronan/hyaluronanE.html

U.S. Pharmacopeia – the National Formulary (XXII revision) (1990). Official Monographs, pp. 644.

Zhang M, James SP, and Rentfrow E (2001A). The effect of IPN surface modification on the tensile and creep properties of UHMWPE. In *27th Annual Meeting Transactions of Society for Biomaterials*, pp.479.

Chapter 5

Hyaluronan Esters

5.1 Introduction

In the UHMWPE-HA micro-composite system, the use of porous preforms made the introduction of HA into UHMWPE much easier than the previously reported solvent swelling IPN method [Beauregard, 1999]. Treatment time for UHMWPE was reduced to several minutes from more than ten days, and the thickness of the modified layer could be controlled. However, removal of the residual solvent and two molding cycles still complicate the process. It would be desirable to mold HA directly with UHMWPE during the thermal process. However, like natural cellulose, hyaluronan (HA) degrades before it melts due to strong intermolecular hydrogen bonding and high crystallinity [Shiraishi, 1989]. The HA derivatives developed in Chapter 2, HA-CTA and silyl HA-CTA, did not melt either, perhaps because the disruption of intermolecular interaction and molecular order was insufficient. Therefore, a novel thermal-processable HA derivative is still required to meet thermal processing requirements.

It has been reported that cellulose could be converted into a thermoplastic material through esterification [Klemm et al., 1998B; Shiraishi et al, 1989]. In principle, cellulose esters are synthesized by employing acid anhydride with a suitable catalyst or acid chloride in the presence of a tertiary base. However, plasticization of low aliphatic acid

esters of cellulose is not sufficient. They exhibit high melting points (e.g., 225-250°C for cellulose 2,5-acetate and above 300°C for cellulose triacetate). These commercial esters melt accompanied by decomposition, so they can be processed only via solution state or in the presence of a large amount of plasticizer [Klemm et al., 1998B]. Several further esterification methods for cellulose diacetate have been reported to produce melt-processable cellulose derivatives [Yoshioka et al., 1996; Lee et al., 2001; Teramoto et al., 2002].

Esterification with high aliphatic acids can effectively confer thermal fluidity to cellulose. Shiraishi et al. [1979A] prepared a series of high aliphatic esters of wood in N_2O_4-DMF in the presence of pyridine with various acid chlorides, from caproyl to stearoyl chloride, and acid anhydrides, from propionic to caproic anhydride, and successfully molded the lauroylated wood meal into a transparent film through hot-pressing [Shiraishi et al, 1989]. Starting from valerate, the melting points of higher aliphatic triesters of cellulose were not beyond 155°C [Klemm et al., 1998B], which are far below the decomposition temperature of cellulose (180-250°C), allowing these cellulose esters to be hot processed.

A special route to synthesize cellulose esters was proposed by Stein and Klemm [1988]. They used trimethylsilyl cellulose as starting materials to prepare cellulose esters, including high aliphatic acid esters. The reaction of trimethylsilyl cellulose with acid chlorides was carried out at 80-160°C for 0.5-1 hour without addition catalysts or solvents. Acylation was demonstrated to occur at the oxygen of the $-OSi(CH_3)_3$ group of silyl cellulose. This rapid, non-solvent reaction was also applied to esterification of HA in this study.

Two classes of HA esters have been patented, or have pending patent applications. One is Hyaff ® developed by Fidia Advanced Biopolymer in Italy. Hyaff is a class of hyaluronan esters with the free carboxyl groups of HA esterified using different types of alcohols [della Valle and Romeo, 1989]. The reaction was reviewed in Section 1.2.6.1. These HA esters can be used in medicine, surgery, cosmetics and other biomedical fields, but they are not thermoplastic (i.e., no melting endotherms) [Barbucci et al., 1993; Rastrelli et al., 1990]. Another class of HA esters was developed by Yui et al. [2002]. They modified the hydroxyl groups of HA with an acid halide carrying photoreactive groups, such as cinnamoyl chloride, in DMF solution in the presence of pyridine. The reaction was reviewed in Section 1.2.6.1. The product dissolved in DMF was subjected to ultraviolet radiation to crosslink HA. The HA derivatives are useful for pharmaceutics, foodstuffs, cosmetics, etc., but the crosslinked polymer cannot melt.

None of the current HA esters are thermoplastic. A series of novel melt-processable HA esters with varying aliphatic chain lengths were created using silyl HA-CTA as the starting material. The synthesis and characterization of these novel HA esters are reported herein. The regeneration of HA from the HA esters via saponification is also reported.

5.2 Materials and Methods

5.2.1 Materials

Silyl HA-CTA was obtained through the methods described in Chapter 2. The original sodium hyaluronate (HyluMed®, medical grade, MW: 1.36×10^6 daltons) was purchased from Genzyme (Cambridge, MA). Acid chlorides, including hexanoyl (caproyl), octanoyl (capryloyl), decanoyl (caprinoyl), lauroyl, palmitoyl, and stearoyl chloride (see Table

5.1), were purchased from Aldrich (Milwaukee, WI), and used as received. DMSO, THF, xylenes, hexane and acetone were purchased from Fisher (Pittsburgh, PA). DMSO and THF were used as received. Xylenes, hexane and acetone were respectively dried by refluxing over Na, CaH_2 and anhydrous $CaSO_4$ and distilled just before use. Pyridine and potassium hydroxide (certified A.C.S) were also obtained from Fisher, but used as received. Ethanol (ACS/USP grade) provided by Pharmco (Brookfield, CT), and used as received.

5.2.2 Reactions

(1) Syntheses of HA Esters

HA esters were synthesized by reacting acid chlorides with HA-CTA in solvents or without solvents. For the non-solvent synthesis, 200mg of silyl HA-CTA were added under N_2 atmosphere to 5-10 equivalents of acid chloride. The mixture was heated for 0.5-1 h at 80°C. The reaction product was a clear, light yellow or brown solution, but once cooled, the solution became a turbid, viscous paste or, in the case of stearate, a solid. Hexane was used to precipitate caproate, caprylate, caprinate and laurate from the product mixtures. Acetone was used to wash the excess of palmitoyl and stearoyl chlorides from the HA esters. After washing or precipitating several times, the resulting HA esters were dried in 50°C vacuum oven until constant weight was obtained.

When performing synthesis with solvents, xylenes were used to form a homogeneous solution and promote reaction. After esterification, xylenes were removed under vacuum, while excess acid chlorides were removed with the same method used in the non-solvent synthesis.

(2) Saponification of HA esters

KOH (5.6106 g) was dissolved in 100 ml of water to make a 1M KOH solution. Equal volumes of acetone and ethanol, and equal volumes of pyridine and ethanol were mixed respectively to obtain 200ml of solvent mixtures. For those esters soluble in acetone, such as caproate, caprylate, caprinate and laurate, 200 mg of HA ester were dissolved in 20 ml of acetone-ethanol mixture, forming a clear solution. Aqueous KOH solution (5 ml) was slowly added to the solution through a pipette with swirling. The saponified HA ester gradually precipitated from solution. After addition of 5 ml water, the solution stood at room temperature for another hour to completely saponify the ester residue. The precipitate was filtered and KOH in the precipitate was removed by dissolving in water and re-precipitating with ethanol several times. The final white particle product was regenerated HA, which was vacuumed in a 50°C oven until a constant weight was obtained.

For those HA esters insoluble in acetone, such as palmitate and stearate, 200mg of ester were dissolved in 20 ml of pyridine-ethanol mixture. The rest of the saponification procedure was the same as above.

5.2.3 Characterization Methods

Fourier Transform Infrared Spectroscopy (FT-IR): HA caproate, caprylate, caprinate and laurate were dissolved in acetone and coated on NaCl disks for FT-IR analysis. HA palmitate and stearate were dissolved in xylenes and cast onto NaCl disks. Regenerated HA from ester saponification was mixed with KBr and pressed into pellets. The FT-IR spectrometer and spectrum-collecting methods are described in Section 2.2.3.

X-Ray Photoelectron Spectroscopy (XPS): HA laurate was dissolved in xylenes and cast into film on glass slide for XPS analysis. The equipment and test conditions are described in Section 2.2.3.

Differential Scanning Calorimetry (DSC) and Thermal Gravimetric Analysis (TGA): The DSC and TG analyses of HA esters were performed on the same instruments used for HA, HA-CTA and silyl HA-CTA, and the test conditions are described in Section 2.2.3.

Hot Stage Microscope Analysis: HA ester film samples were prepared by evaporating solutions of HA ester in organic solvents (e.g., acetone for caproate, xylenes for laurate), which were placed between a microscope slide and a coverslip. The slide was placed on a hot stage mounted on a Nikon polarizing light microscope. The polymer was heated at a rate of 20°C/min and photomicrographs were taken with a Nikon FX-35DX camera.

5.3 Results and Discussion

5.3.1 Synthesis of HA Esters

Compared with native HA, silyl HA-CTA used as a starting material is more reactive, making it useful as the intermediate of many further modifications of HA, including esterification. The trimethylsilyl groups of silyl HA-CTA are more easily replaced than the active hydrogen in HA hydroxyl groups. Esterification with silyl HA-CTA as a starting material (Figure 5.1) was carried out without addition of any catalysts, and the reaction took place at a very high rate (within 0.5-1 hours). The only by-product was trimethylchlorosilane (TMCS), which has a low boiling point (57°C), and can be evaporated at the reaction temperature (80°C).

The fact that the acylation takes place at the oxygen of the trimethylsilyloxy group -O-$Si(CH_3)_3$ in the silyl HA-CTA can be demonstrated by the complete removal of trimethylsilyl groups from HA esters. The FT-IR spectrum of HA palmitate is shown in Figure 5.2 in comparison with HA-CTA and silyl HA-CTA. The spectra of all HA esters are similar, so the spectrum of palmitate is used as a representative. All the characteristic absorption bands related to trimethylsilyl groups, including bands at 1250, 879, 847 and 758 cm^{-1}, disappear in the HA ester spectra. A strong, new peak at 1753 cm^{-1} is observed for the HA ester, attributable to the carbonyl groups in saturated esters [Smith, 1998], indicating the introduction of a large amount of acyl groups with acylation. A strong peak near 1160cm^{-1} associated with ester C-C-O asymmetric stretching also shows in the HA ester spectrum. The intensity of bands at 2926 and 2855 cm^{-1} also significantly increases compared to the silyl HA-CTA spectrum. This is due to the introduced long aliphatic chains of HA esters.

The C1s XPS high resolution spectrum of HA laurate is shown in Figure 5.3. Like silyl HA-CTA, the C1s spectrum of HA ester can also be best fitted with four peak components: C0, C1, C2 and C3, and their definition and position are identical to that of silyl HA-CTA described in Section 2.3.2. The C3 component (associated with -O-C=O and -HN-C=O groups) for the HA ester increases to 5.6% from 4.0% in silyl HA-CTA, and its intensity almost doubles that of the C2 peak (assigned to O-C-O and C=O). In contrast, in silyl HA-CTA, the C3 peak area is inferior to C2. The increase of C3 peak percentage and intensity relative to C2 can be explained with the introduction of large amounts of ester groups during esterification. The number of CHx and C-C units in

lauroyl groups ($CH_3(CH_2)_{10}C=O$) exceeds that in $Si(CH_3)_3$, so the C0 component also shows a higher percentage in HA laurate (81.0%) than in silyl HA-CTA (78.1%).

The N1s XPS high resolution spectra of HA laurate and silyl HA-CTA are shown in Figure 5.4. The N1s signal of the ester consists of two components: ammonium salt N+ and amide N. The intensity of ammonium salt N+ signal is smaller than that of amide N signal in the ester sample, but they are almost equal to that observed in silyl HA-CTA. This may suggest that the acid chloride also attacked –CTA groups during esterification, but this attack was not dominant, because most ammonium salt N+ groups still remain.

5.3.2 Regeneration of HA from HA Esters

Ester bonds are susceptible to hydrolytic cleavage, and under alkaline conditions, an irreversible saponification of ester groups can occur [Klemm et al., 1998B]. Therefore, ester groups are removed from HA esters with saponification. Furthermore, alkaline metal cations (e.g. Na^+ and K^+) with sufficiently high concentration can displace the –CTA groups in the ester [Scott, 1960], resulting in a regenerated HA. It was reported that saponification of cellulose esters was normally performed in an alcoholic alkali solution [Klemm et al., 1998A; Shiraishi et al., 1979B]. In order to increase wetting and thus reaction of the hydrophobic ester, a water-miscible and ester-soluble organic solvent was often added. In ASTM D 817-96, acetone or pyridine was used with methanol to dissolve cellulose esters with high content of propionyl or butyryl substitutions. A mixture of acetone and ethanol was used for saponification of these esters, because HA esters from caproate to laurate are soluble in acetone. HA palmitate and stearate are insoluble in acetone, but dissolve in pyridine, so a pyridine-ethanol mixture was used for them.

The FTIR spectrum of HA regenerated from saponification of HA caprylate is shown in Figure 5.5. All the peaks characteristic of absorptions for –CTA and capryloyl esters are gone. There is no difference between the spectra of regenerated HA and original HA, indicating the complete removal of –CTA and ester groups through saponification.

5.3.3 Properties of HA Esters

Each disaccharide unit of HA contains four hydroxyl groups, one amide and one carboxylic acid group. Due to the strong intra- and inter-molecular hydrogen bonds, HA is highly crystalline and insoluble in organic solvents, and cannot be transformed into the molten state before its decomposition. From thermogravimetric data in Figure 5.6, it can be seen that HA begins to degrade around 212°C, but no melting point can be found below that temperature (Figure 5.7).

Introduction of aliphatic acyl groups to HA was effective in disrupting the strong HA intermolecular bonding, reducing the crystallinity and producing appreciable thermoplasticization, similar to that observed in esterified cellulose [Shiraishi et al., 1979B]. This is confirmed by the melting endothermic peaks in the DSC thermograms of HA laurate and caproate (Figure 5.7). For laurate, a broad endotherm is observed ranging from 76°C to 105°C with a peak at 97.8°C, while caproate shows a melting peak starting from 175°C with the peak at 191.7°C. The TG results (Figure 5.6) show that HA laurate begins degrading at about 191°C, while caproate begins degrading at approximately 170°C. The hot-stage microscope photographs of HA laurate are shown in Figure 5.8. Melting liquid droplets became obvious in laurate at approximately 100°C, and with increasing temperature, the droplets became bigger and bigger until they joined to form a

completely flowable melt. On the hot stage the HA caproate did not appear to melt until 190°C, but at this temperature the liquid also showed a brownish appearance typical of degradation. Therefore, HA laurate is melt-processable, but caproate melts with decomposition due to insufficient disruption of hydrogen bonds and crystal structure. The melting onsets determined using the hot-stage microscope coincided with the peaks of the endotherms in the corresponding DSC thermograms, but not with the endotherm onsets. This is probably due to the higher heating rate used in the hot-stage and the difficulty of detecting the first-formed liquid drops in the micrographs.

The melting temperature and the starting points of degradation for various HA esters are summarized in Table 5.1. Obviously, the intermolecular interaction between the polymer chains decreases with increasing length of ester side chains, as indicated by the change in melting points. The higher aliphatic acid chloride was more effective in conferring thermoplasticity to HA. Starting from caprinate, higher aliphatic esters of HA melt far before the decomposition occurs, and thus can be melt processed. On the other hand, caproyl and capryloyl are not sufficiently large enough to disturb the molecular order of HA, so HA caproate and caprylate did not achieve complete thermal fluidity before the onset of degradation.

Degradation points of HA esters depend on the balance between two factors: a decrease in crystallinity (molecular order) and an increase in the length of acyl groups. From caproate to palmitate, the effect of acyl group chain length seems to dominate, so the degradation temperature increases with the carbon number of the ester chain. However, with stearate, the effect of molecular order disruption seems to dominate, so the degradation temperature of HA stearate is lower than that of palmitate.

The solubility of HA esters were also investigated and the results are summarized in Table 5.2. HA esters from caproate to laurate are soluble in acetone, while palmitate and stearate are soluble in hexane, indicating that the hydrophobicity of HA esters increases with the side chain length. Xylenes are a good solvent for all of these esters.

From the above evidence, HA ester melting points and solubility in organic solvents can be controlled by modulating the chain length of acyl groups. The resultant thermoplastic HA esters can be hot molded into films, sheets, and any desired shapes. They can be used alone or mixed with some other biomedical grade thermoplastics, such as UHMWPE. Crosslinkers, such as blocked polyisocyanate, can also be used during molding to obtain a permanent three-dimensional HA ester network. Finally, the acyl groups can be easily removed through saponification in order to return HA to its native state after molding.

5.4 Conclusions

A series of HA esters were successfully created through the acylation reaction of silyl HA-CTA with acid chlorides. The disappearance of all characteristic infrared absorption bands assigned to the $-OSi(CH_3)_3$ groups and the appearance of the strong ester carbonyl peak confirmed the completion of esterification. In this esterification, some –CTA groups attached to carboxyl groups might also be attacked by acid chlorides. This was reflected by the decrease in intensity of the N^+ peak component in high resolution N1s XPS spectrum.

Esterification with high aliphatic acid chlorides was demonstrated to be an effective method for imparting thermoplasticity to HA. HA caprinate, laurate, palmitate and

stearate had melting peaks far below their degradation temperatures, providing a large window for safe hot processing of the polymers. Caproyl and capryloyl are not long enough to disrupt the strong HA intermolecular interactions and molecular arrangement, so their corresponding HA esters were not melt-processable.

The ester groups could be completely removed through saponification. The FT-IR analysis showed that the HA regenerated from HA esters had the same structure as native HA, indicating esterification and saponification did not damage the backbone of HA.

5.5 Tables

Table 5.1 Properties of HA and its aliphatic esters

Material	Acid Chlorides	Formula of Acid Chlorides	Melting Points (°C)	Starting Points of Degradation (°C)
HA			No*	212
HA-CTA			No	175
Silyl HA-CTA			No	161
Caproate	Hexanoyl	$CH_3(CH_2)_4COCl$	191.7	170
Caprylate	Octanoyl	$CH_3(CH_2)_6COCl$	188.9	184
Caprinate	Decanoyl	$CH_3(CH_2)_8COCl$	156.7	187
Laurate	Lauroyl	$CH_3(CH_2)_{10}COCl$	97.8	191
Palmitate	Palmitoyl	$CH_3(CH_2)_{14}COCl$	96.4	200
Stearate	Stearoyl	$CH_3(CH_2)_{16}COCl$	88.3	194

*No melting temperature: polymer degrades before melting.

Table 5.2 Solubility of HA esters in organic solvents

HA Esters	DMSO	THF	Acetone	Xylenes	Hexane
Caproate	Swelling	+	+	+	–
Caprylate	Swelling	+	+	+	–
Caprinate	Swelling	+	+	+	–
Laurate	–	+	+	+	–
Palmitate	–	–	–	+	+
Stearate	–	–	–	+	+

"+" soluble; "–" insoluble.

5.6 Figures

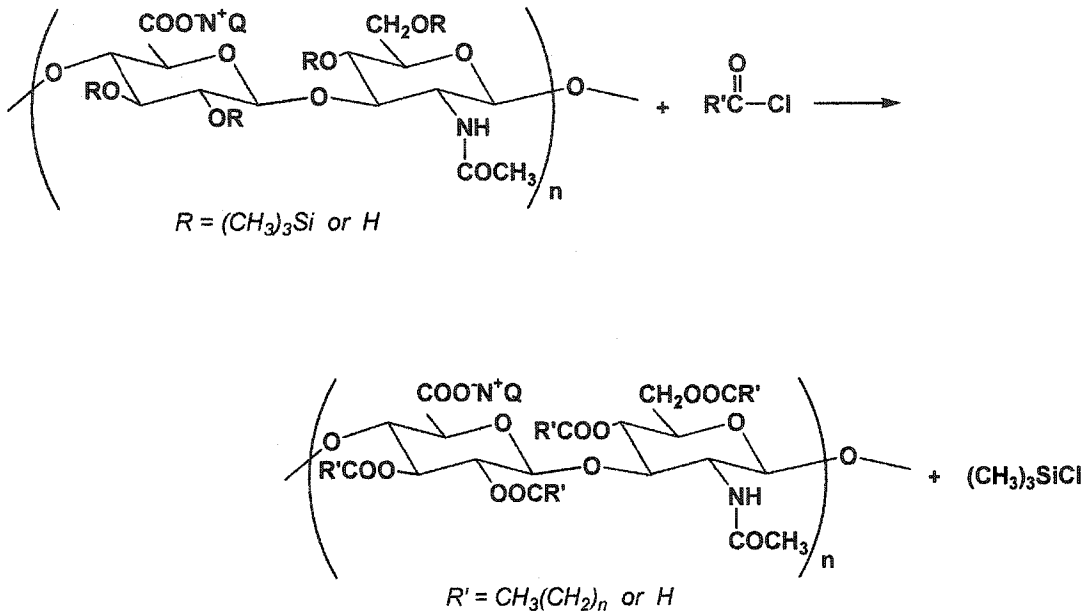

Figure 5.1 Acylation of silyl HA-CTA

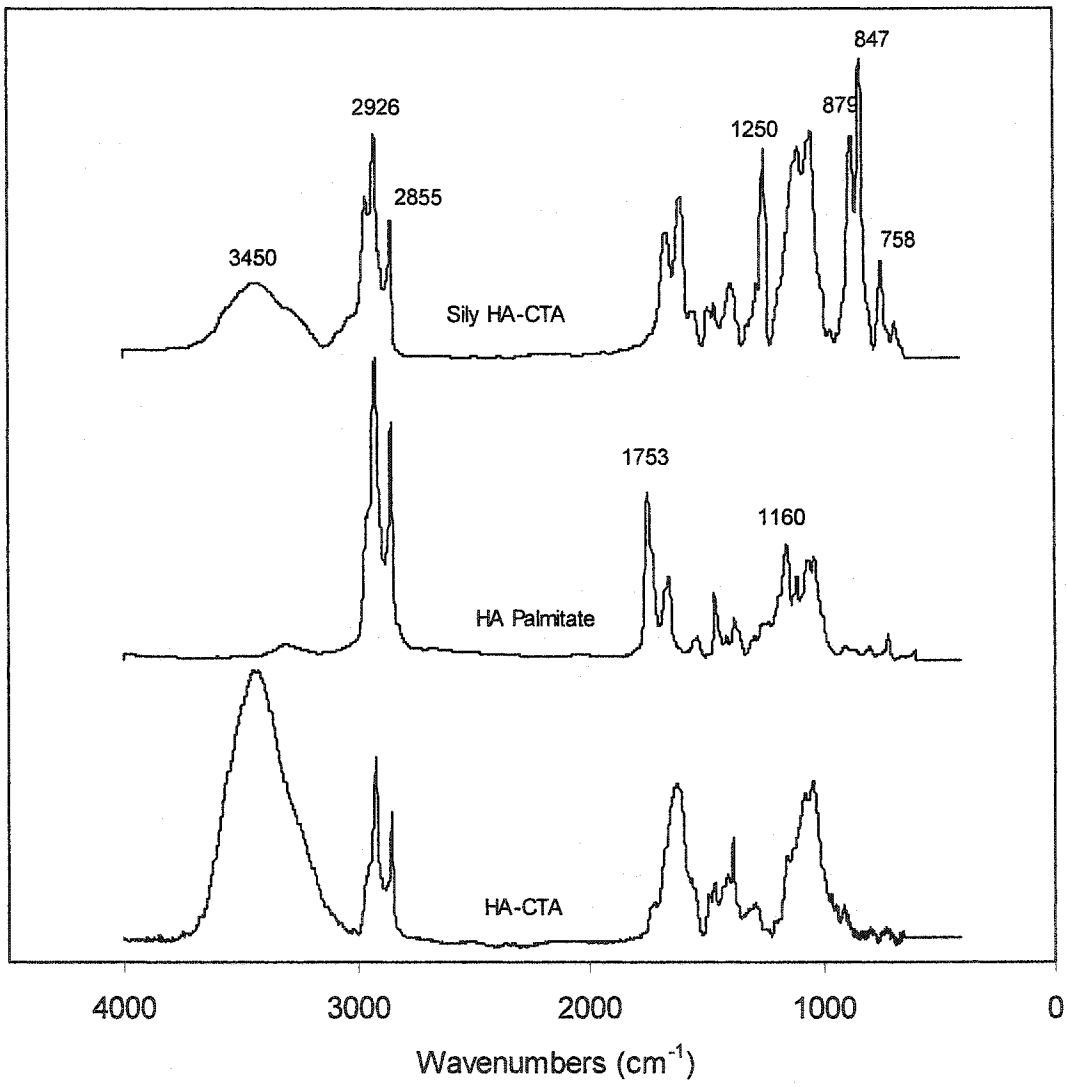

Figure 5.2 FT-IR spectra of silyl HA-CTA, HA palmitate and HA-CTA

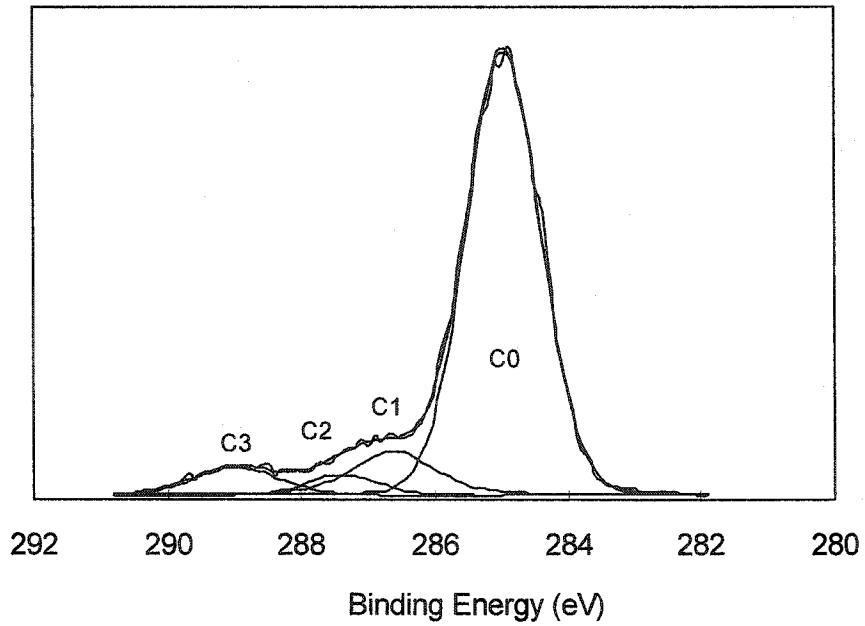

Figure 5.3 High-resolution C1s XPS spectrum of HA laurate

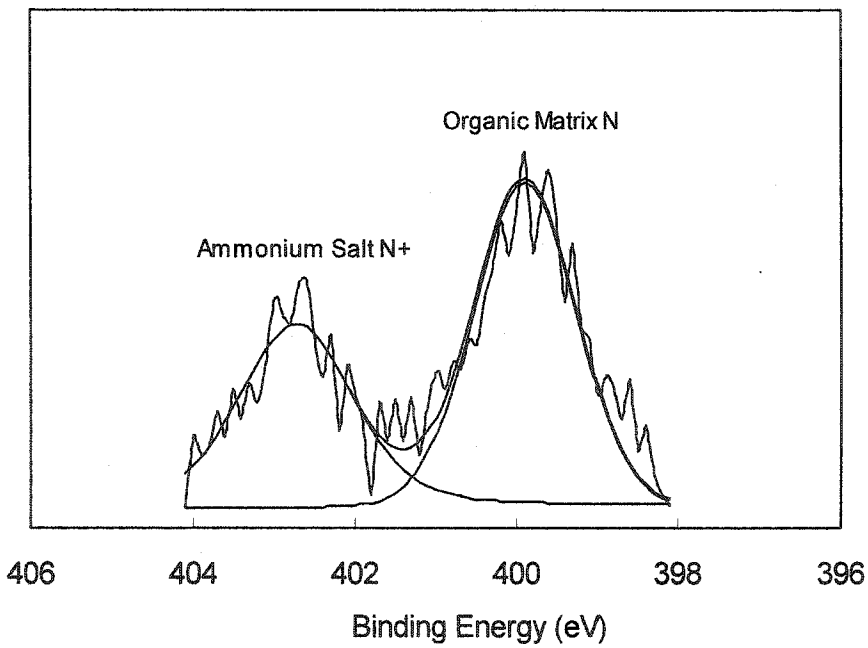

Figure 5.4 High-resolution N1s XPS spectrum of HA laurate

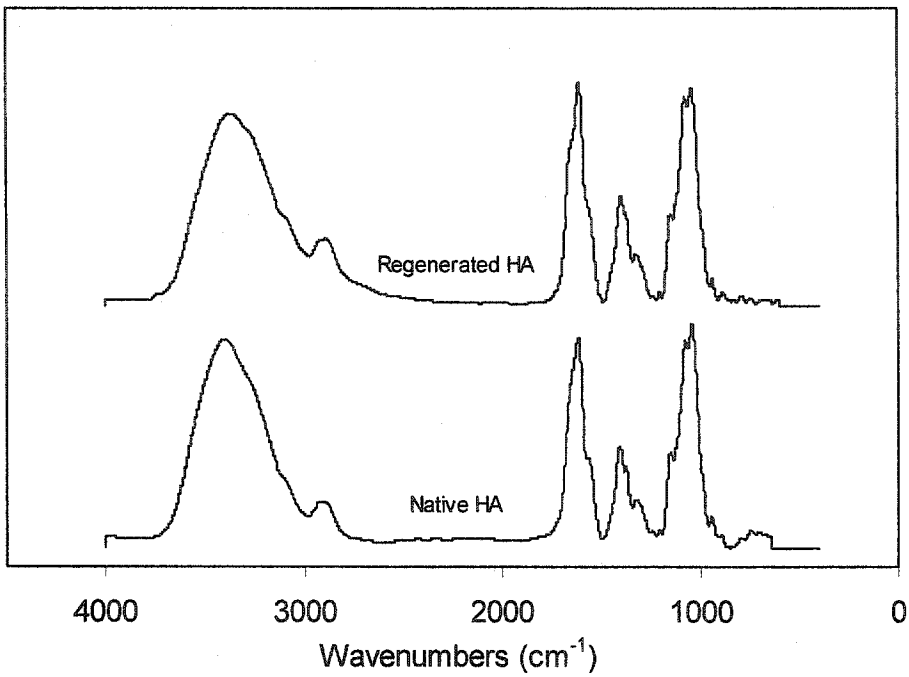

Figure 5.5 FT-IR spectra of regenerated HA from saponification and native HA

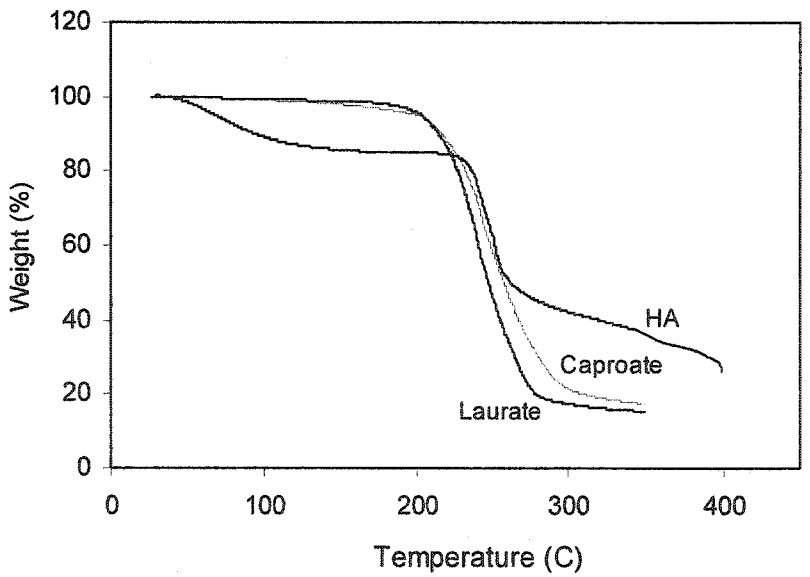

Figure 5.6 TG of HA, HA caproate and laurate

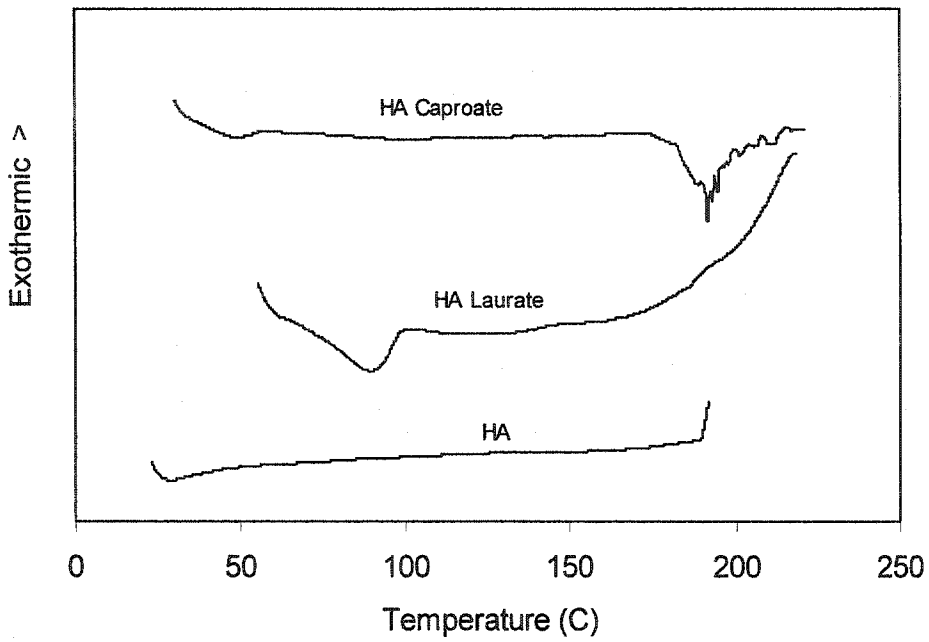

Figure 5.7 DSC of HA, HA caproate and laurate

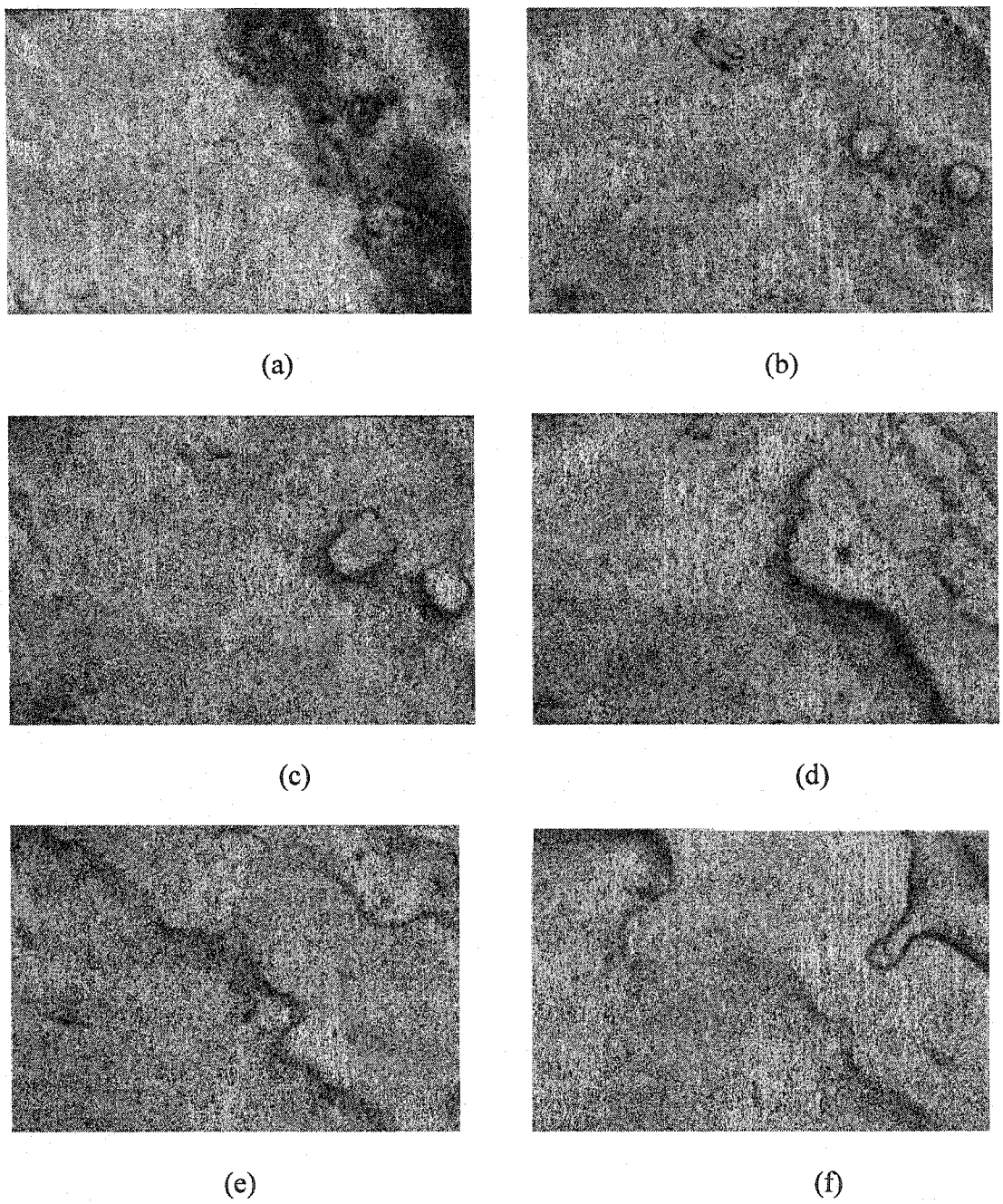

Figure 5.8 Optical micrographs of HA laurate at (a) room temperature; (b) 100°C; (c) 120°C; (d) 140°C; (e) 160°C; (f) 180°C

5.7 References

Barbucci R, Magnani A, and Baszkin A et al. (1993). Physical-chemical surface characterization of hyaluronic acid derivatives as a new class of biomaterials. *Journal of Biomaterials Science, Polymer Edition*, 4: 245-273.

Beauregard GP (1999). Synthesis and characterization of a biomimetic UHMWPE-based interpenetrating polymer network for use as an orthopedic biomaterial. Ph.D dissertation. Colorado State University, Fort Collins, Colorado.

della Valle F and Romeo A (1989). Esters of hyaluronic acid. US Patent 4851521.

Klemm D, Philipp B, and Heinze T et al (1998A). *Comprehensive Cellulose Chemistry (Volume 1): Fundamentals and Analytical Methods*. Wiley-VCH: Weinheim, Germany, pp.235.

Klemm D, Philipp B, and Heinze T et al (1998B). *Comprehensive Cellulose Chemistry (Volume 2): Functionalization of Cellulose*. Wiley-VCH: Weinheim, Germany, pp.164-198.

Lee SH and Shiraishi N (2001). Plasticization of cellulose diacetate by reaction with maleic anhydride, glycerol, and citrate eaters during melting processing. *Journal of Applied Polymer Science*, 81: 243-250.

Rastrelli A, Beccaro M, and Biviano F et al. (1990). Hyaluronic acid esters, a new class of semisynthetic biopolymers. In *Proceedings of the 8th European Conference on Biomaterials* (edited by Heimke G et al.). Elsevier Science Publishers B.V.: Amsterdam, 9: 199-205.

Scott JE (1960). Aliphatic ammonium salts in the assay of acidic polysaccharides from tissues. *Methods of Biochemical Analysis*, 8: 145-197.

Shiraishi N, Matsunaga T, and Yokota T (1979A). Preparation of higher aliphatic acid esters of wood in an N_2O_4-DMF cellulose solvent medium. *Journal of Applied Polymer Science*, 24:2347-2359.

Shiraishi N, Matsunaga T, and Yokota T (1979B). Thermal softening and melting of esterified wood preparation in an N_2O_4-DMF cellulose solvent medium. *Journal of Applied Polymer Science*, 24:2361-2368.

Shiraishi N (1989). Plasticization of wood and its application. In *Cellulosics Utilization* (edited by Inagaki H and Phillips GO). Elsevier Science Publishers Ltd: New York, NY, pp.97-109.

Smith B (1998). *Infrared Spectral Interpretation*. CRC Press: New York, pp.158-160.

Stein A and Klemm D (1988). Syntheses of cellulose derivatives via O-triorganosilyl cellulose, 1. *Makromolekulare Chemie, Rapid Communication*, 9: 569-573.

Teramoto Y, Yoshioka M, Shiraishi N, and Nishio Y (2002). Plasticization of cellulose diacetate by graft copolymerization of ε–caprolactone and lactic Acid. *Journal of Applied Polymer Science*, 84: 2621-2628.

Yoshioka M, Miyazaki T, and Shiraishi N (1996). Plasticization of cellulose derivatives by reactive plasticizers I. *Mokuzai Gakkaishi*, 42: 406-416.

Yui N, Ooya T and Sato I (2002). Chemically modified hyaluronic acid or salts thereof, and a process for producing thereof. US Patent Application, No. 20020143171.

Chapter 6

Research Summary and Future Work

6.1 Research Summary

The goal of this research was to modify the surface of UHMWPE via introduction of hyaluronan to reduce its wear and enhance its lubrication. Hyaluronan could potentially be introduced into UHMWPE through solvent infiltration or through a blending in the melt and molding. Two novel classes of hyaluronan derivatives were developed to meet the different process requirements of solvent infiltration and melt blending. Silylated HA was hydrophobic and soluble in regular organic solvents, so it was used for the solvent method. UHMWPE porous preforms were used instead of bulk solid material, so that prolonged swelling of UHMWPE was not required and to achieve more precise control over the HA concentration and thickness of the surface layer. In xylenes solution, silylated HA quickly diffused into the connected pores of the preforms, so the process was fast and simple. The final micro-composites obtained through appropriate treatment had uniform films of HA on its surface, which were water wettable, lubricious, and stable. The presence of HA did significantly affect the tensile properties of UHMWPE, but the changes were acceptable. Almost all the samples (including non-treated controls) exhibited inferior mechanical properties due to poor consolidation during the final molding process. However, improvements in the overall molding process are easily

achievable by increasing the molding temperatures used. There is a range of safe molding temperatures, above that used in the current samples and below that which would degrade the HA, which should result in much improved tensile properties for all samples (controls and micro-composites).

The presence of HA on the surface of the micro-composites significantly reduced the wear and wear rate of UHMWPE for certain sample treatment and re-molding processes. Incomplete consolidation, high HA content within the micro-composite, insufficient HA on the surface, low crosslinking density and weak adhesion of coating after consolidation weakened the lubrication achieved by micro-composites. By optimizing treatment parameters and improving molding conditions, a micro-composite with controlled qualities can be obtained, and is expected to have much better wear-resistance than the current materials.

The silylated HA developed for the solvent infiltration method has other potential uses because it can be dissolved in a wide range of solvents, such as acetone, THF, 1,2-dichloroethane, xylenes and hexane, by modulating its degree of silylation (DS). This provides an easy way to blend HA with other organic-soluble materials, such as regular polyethylene, polystyrene, polypropylene, and polyurethane etc. Biomaterials based on HA and other non-toxic, non-carcinogenic hydrophobic polymers will find wide application in the biomedical and sanitary fields. These materials can be manufactured in various forms, such as film, membrane, sponge, hydrogel, guide channel, thread, gauze, non-woven tissue, etc. HA with the native structure can easily be regenerated from the silyl HA via hydrolysis.

Although microcomposite samples were not made via the melt blending process, significant progress was made towards the development of such a method. A series of HA esters were synthesized from silylated HA as the starting material. When the chain length of the acyl groups was large enough (> 10 C), the HA ester melted before degrading. Thus, a thermoplastic (i.e.,melt-processable) HA was created. The melting temperature of HA esters, which was controlled by changing the acyl groups, decreased with increased acyl chain length. In the future an HA ester with a melting point matching that of UHMWPE can be selected to form an interpenetrating polymer network between UHMWPE and HA through in situ hot molding.

The thermoplastic HA esters can be hot molded into films, sheets, and various other shapes. They can be used alone or mixed with other biomedical grade thermoplastics, such as UHMWPE, polypropylene, and polystyrene. Crosslinkers, such as blocked polyisocyanate (the isocyanate groups can be released at the controlled temperature), could also be used during molding to obtain a permanent three-dimensional HA ester network. Finally, the acyl groups of the HA esters can easily be removed through saponification to regenerate HA to a structure similar to its native state after molding.

6.2 Future Work

6.2.1 Silylation

HMDS has been demonstrated effective in silylating hyaluronan, and the product was easily separated, however the reaction speed was quite slow. A more active silylation agent, such as TMCS, may be helpful. However, the impurities in TMCS caused crosslinking of the silylated HA, and the effort to remove the impurities were not

successful. Cooper et al. [1981] have reported a method to produce TMCS without highly chlorinated impurities that was not attempted in the present study. They reacted HMDS with hydrogen chloride based on stoichiometric amounts. The ammonium chloride by-product was separated from TMCS via filtering. This method will be attempted in the future, and the efficiency of HA silylation is expected to increase largely with the use of pure TMCS.

6.2.2 Micro-composites

Many parameters that might affect the properties of UHMWPE-HA micro-composites were not investigated in this dissertation, including the type of crosslinker, the temperature, pressure, time and cooling rate during re-molding. These factors will be studied in the future. UHMWPE porous preforms are the matrix of micro-composites, whose properties directly determined the quality of the final composites; however, no control samples with different preform parameters were investigated in the present study. In the future, simple and effective methods should be developed to characterize the porosity, pore sizes and distribution, and their effect on the properties of the composites should be investigated. Finally a protocol should be made to control the quality of the UHMWPE porous preforms and the final consolidated product.

The porous preform treatment methods and molding processes influence the properties of the micro-composite via changing its micro-structure and morphology. The structure and morphology of the micro-composite, and their relationship with the processes need to be investigated in the future.

The effect of the thickness of the porous surface layer on both mechanical and tribological properties of the micro-composite will be examined for the determination of an optimal porous thickness and the balance of the material properties. Also, efforts to create porous layers with a gradient in porosity (more at the surface and decreasing amounts towards the bulk UHWMPE) will be made. This might improve the delamination resistance of the microcomposite.

Finally, other mechanical properties, such as creep, fatigue, toughness, hardness and resistance to delamination of the surface layer (i.e., surface layer shear strength) will be examined.

6.2.3 HA Esters

A considerable amount of work will be required to produce an interpenetrating polymer network between HA esters and UHMWPE via the melt blending method. First, an appropriate HA ester needs to be selected so that its melting temperature and flow state (i.e., viscosity at molding temperature) match that of UHMWPE. Second, an appropriate crosslinker needs to be selected so that the rheology of the HA ester during molding will match the molding conditions of UHMWPE, especially the pressure window. A blocked polyisocyanate can be used for this purpose, because its isocyanate groups are masked at low temperature, but become active at a defined high temperature with the removal of the masking groups By using an appropriately blocked polyisocyanate, the gel point of the HA ester could be designed to coincide with the pressure application point of UHMWPE. Third, an appropriate molding cycle will be determined to consolidate the material and achieve good comprehensive properties.

6.3 References

Cooper GK, Sandberg KR, and Hinck JF (1981). Trimethylsilyl cellulose as precursor to regenerated cellulose fiber. Journal of Applied Polymer Science, 26: 3828-3835.